Using K-means and Border Element Method to Design Phased Arrays with Subarray-only Amplitude and Phase Control

P. Rocca, L. Poli, A. Polo, and A. Massa

1

Contents

Legenda

EM: Excitation Matching

BEM: Border Element Method

CPM: Contiguous Partition Method

SLL: Sidelobe Level

HPBW: Half-Power Beamwidth

1 Numerical Validation - The K-means-based Excitation Matching Method

1.1 Reliability Analysis

OBJECTIVE: Verify the reliability of the proposed $K - means$ algorithm. A statistical analysis will be carried out in order to evaluate the performance of the method when randomly changing the initialization of the array partitions. The size of the problem is fixed (number of elements: $N = 32$) as well as the desired beam pointing angle, but different number of clusters are considered, form $Q = 12$ up to $Q = 28$ (namely, the values that will be considered in the following Sections).

Array Parameters

- Number of elements: $N = 32$

- Number of subarrays: $Q = 12, 16, 20, 24, 28$

- Inter-element spacing: $d = \lambda/2$

- Taylor excitation amplitudes, $SLL_{ref} = -30$ [dB]

- Pointing angle: $\theta_0 = -5$ [deg]

K-means Clustering Parameters

- Number of iterations: $I = 100$

- Number of executions: $R = 1000$

1.1.1 Taylor Pattern, $N = 32$, $SLL_{ref} = -30$ [dB], $\theta_0 = -5$ [deg]

	min	max	μ	σ^2	η [%]
$Q = 12$	1.43×10^{-2}	2.22×10^{-2}	1.64×10^{-2}	1.61×10^{-6}	2.1
$Q = 16$	8.16×10^{-3}	1.47×10^{-2}	8.76×10^{-3}	5.06×10^{-7}	11.5
$Q = 20$	4.23×10^{-3}	5.69×10^{-3}	5.02×10^{-3}	9.84×10^{-8}	0.4
$Q = 24$	1.83×10^{-3}	4.17×10^{-3}	2.12×10^{-3}	1.07×10^{-7}	1.8
$Q = 28$	3.47×10^{-4}	6.63×10^{-4}	4.25×10^{-4}	1.86×10^{-8}	75.2

Table I: *Reliability Analysis* - Statistics: Minimum value (min), maximum value (max), mean value (μ) and variance (σ^2) of the excitation matching error Ψ along with the "successful rate" (η, ratio between the number runs which converge toward the best solution found by the algorithm over the total number of runs).

OUTCOMES:

- The performance of the method and the achieved solutions significantly depend on the initial clustering. However, the data in Tab. I show that generally the mean value is very close to the minimum one (e.g., $\mu\rfloor_{Q=16} = 8.76 \times 10^{-3}$ vs. $\min_{r=1,...,R} \Psi_r\rfloor_{Q=16} = 8.16 \times 10^{-2}$, where $\mu = E\{\Psi\} = \frac{1}{R}\sum_{r=1}^{R} \Psi_r$) and the variance is very low (e.g., $\sigma^2\rfloor_{Q=16} = 5.06 \times 10^{-7}$, where $\sigma^2 = \frac{1}{R}\sum_{r=1}^{R}\{\Psi_r - \mu\}^2$) except for the case with $Q = 20$ where the mean value is closer to the maximum one ($\mu\rfloor_{Q=20} = 5.02 \times 10^{-3}$ closer to $\max_{r=1,...,R} \Psi_r\rfloor_{Q=20} = 5.69 \times 10^{-3}$ instead of $\min_{r=1,...,R} \Psi_r\rfloor_{Q=20} = 4.23 \times 10^{-3}$). In such a case (i.e., $Q = 20$), the successful rate is very low (i.e., $\eta\rfloor_{Q=20} = 0.4\%$);

- Due to the stochastic nature of the algorithm $R = 100$ runs will be executed in the next Sections, and only the best solution will be selected and analyzed.

1.2 Taylor Patterns - Analysis varying Q for Different Values of Reference Sidelobe Level SLL_{ref}

OBJECTIVE: In the previous Section the values reported in Tab. I clearly show that the excitation matching error Ψ decreases when the number of subarrays Q increases. This Section is aimed at studying the performance of the $K - means$ algorithm when changing the reference pattern, and more precisely when decreasing its sidelobe level, by evaluating all the figure of merit. The performance will be analyzed also considering different values of Q, in order to confirm the outcome of the previous Section. The size of the problem is kept fixed (number of elements: $N = 32$) as well as the desired beam pointing angle.

Array Parameters

- Number of elements: $N = 32$

- Number of subarrays: $Q = 12,\ 16,\ 20,\ 24,\ 28,\ 32$

- Inter-element spacing: $d = \lambda/2$

- Taylor excitation amplitudes, $SLL_{ref} = -20,\ -25,\ -30,\ -35,\ -40$ [dB]

- Pointing angle: $\theta_0 = -10$ [deg]

K-means Clustering Parameters

- Number of iterations: $I = 100$

- Number of executions: $R = 100$

1.2.1 Taylor Pattern, $N = 32$, $SLL_{ref} = -20$ [dB], $\theta_0 = -10$ [deg]
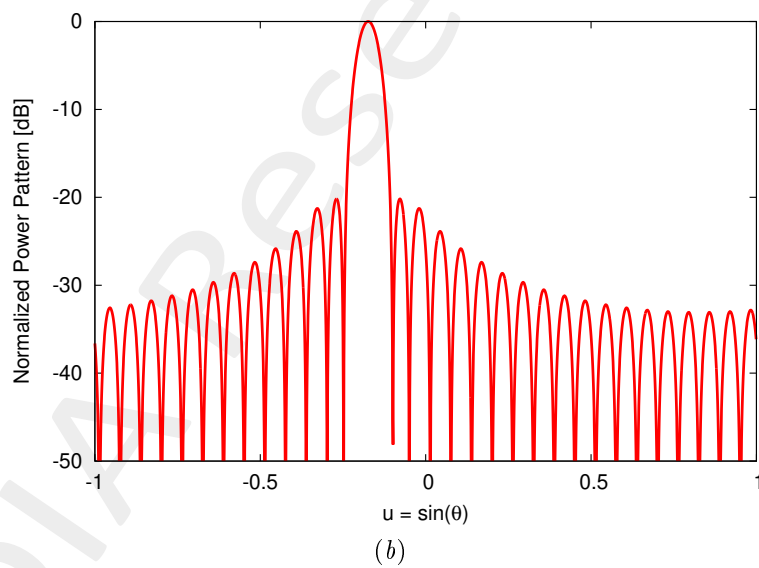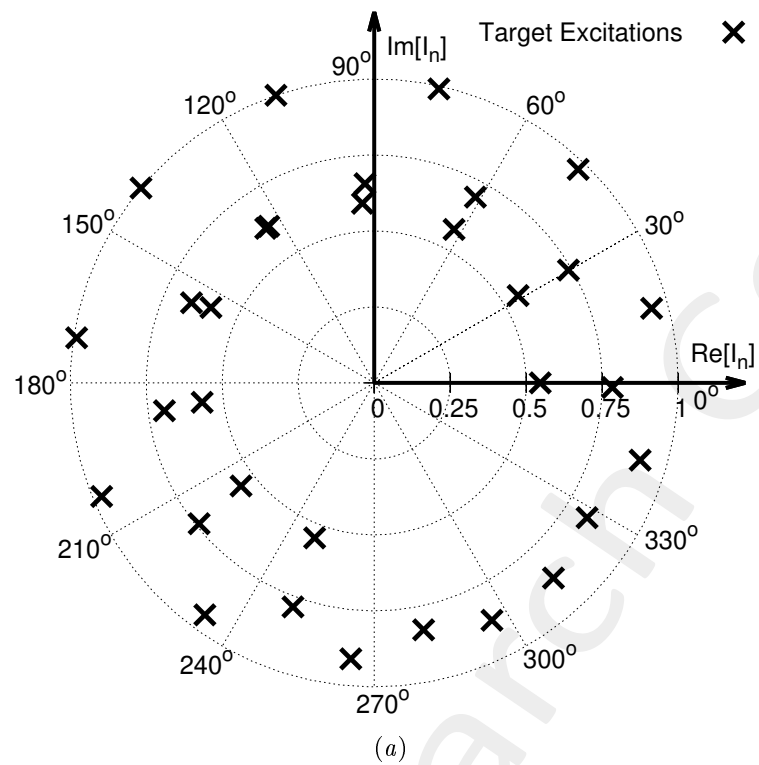
Target Solution

(a)

(b)

Figure 1: *Target solution* - (a) target excitations and (b) corresponding radiation pattern.

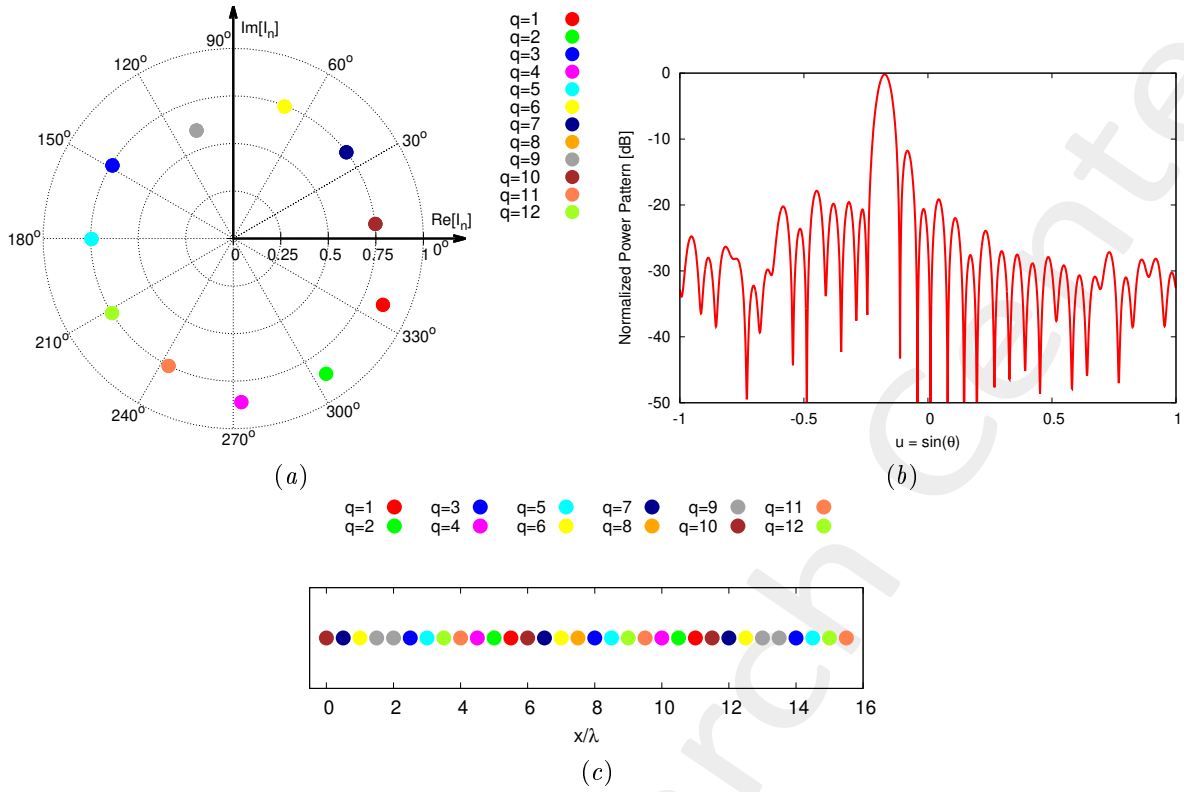**$Q = 12$ - Excitation Matching (EM) K-means Solution**

(a)

(b)

(c)

Figure 2: *K-means solution* - (a) Optimized excitations, (b) arising radiation pattern and (c) subarray configuration.

$Q = 16$ - Excitation Matching (EM) K-means Solution

(a)

(b)

(c)

Figure 3: *K-means solution* - (a) Optimized excitations, (b) arising radiation pattern and (c) subarray configuration.

$Q = 20$ - Excitation Matching (EM) K-means Solution

Figure 4: *K-means solution* - (a) Optimized excitations, (b) arising radiation pattern and (c) subarray configuration.

$Q = 24$ - Excitation Matching (EM) K-means Solution
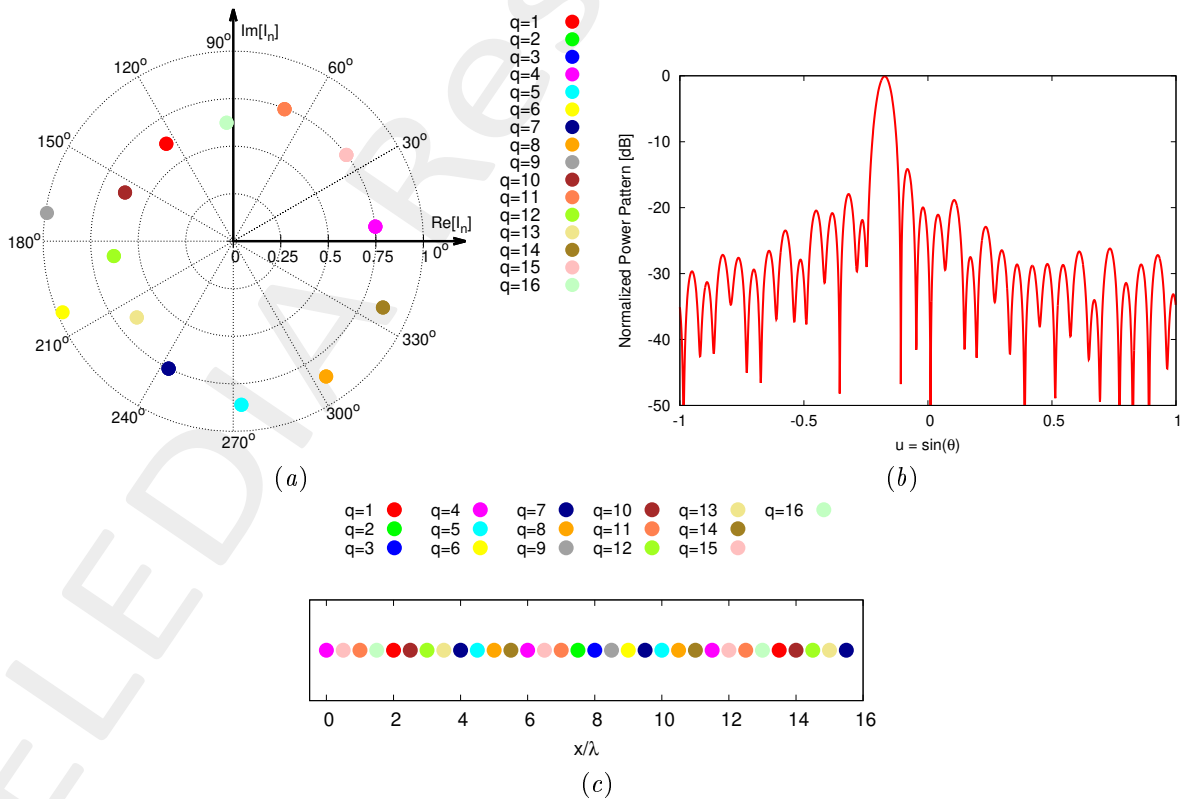

Figure 5: *K-means solution* - (a) Optimized excitations, (b) arising radiation pattern and (c) subarray configuration.

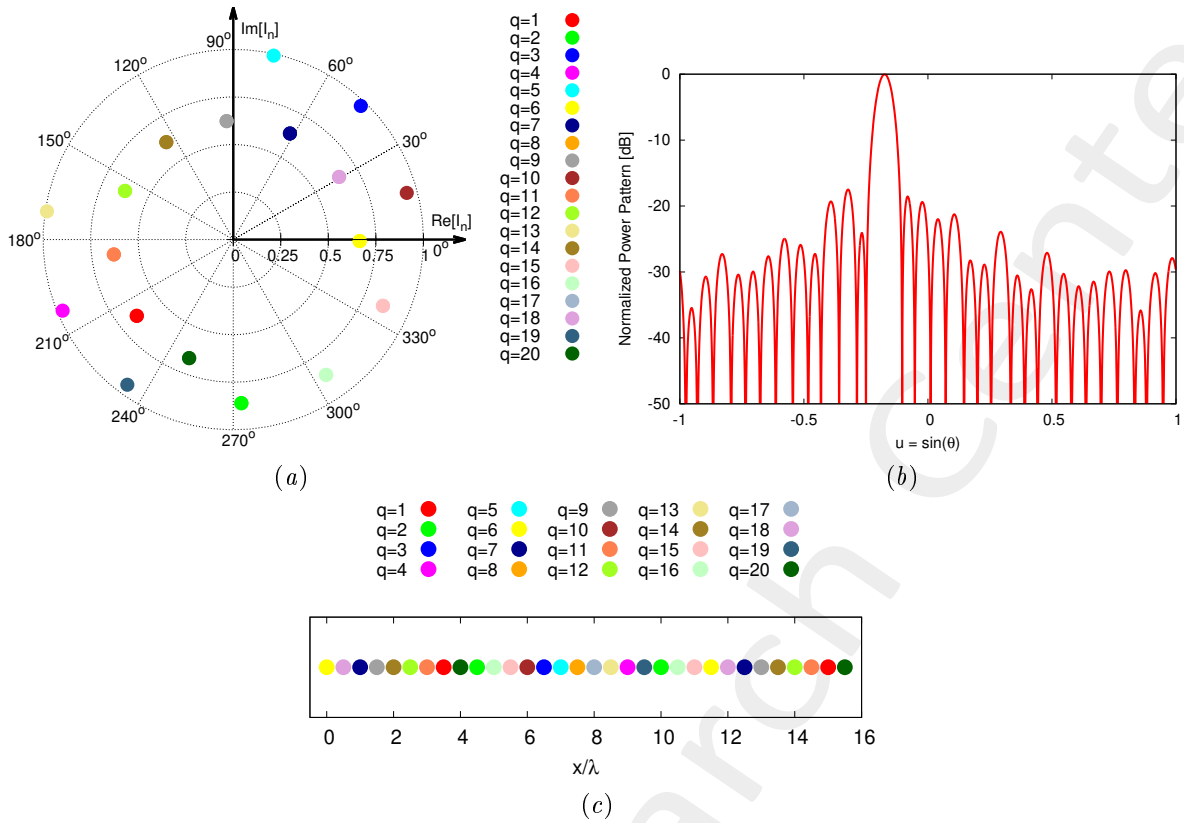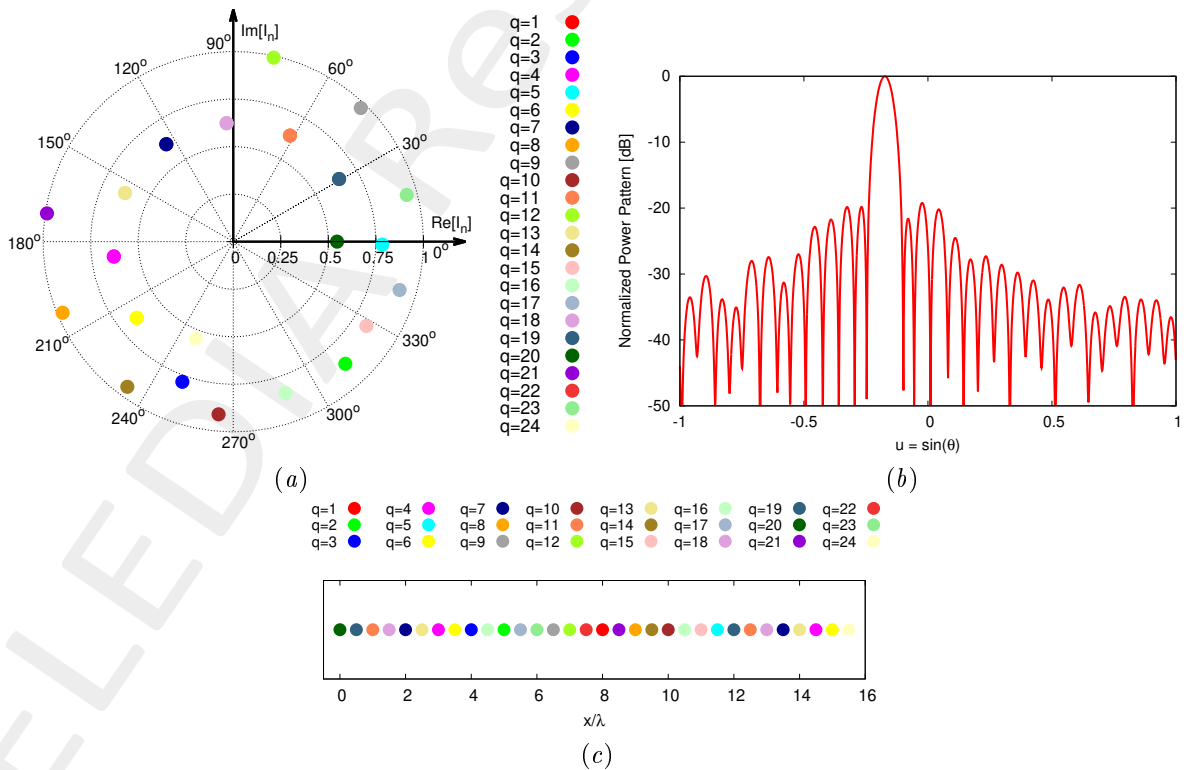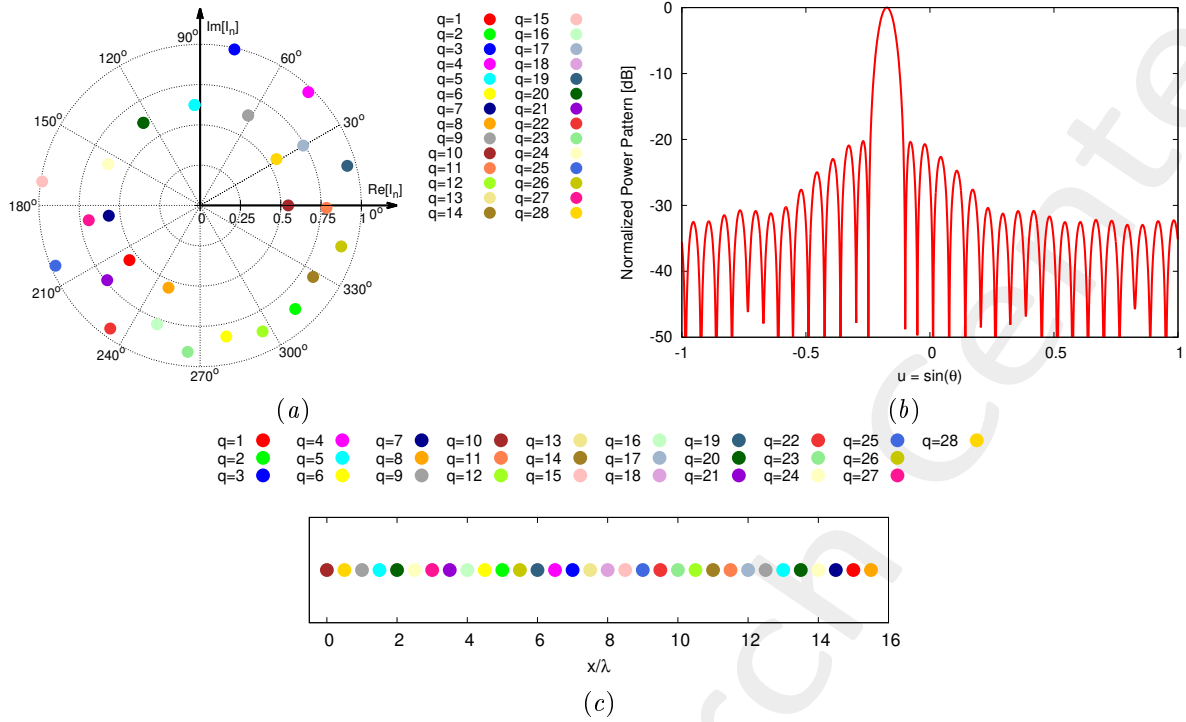**$Q = 28$ - Excitation Matching (EM) K-means Solution**

Figure 6: *K-means solution* - (a) Optimized excitations, (b) arising radiation pattern and (c) subarray configuration.

Pattern Features Resume

	SLL [dB]	$HPBW$ [deg]	$D_{\max}$ [dB]	Δ	Ψ
$Q = 12$	-11.56	3.30	17.90	5.34×10^{-2}	3.28×10^{-2}
$Q = 16$	-14.06	3.38	17.91	3.02×10^{-2}	1.86×10^{-2}
$Q = 20$	-17.46	3.49	17.88	1.06×10^{-2}	6.51×10^{-3}
$Q = 24$	-19.21	3.54	17.88	4.11×10^{-3}	2.53×10^{-3}
$Q = 28$	-20.25	3.57	17.87	6.34×10^{-4}	3.89×10^{-4}
$Q = 32$	-20.18	3.58	17.87	0.00	0.00

Table II: *K-means solution* - Sidelobe level, SLL, half-power beamwidth, $HPBW$, directivity peak, $D_{\max}$, pattern matching error, Δ, and fitness, Ψ, values.

1.2.2 Taylor Pattern, $N = 32$, $SLL_{ref} = -25$ [dB], $\theta_0 = -10$ [deg]

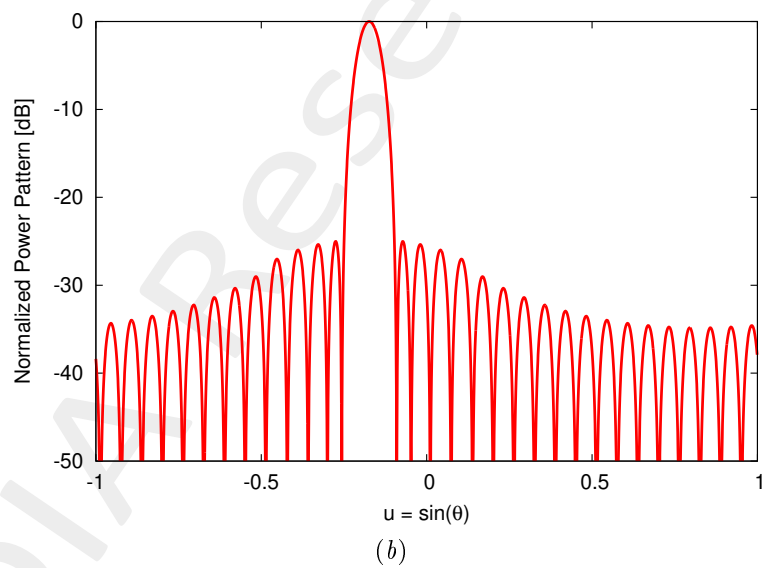**Target Solution**

(a)

(b)
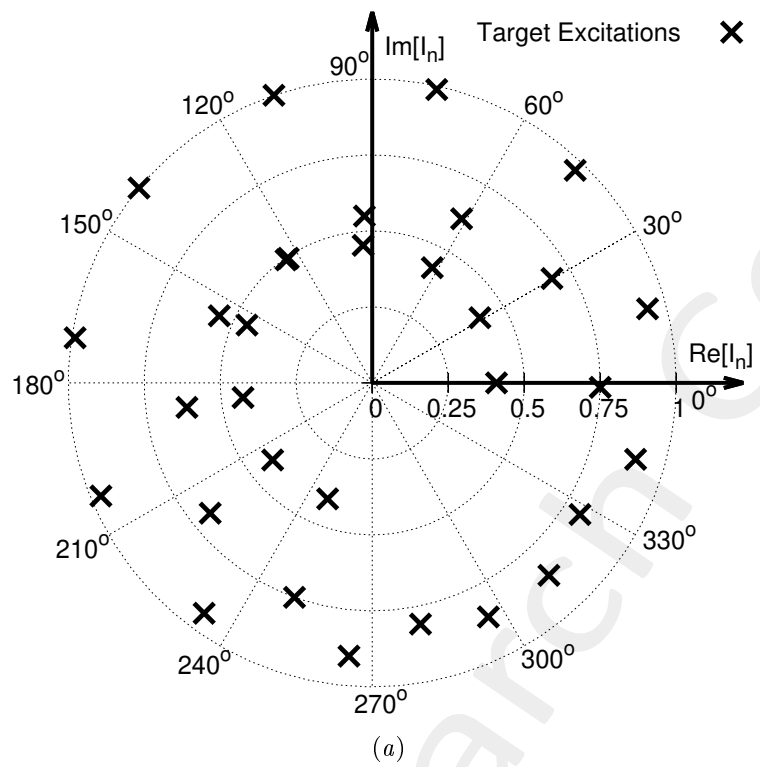
Figure 7: *Target solution* - (a) target excitations and (b) corresponding radiation pattern.

$Q = 12$ - Excitation Matching (EM) K-means Solution

(a)

(b)

(c)

Figure 8: *K-means solution* - (a) Optimized excitations, (b) arising radiation pattern and (c) subarray configuration.

$Q = 16$ - Excitation Matching (EM) K-means Solution

(a)

(b)

(c)

Figure 9: *K-means solution* - (a) Optimized excitations, (b) arising radiation pattern and (c) subarray configuration.

$Q = 20$ - Excitation Matching (EM) K-means Solution

(a)

(b)

(c)

Figure 10: *K-means solution* - (a) Optimized excitations, (b) arising radiation pattern and (c) subarray configuration.

$Q = 24$ - Excitation Matching (EM) K-means Solution
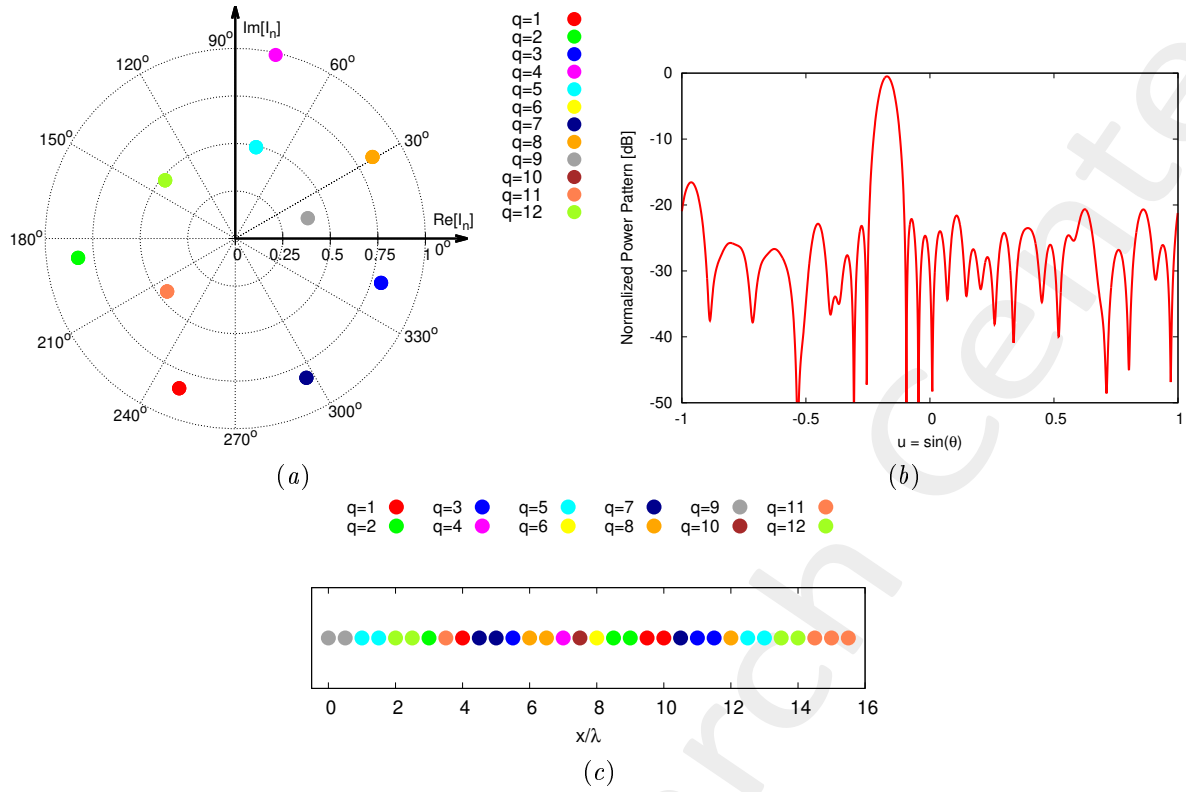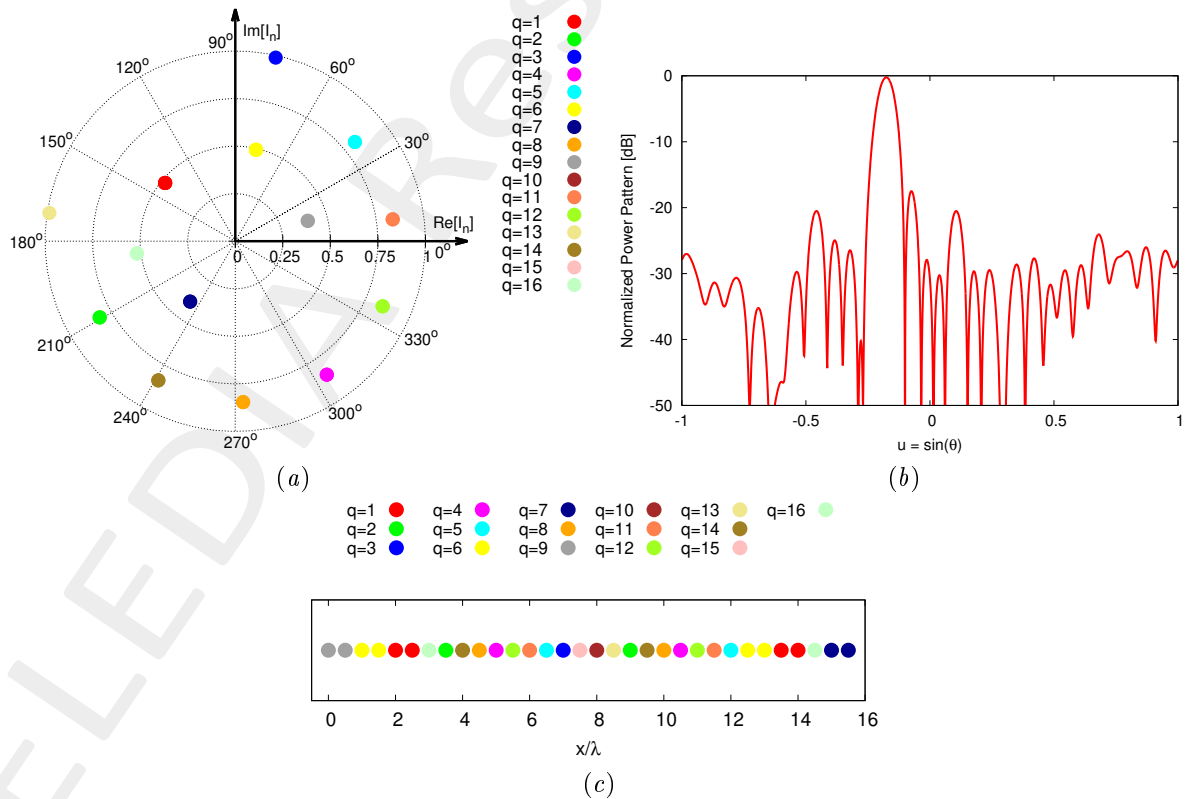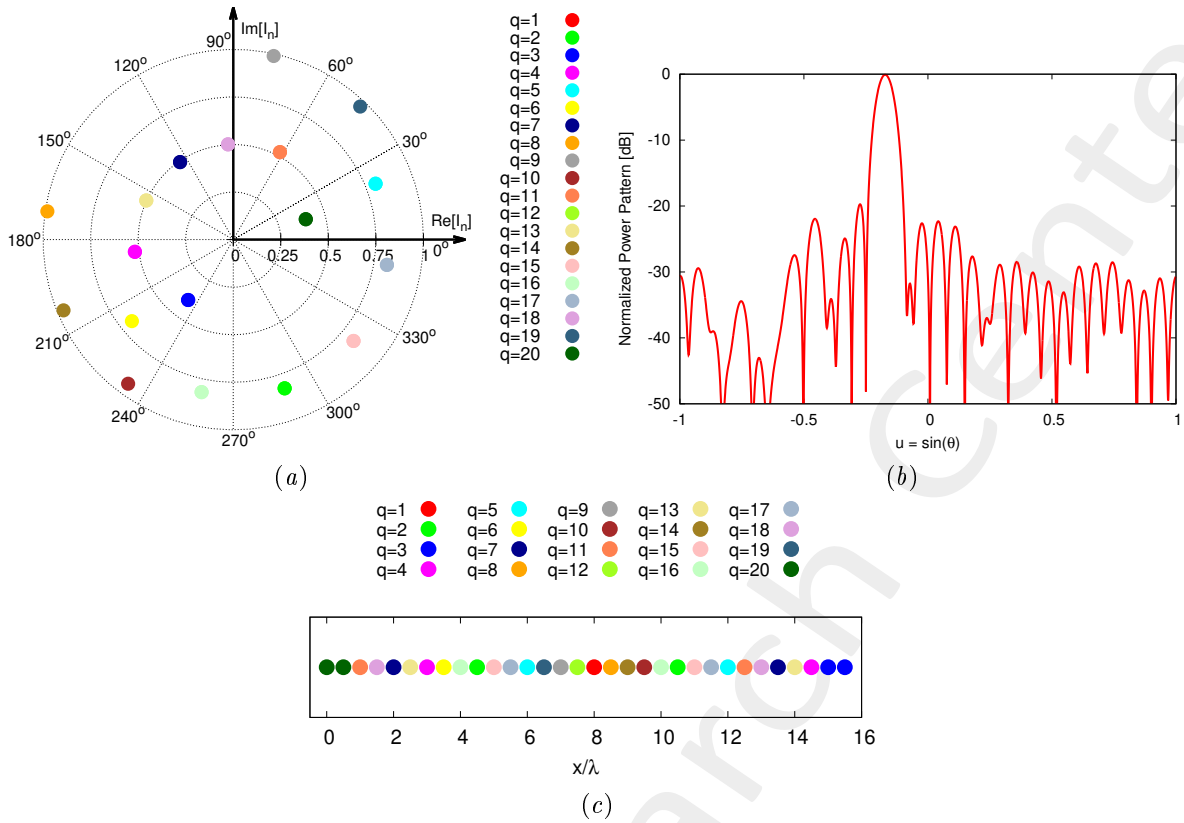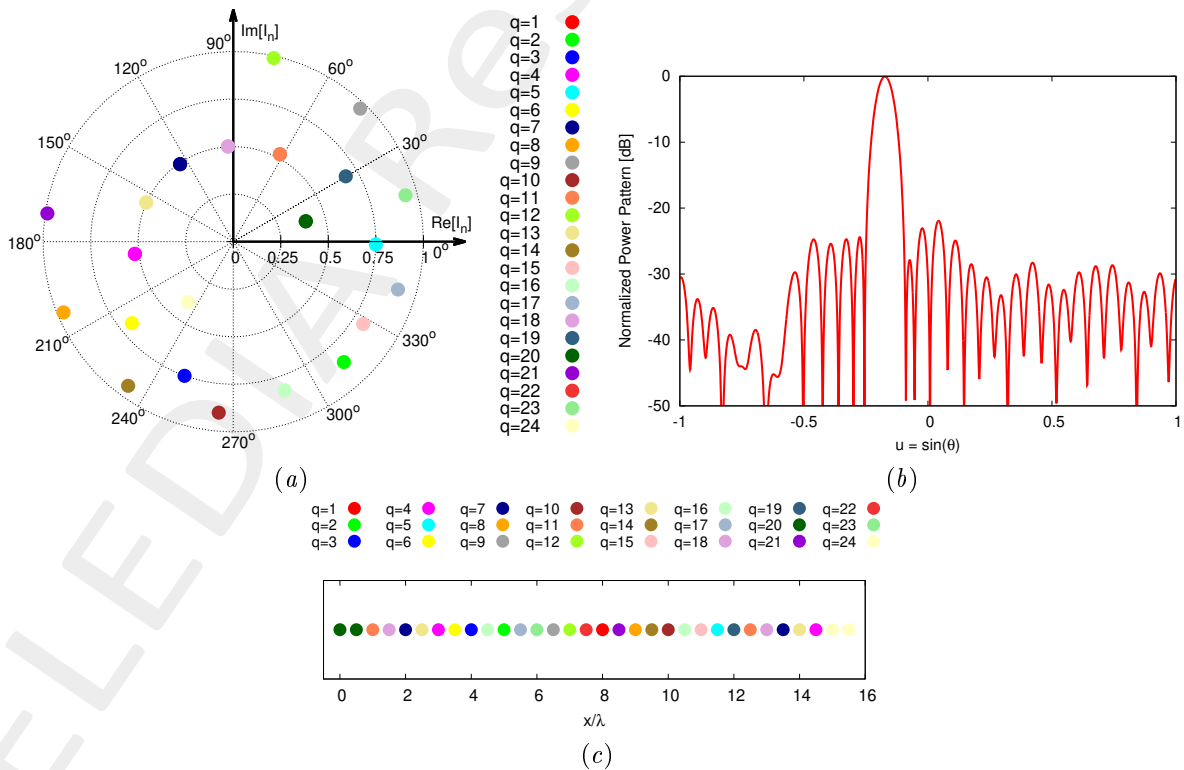

(a)

(b)

(c)

Figure 11: *K-means solution* - (a) Optimized excitations, (b) arising radiation pattern and (c) subarray configuration.

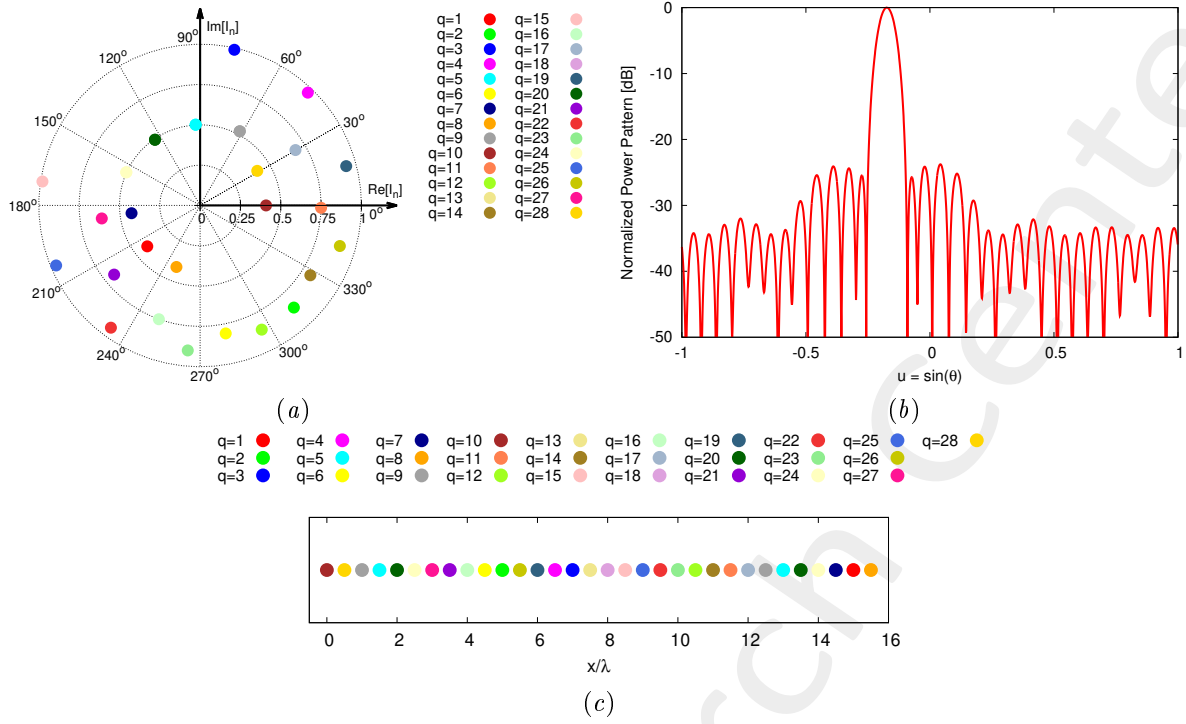**$Q = 28$ - Excitation Matching (EM) K-means Solution**

Figure 12: *K-means solution* - (a) Optimized excitations, (b) arising radiation pattern and (c) subarray configuration.

Pattern Features Resume

	SLL [dB]	$HPBW$ [deg]	$D_{\max}$ [dB]	Δ	Ψ
$Q = 12$	-16.06	3.74	17.45	6.29×10^{-2}	3.41×10^{-2}
$Q = 16$	-17.67	3.78	17.56	3.23×10^{-2}	1.75×10^{-2}
$Q = 20$	-19.64	3.77	17.63	1.54×10^{-2}	8.38×10^{-3}
$Q = 24$	-21.87	3.80	17.63	6.85×10^{-3}	3.72×10^{-3}
$Q = 28$	-23.76	3.78	17.67	1.55×10^{-3}	8.42×10^{-4}
$Q = 32$	-25.01	3.80	17.66	0.00	0.00

Table III: *K-means solution* - Sidelobe level, SLL, half-power beamwidth, $HPBW$, directivity peak, $D_{\max}$, pattern matching error, Δ, and fitness, Ψ, values.

1.2.3 Taylor Pattern, $N = 32$, $SLL_{ref} = -30$ [dB], $\theta_0 = -10$ [deg]

Target Solution

(a)

(b)
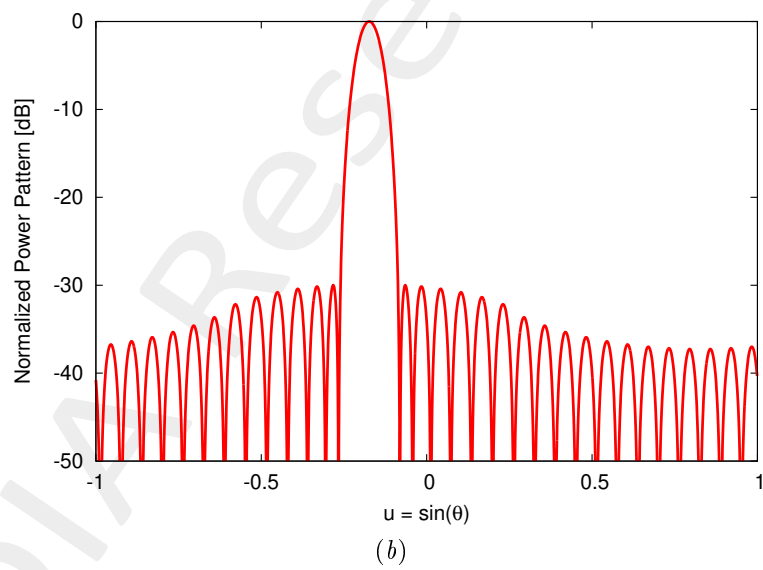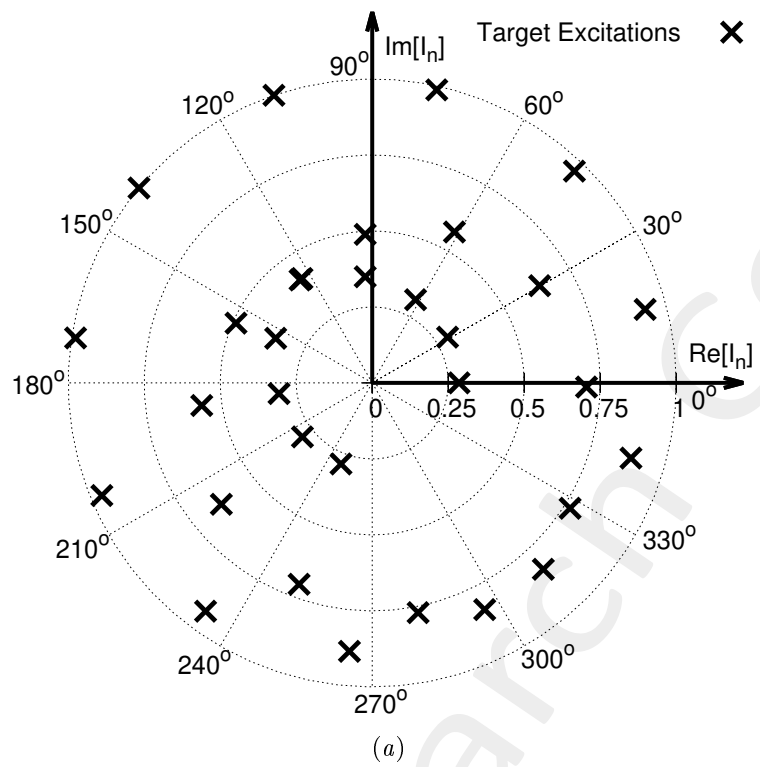
Figure 13: *Target solution* - (a) target excitations and (b) corresponding radiation pattern.

$Q = 12$ - Excitation Matching (EM) K-means Solution

(a)

(b)

(c)

Figure 14: *K-means solution* - (a) Optimized excitations, (b) arising radiation pattern and (c) subarray configuration.

$Q = 16$ - Excitation Matching (EM) K-means Solution

(a)

(b)

(c)

Figure 15: *K-means solution* - (a) Optimized excitations, (b) arising radiation pattern and (c) subarray configuration.

$Q = 20$ - Excitation Matching (EM) K-means Solution

(a)

(b)

(c)

Figure 16: *K-means solution* - (a) Optimized excitations, (b) arising radiation pattern and (c) subarray configuration.

$Q = 24$ - Excitation Matching (EM) K-means Solution

(a)

(b)

(c)

Figure 17: *K-means solution* - (a) Optimized excitations, (b) arising radiation pattern and (c) subarray configuration.

$Q = 28$ - Excitation Matching (EM) K-means Solution

Figure 18: *K-means solution* - (a) Optimized excitations, (b) arising radiation pattern and (c) subarray configuration.

Pattern Features Resume

	SLL [dB]	$HPBW$ [deg]	$D_{\max}$ [dB]	Δ	Ψ
$Q = 12$	-17.31	3.98	17.21	6.59×10^{-2}	3.23×10^{-2}
$Q = 16$	-19.41	4.07	17.24	3.44×10^{-2}	1.69×10^{-2}
$Q = 20$	-21.53	4.04	17.34	1.81×10^{-2}	8.86×10^{-3}
$Q = 24$	-25.36	4.05	17.37	7.89×10^{-3}	3.87×10^{-3}
$Q = 28$	-27.96	4.04	17.41	2.01×10^{-3}	9.87×10^{-4}
$Q = 32$	-30.00	4.04	17.42	0.00	0.00

Table IV: *K-means solution* - Sidelobe level, SLL, half-power beamwidth, $HPBW$, directivity peak, $D_{\max}$, pattern matching error, Δ, and fitness, Ψ, values.

1.2.4 Taylor Pattern, $N = 32$, $SLL_{ref} = -35$ [dB], $\theta_0 = -10$ [deg]

Target Solution

(a)

(b)
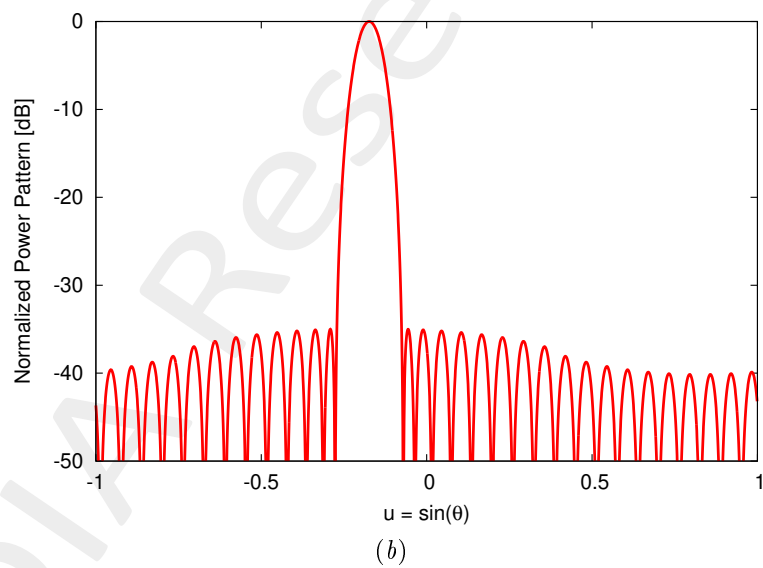
Figure 19: *Target solution* - (a) target excitations and (b) corresponding radiation pattern.
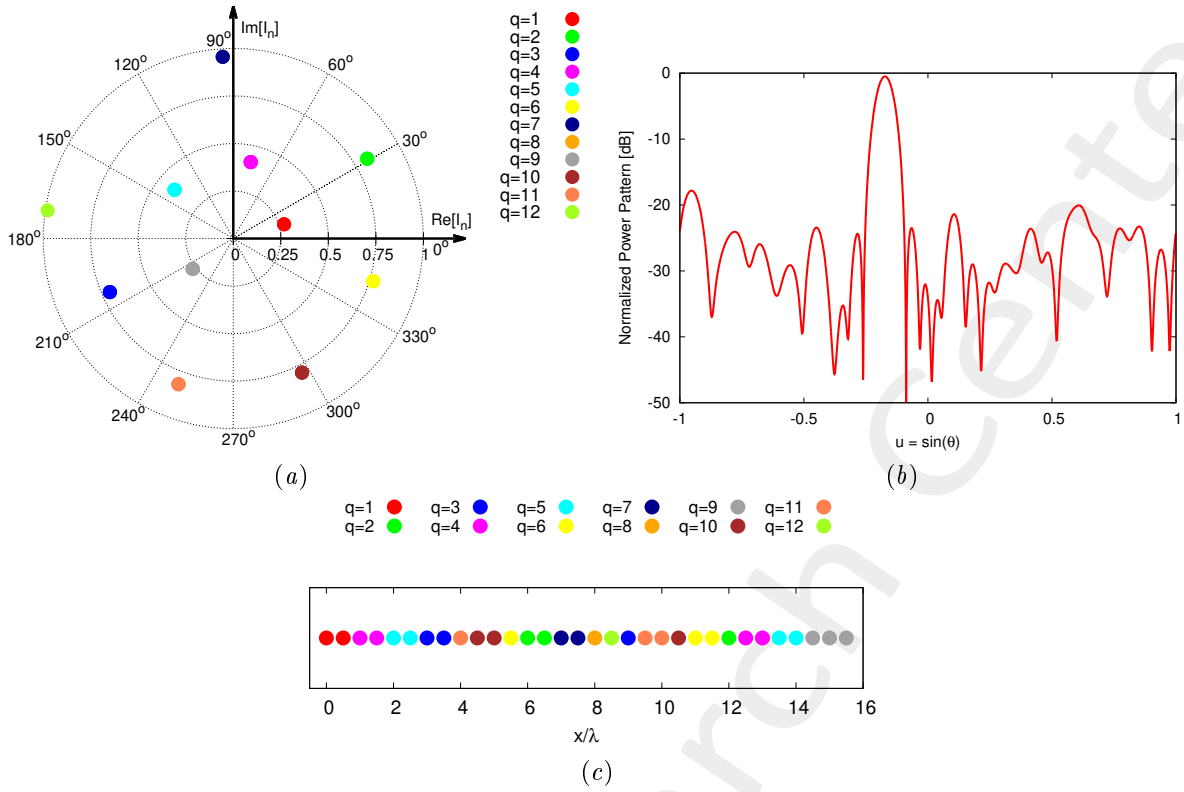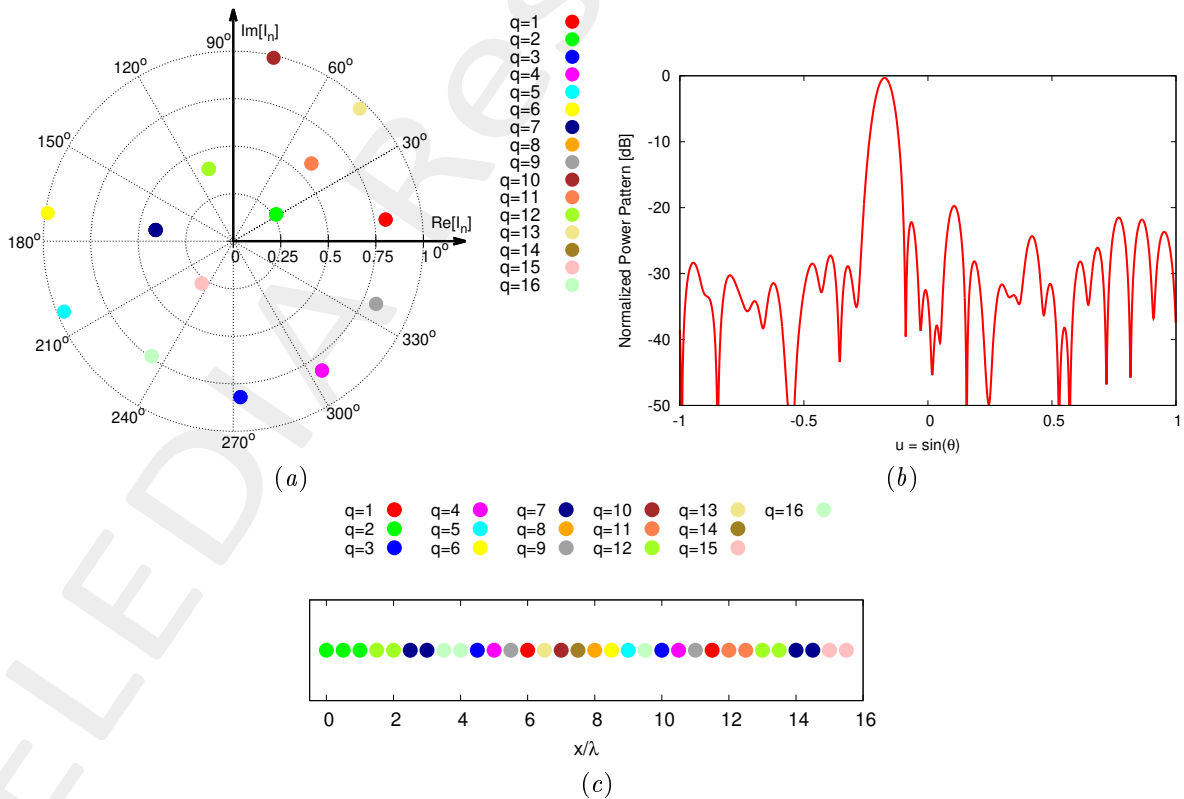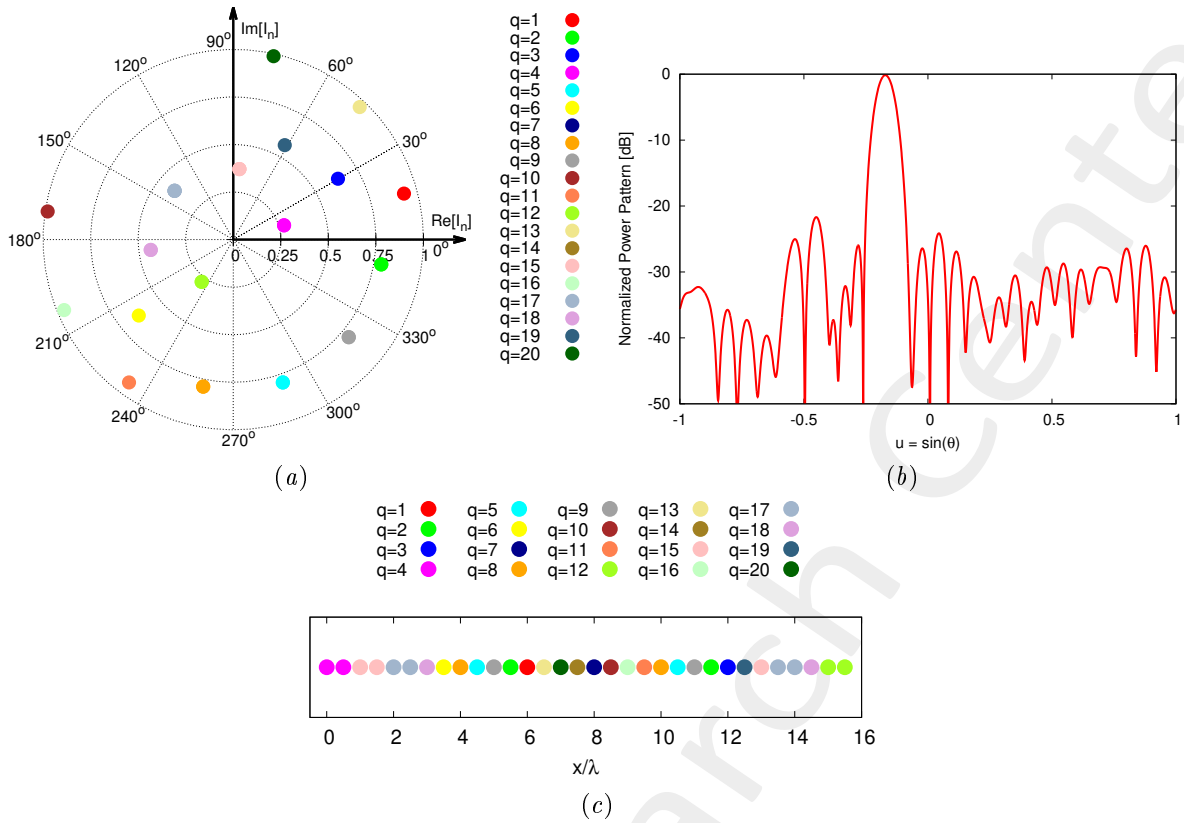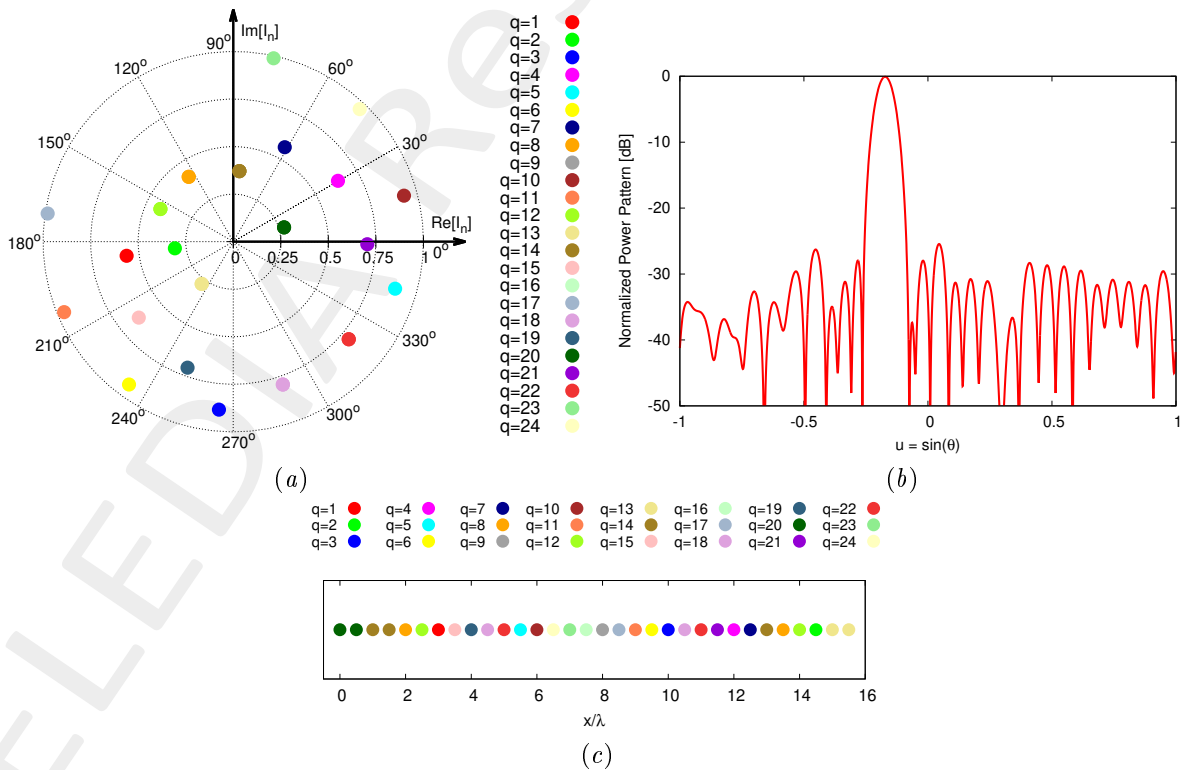
$Q = 12$ - Excitation Matching (EM) K-means Solution

(a)

(b)

(c)

Figure 20: *K-means solution* - (*a*) Optimized excitations, (*b*) arising radiation pattern and (*c*) subarray configuration.
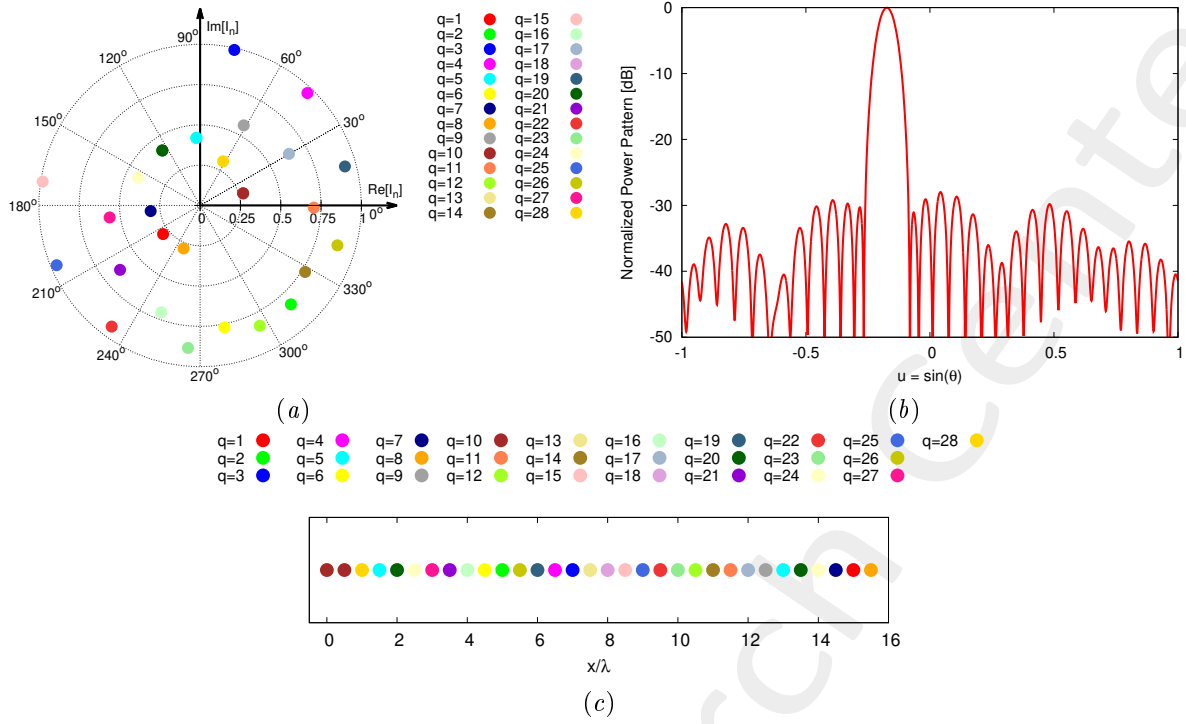
$Q = 16$ - Excitation Matching (EM) K-means Solution

(a)

(b)

(c)

Figure 21: *K-means solution* - (*a*) Optimized excitations, (*b*) arising radiation pattern and (*c*) subarray configuration.

$Q = 20$ - Excitation Matching (EM) K-means Solution

Figure 22: *K-means solution* - (a) Optimized excitations, (b) arising radiation pattern and (c) subarray configuration.

$Q = 24$ - Excitation Matching (EM) K-means Solution

Figure 23: *K-means solution* - (a) Optimized excitations, (b) arising radiation pattern and (c) subarray configuration.

$Q = 28$ - Excitation Matching (EM) K-means Solution

(a)   (b)

(c)

Figure 24: *K-means solution* - (a) Optimized excitations, (b) arising radiation pattern and (c) subarray configuration.

Pattern Features Resume

	SLL [dB]	$HPBW$ [deg]	$D_{\max}$ [dB]	Δ	Ψ
$Q = 12$	-16.09	4.26	16.87	6.84×10^{-2}	3.10×10^{-2}
$Q = 16$	-19.97	4.33	17.00	3.33×10^{-2}	1.50×10^{-2}
$Q = 20$	-25.06	4.34	17.05	1.62×10^{-2}	7.32×10^{-3}
$Q = 24$	-28.45	4.34	17.09	6.45×10^{-3}	2.92×10^{-3}
$Q = 28$	-32.83	4.30	17.14	1.52×10^{-3}	6.89×10^{-4}
$Q = 32$	-35.01	4.28	17.17	0.00	0.00

Table V: *K-means solution* - Sidelobe level, SLL, half-power beamwidth, $HPBW$, directivity peak, $D_{\max}$, pattern matching error, Δ, and fitness, Ψ, values.

1.2.5 Taylor Pattern, $N = 32$, $SLL_{ref} = -40$ [dB], $\theta_0 = -10$ [deg]

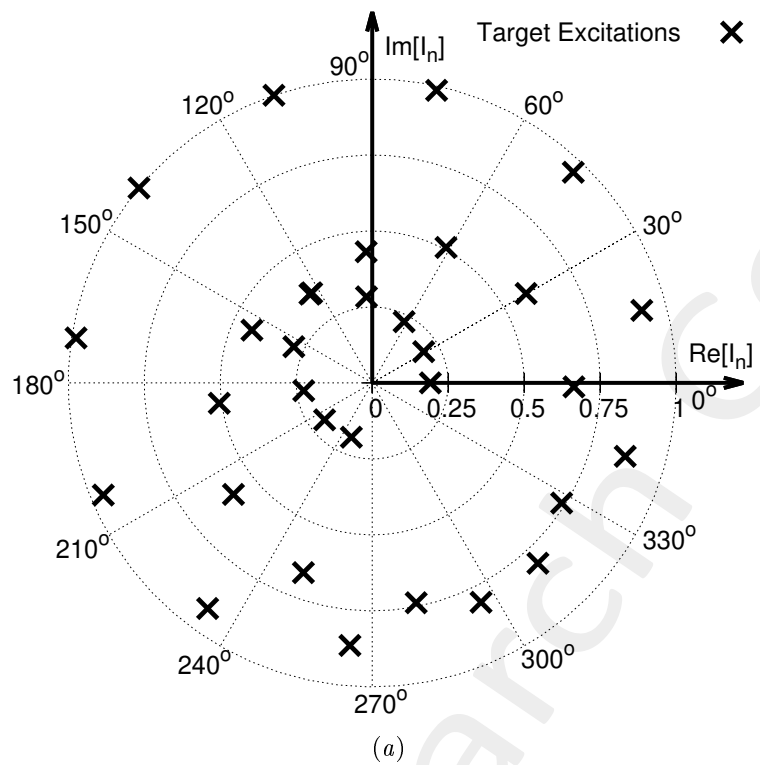**Target Solution**

(a)

(b)
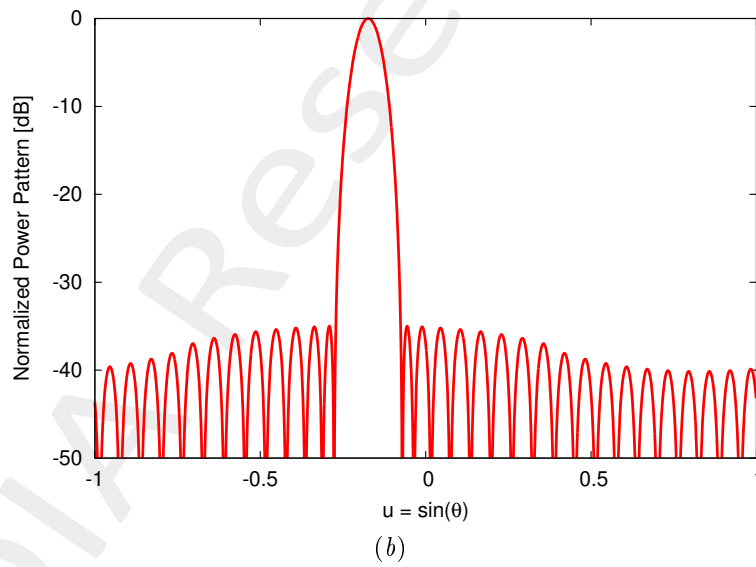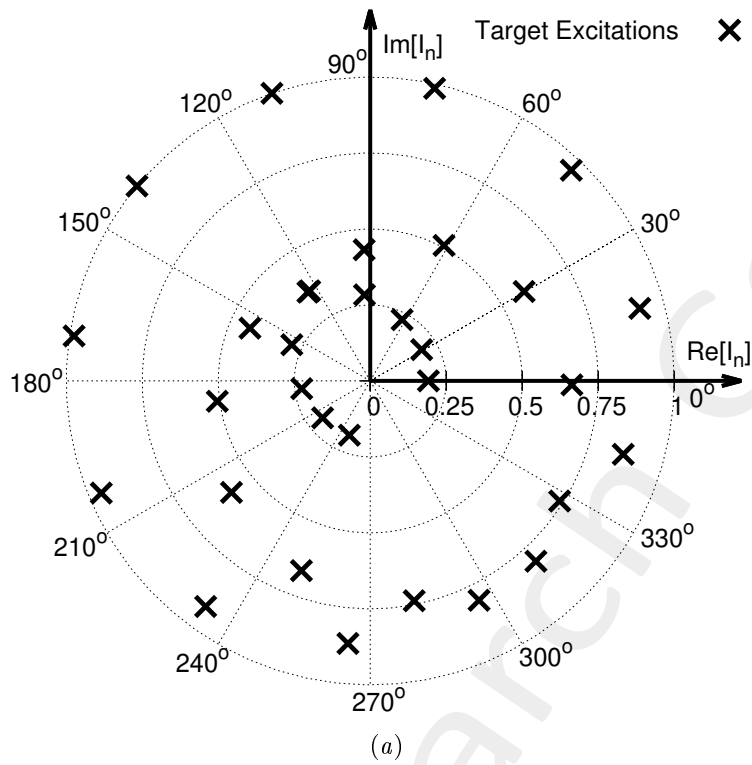
Figure 25: *Target solution* - (a) target excitations and (b) corresponding radiation pattern.

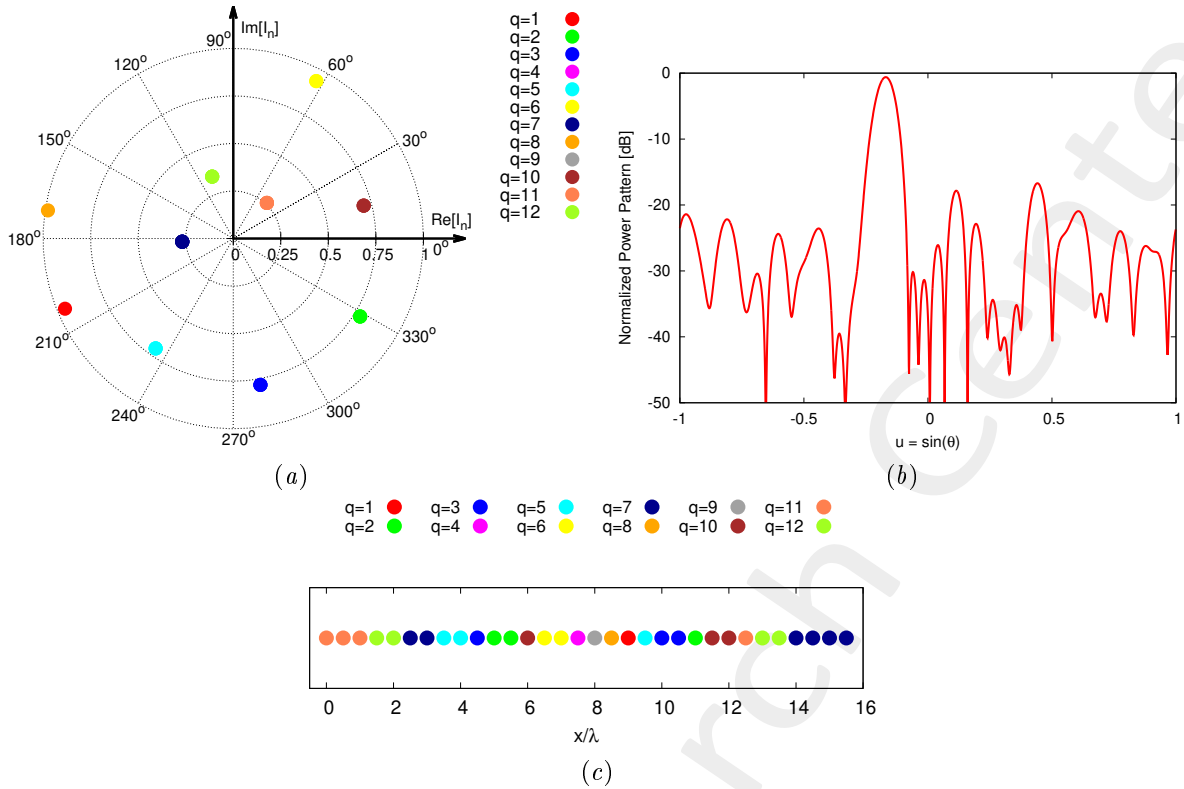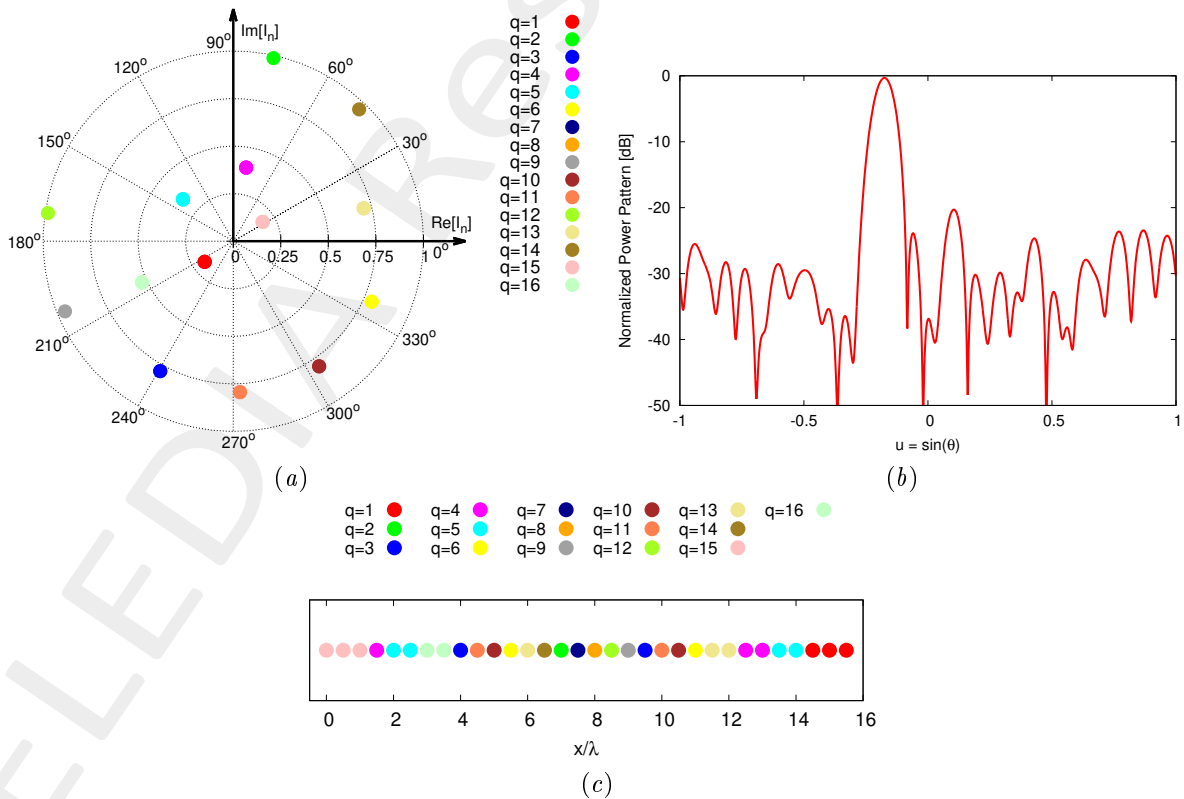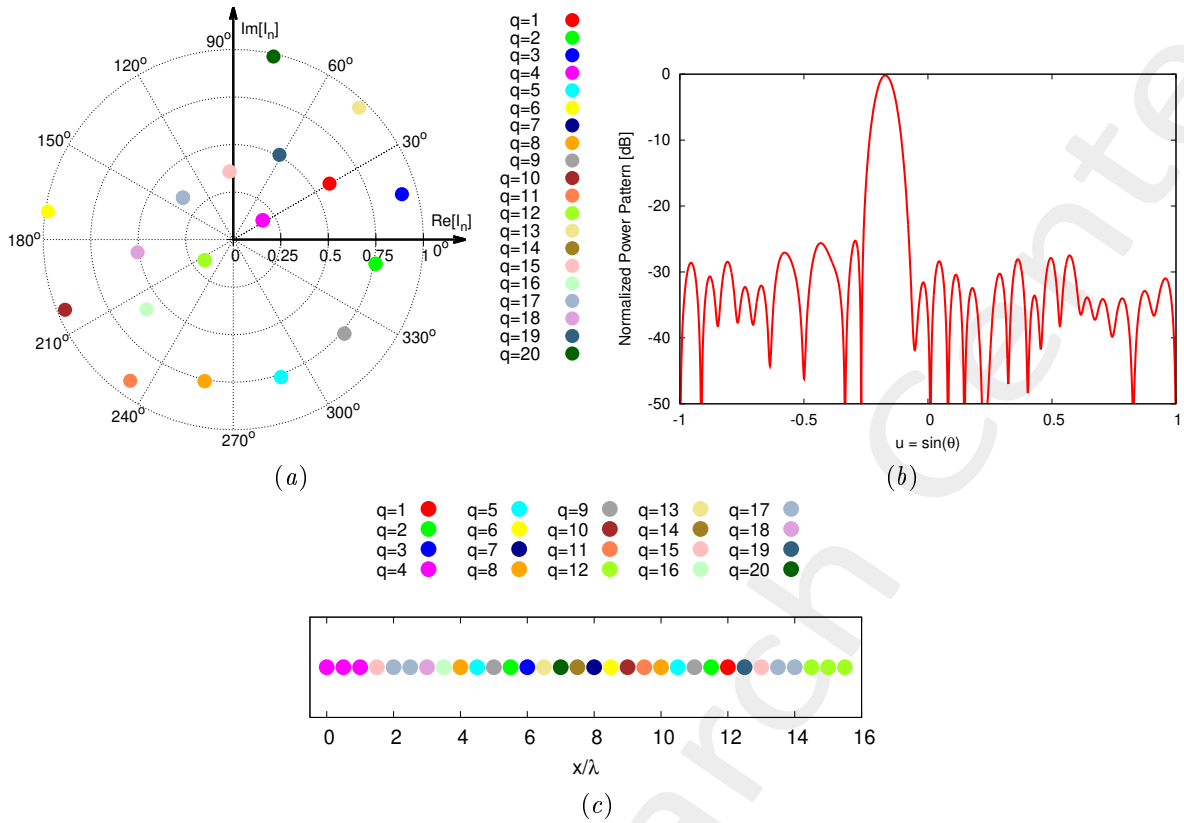**$Q = 12$ - Excitation Matching (EM) K-means Solution**

(a)

(b)

(c)
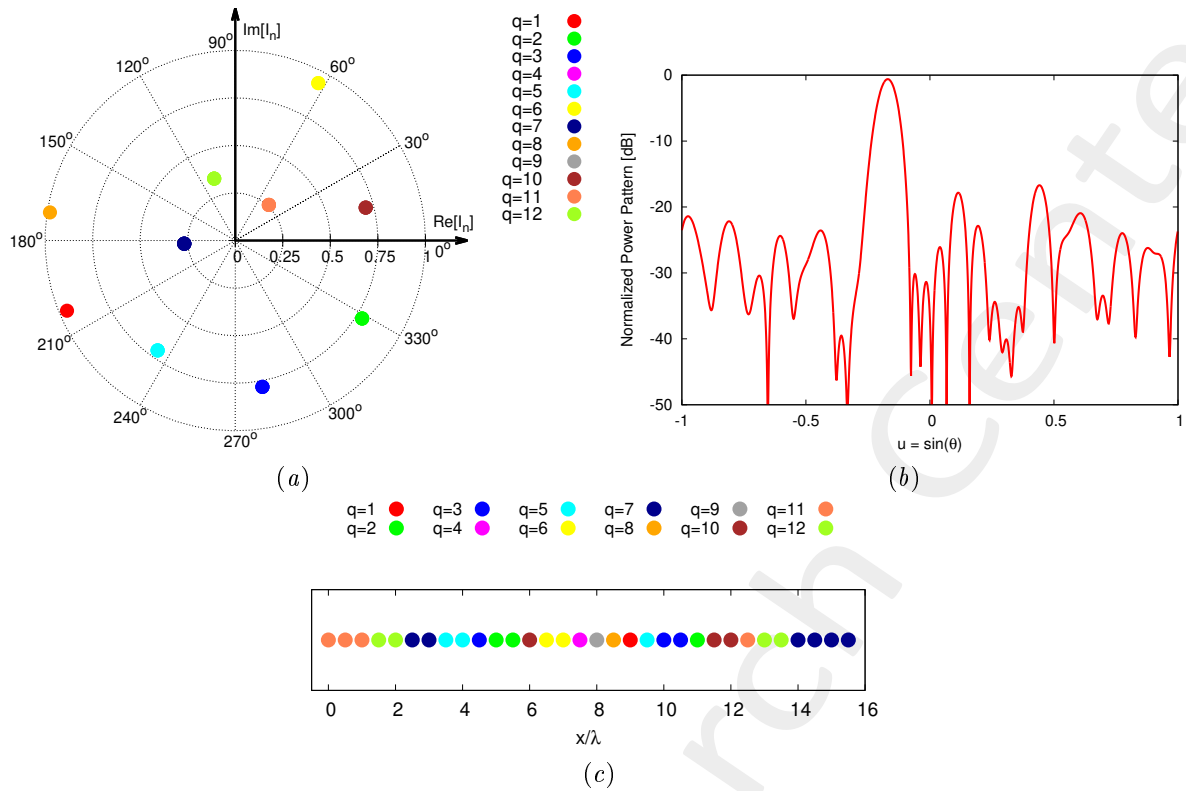
Figure 26: *K-means solution* - (*a*) Optimized excitations, (*b*) arising radiation pattern and (*c*) subarray configuration.

$Q = 16$ - Excitation Matching (EM) K-means Solution

(a)

(b)

(c)
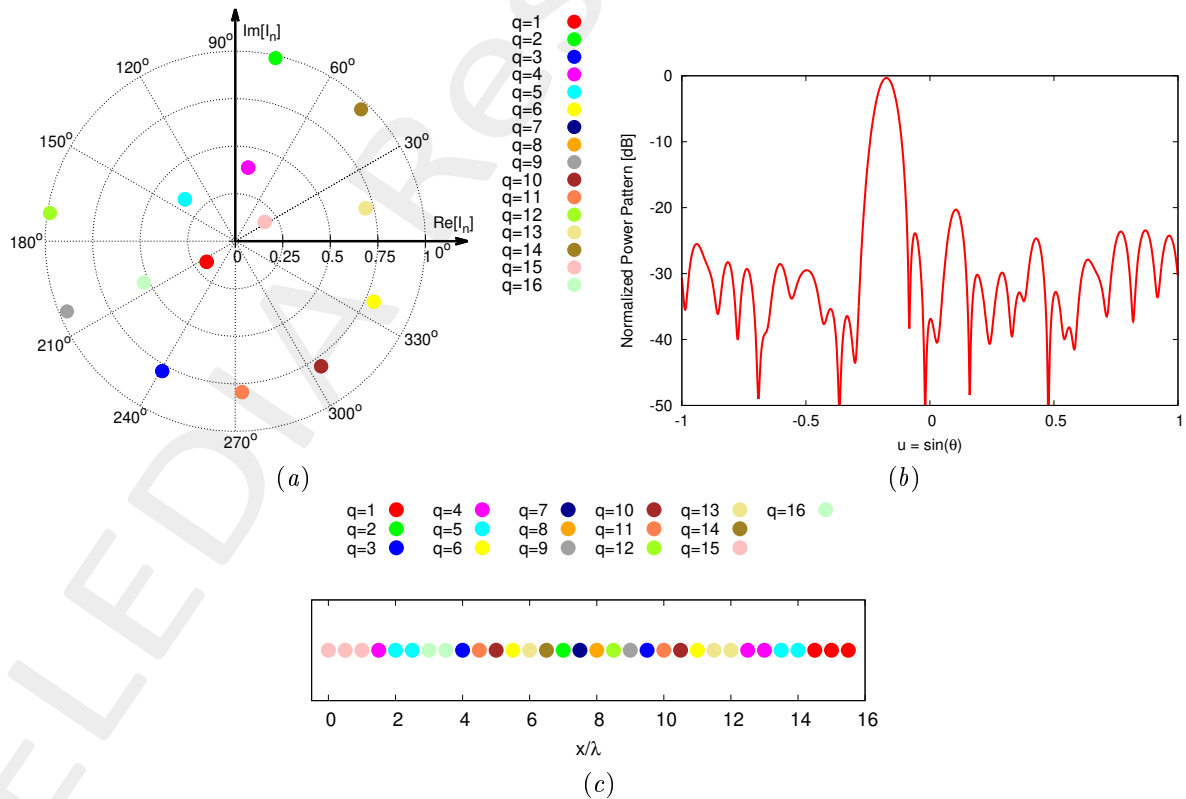
Figure 27: *K-means solution* - (*a*) Optimized excitations, (*b*) arising radiation pattern and (*c*) subarray configuration.
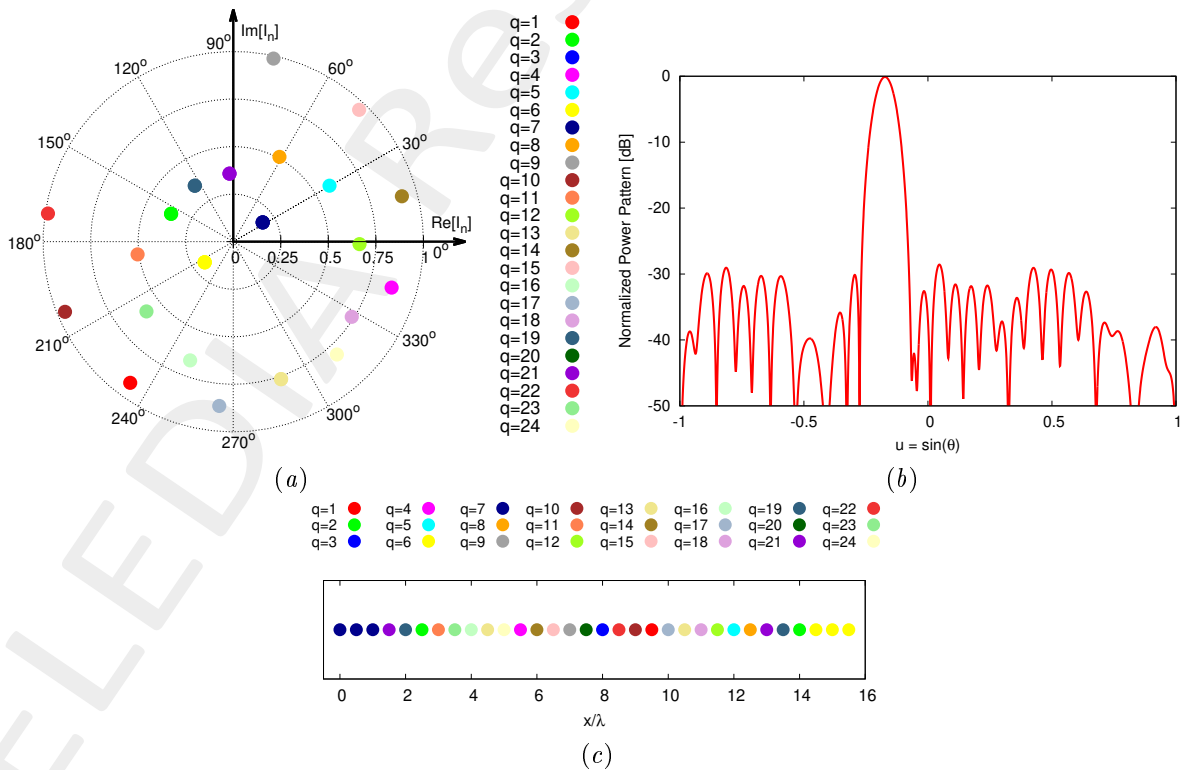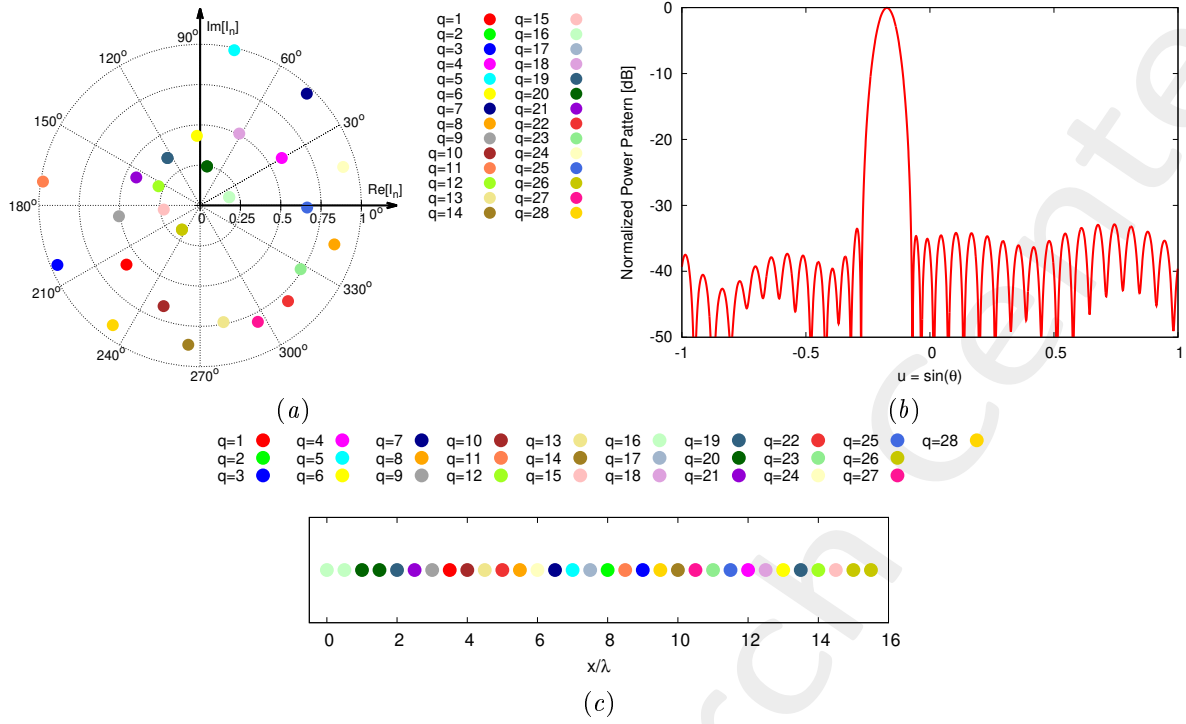
$Q = 20$ - Excitation Matching (EM) K-means Solution

(a)

(b)

(c)
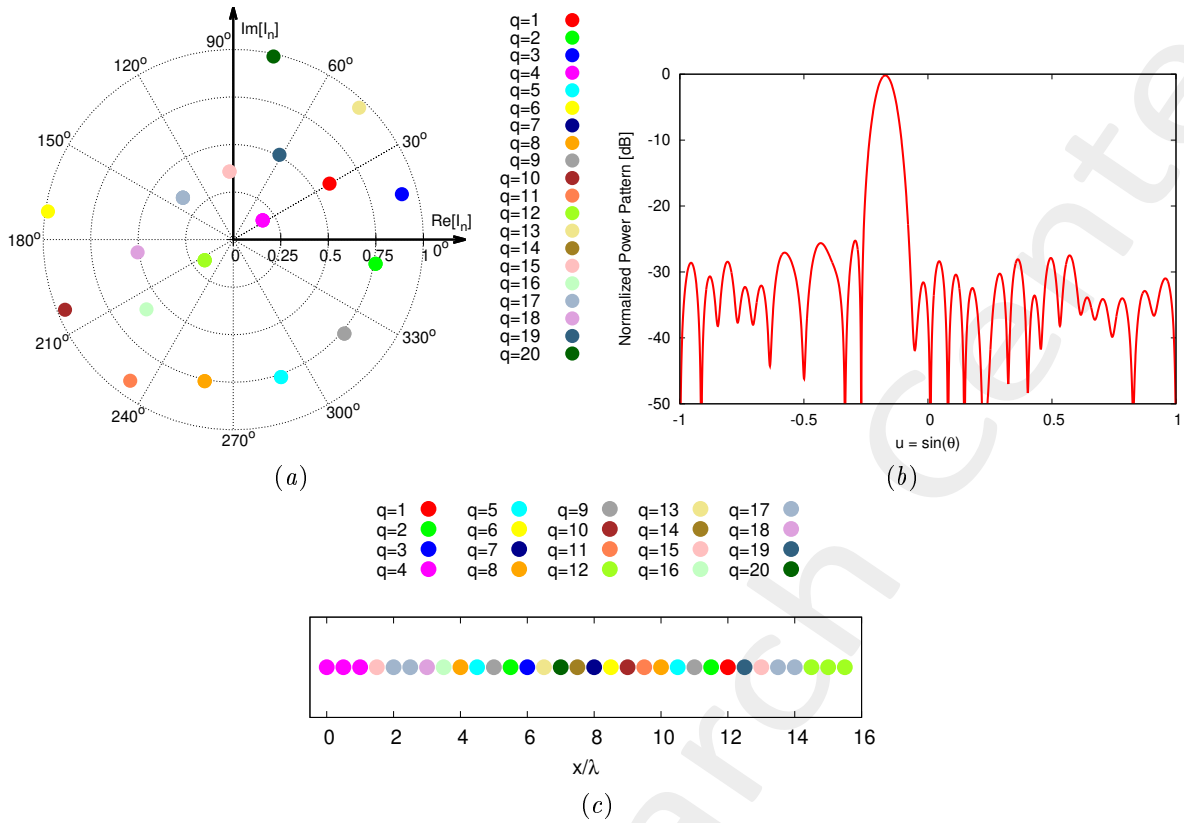
Figure 28: *K-means solution* - (a) Optimized excitations, (b) arising radiation pattern and (c) subarray configuration.

$Q = 24$ - Excitation Matching (EM) K-means Solution

(a)

(b)

(c)
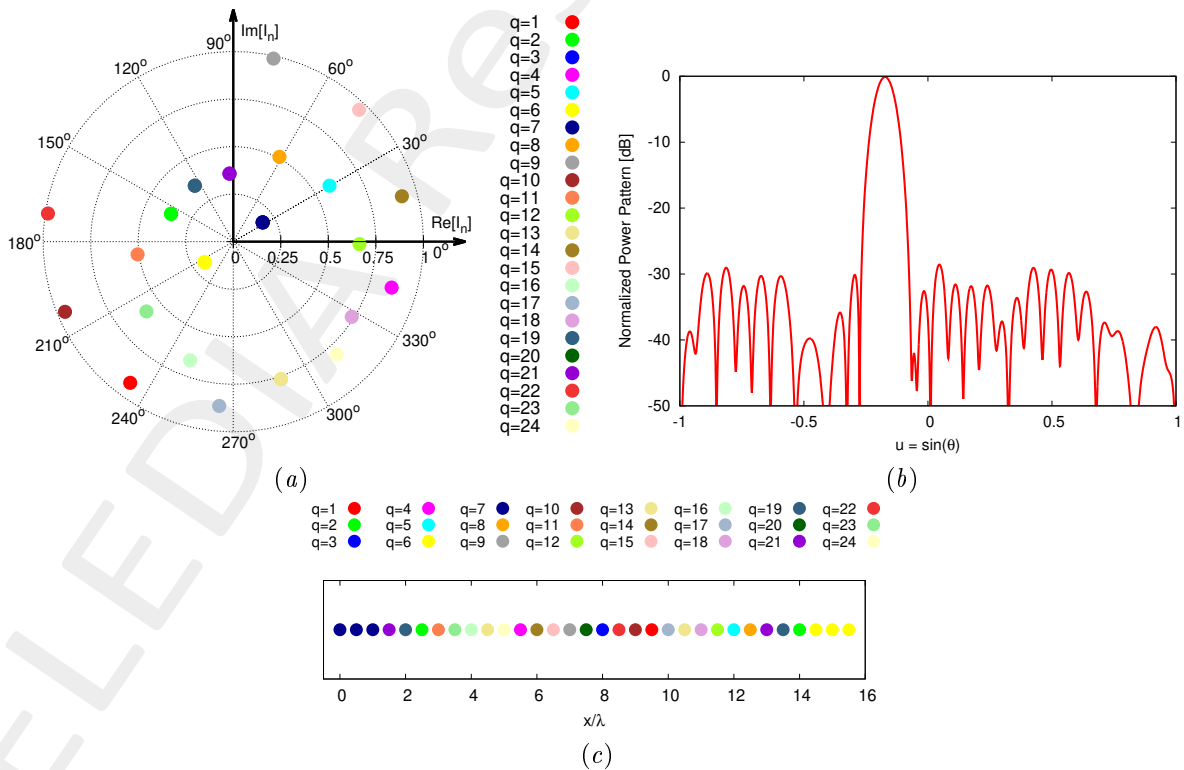
Figure 29: *K-means solution* - (a) Optimized excitations, (b) arising radiation pattern and (c) subarray configuration.

$Q = 28$ - Excitation Matching (EM) K-means Solution
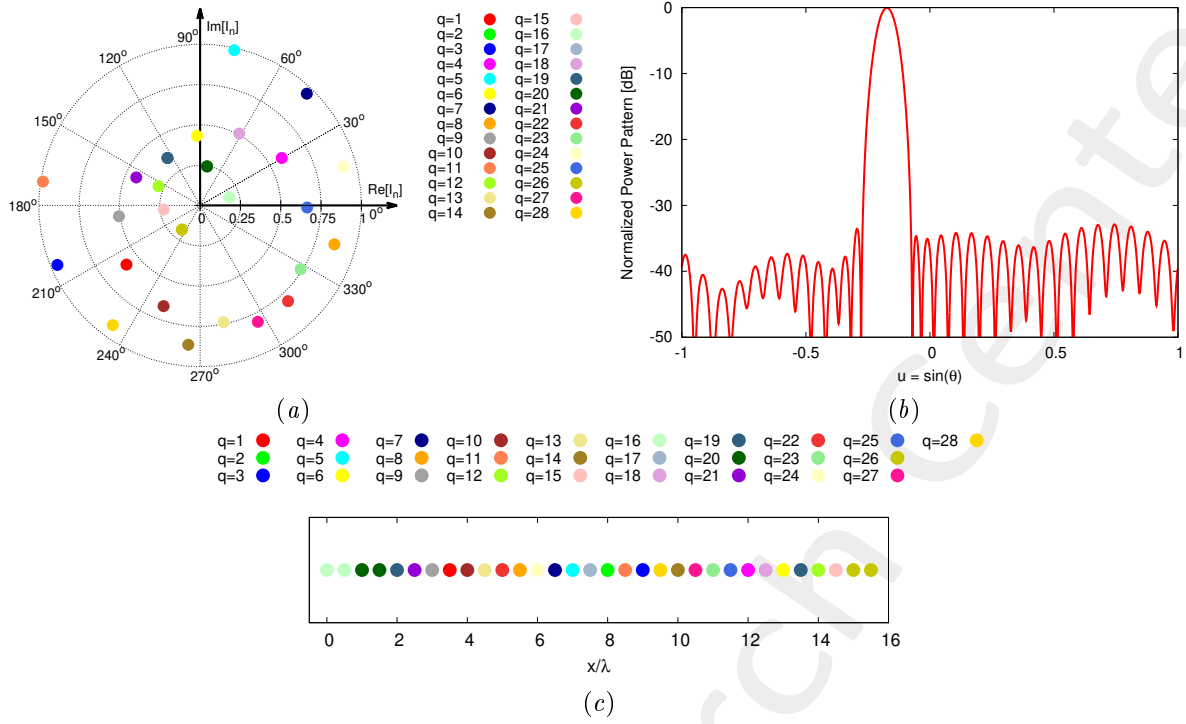
Figure 30: *K-means solution* - (a) Optimized excitations, (b) arising radiation pattern and (c) subarray configuration.

Pattern Features Resume

|	SLL [dB]	$HPBW$ [deg]	$D_{\max}$ [dB]	Δ	Ψ
$Q = 12$	-16.36	4.66	16.52	6.70×10^{-2}	2.84×10^{-2}
$Q = 16$	-20.10	4.52	16.80	3.27×10^{-2}	1.39×10^{-2}
$Q = 20$	-24.95	4.56	16.83	1.48×10^{-2}	6.28×10^{-3}
$Q = 24$	-29.72	4.54	16.88	5.06×10^{-3}	2.14×10^{-3}
$Q = 28$	-34.96	4.52	16.92	9.80×10^{-4}	4.15×10^{-4}
$Q = 32$	-39.97	4.49	16.95	0.00	0.00

Table VI: *K-means solution* - Sidelobe level, SLL, half-power beamwidth, $HPBW$, directivity peak, $D_{\max}$, pattern matching error, Δ, and fitness, Ψ, values.

1.2.6   Comparative Resume

Analysis vs. Q, $\theta_0 = -5$ [deg]

Figure 31: *K-means solutions* - Sidelobe level, SLL, half-power beamwidth, $HPBW$, directivity peak, D_{max}, pattern matching error, Δ, and fitness, Ψ, values as a function of the number of subarrays, Q.

Analysis vs. Q, $\theta_0 = -10$ [deg]

(a)

(b)

(c)

(d)

(e)

Figure 32: *K-means solutions* - Sidelobe level, SLL, half-power beamwidth, $HPBW$, directivity peak, $D_{\max}$, pattern matching error, Δ, and fitness, Ψ, values as a function of the number of subarrays, Q.

(a)

(b)

(c)

(d)

(e)

Figure 33: *K-means solutions* - Sidelobe level, SLL, half-power beamwidth, $HPBW$, directivity peak, D_{max}, pattern matching error, Δ, and fitness, Ψ, values as a function of the number of subarrays, Q.

(a)

(b)

(c)

(d)

(e)

Figure 34: *K-means solutions* - Sidelobe level, SLL, half-power beamwidth, $HPBW$, directivity peak, $D_{\max}$, pattern matching error, Δ, and fitness, Ψ, values as a function of the target sidelobe level, SLL_{ref}.

(a)

(b)

(c)

(d)

(e)

Figure 35: *K-means solutions* - Sidelobe level, SLL, half-power beamwidth, $HPBW$, directivity peak, D_{max}, pattern matching error, Δ, and fitness, Ψ, values as a function of the target sidelobe level, SLL_{ref}.

Analysis vs. SLL_{ref}, $\theta_0 = -15$ **[deg]**

(a)

(b)

(c)

(d)

(e)
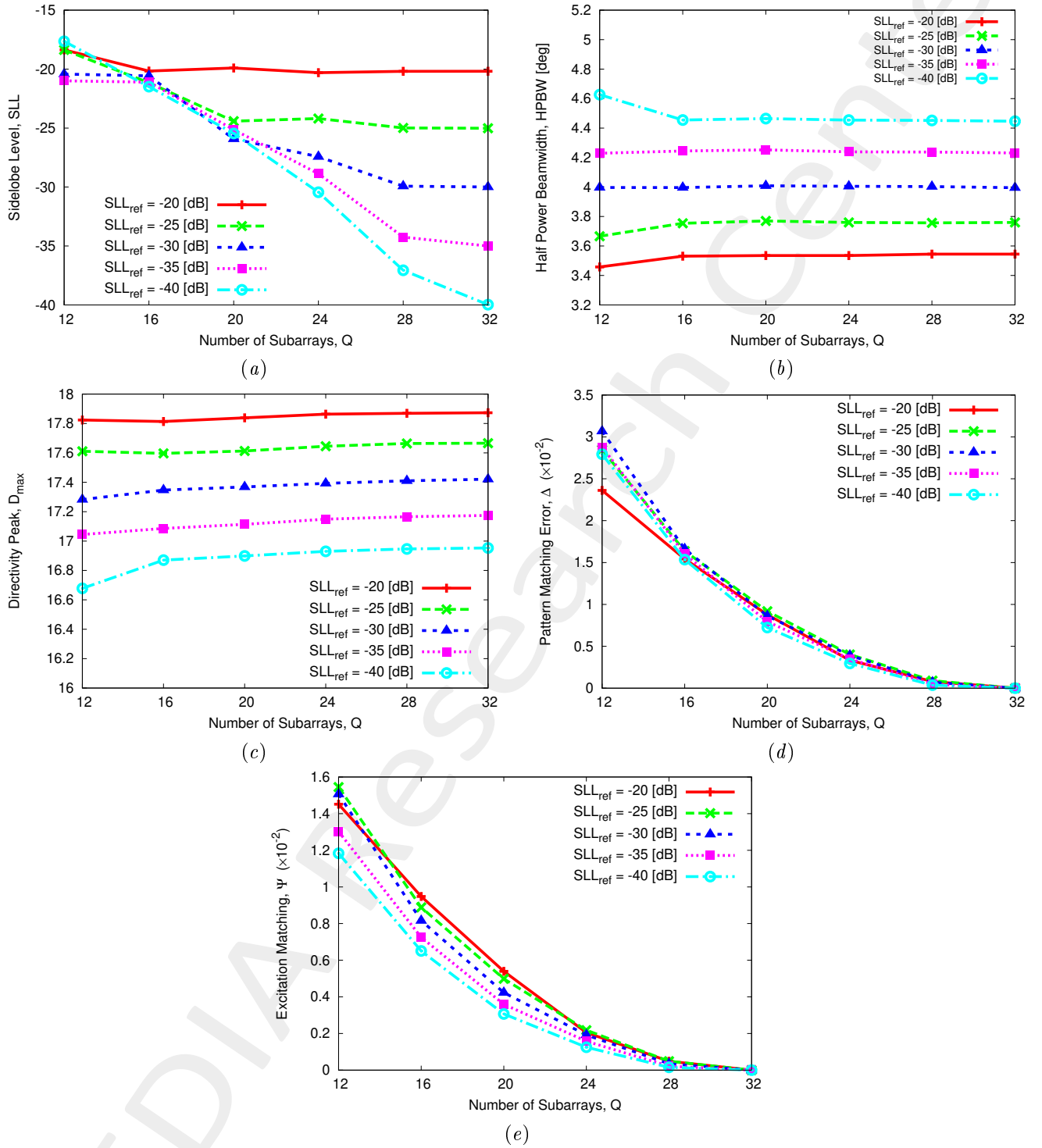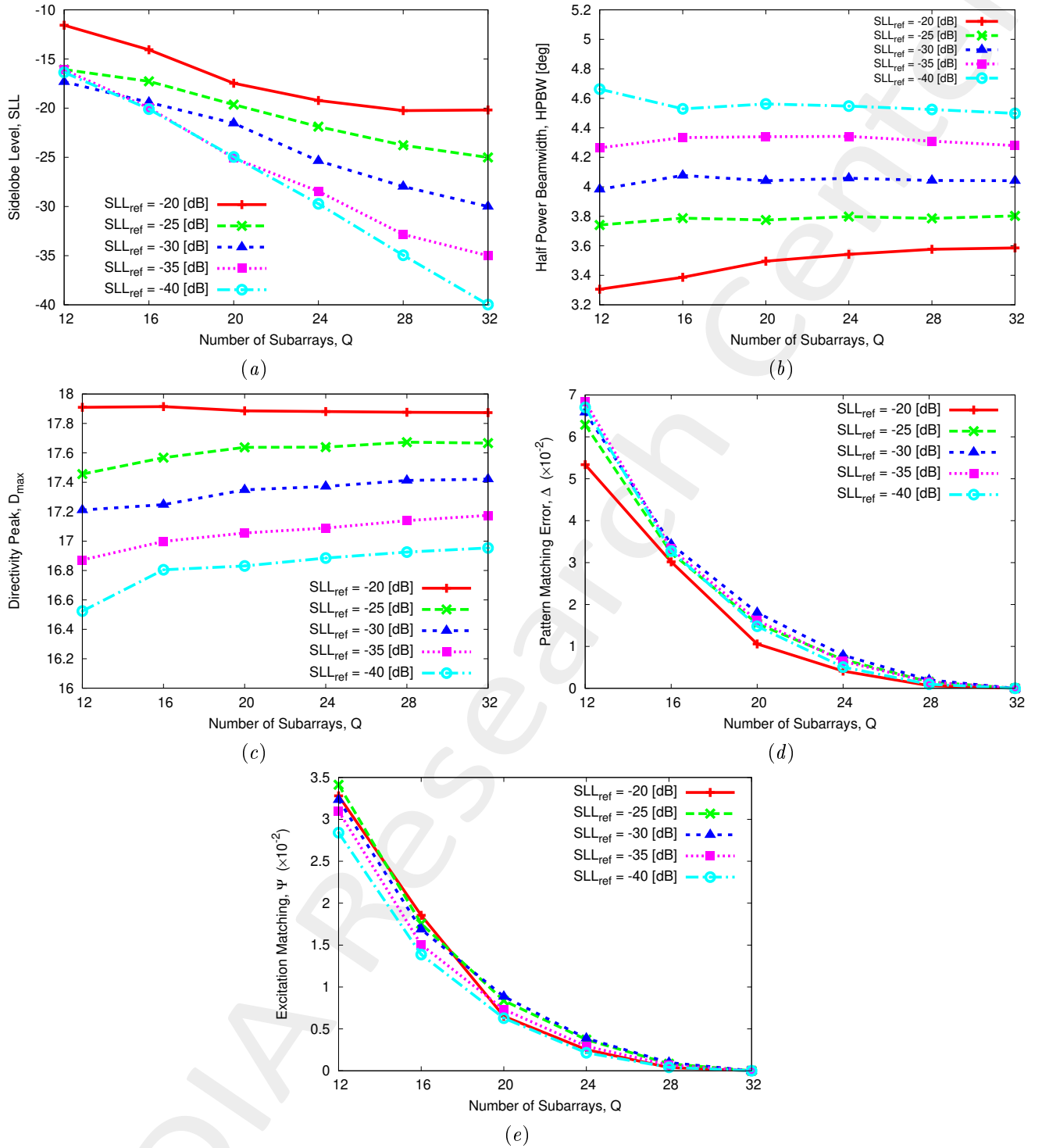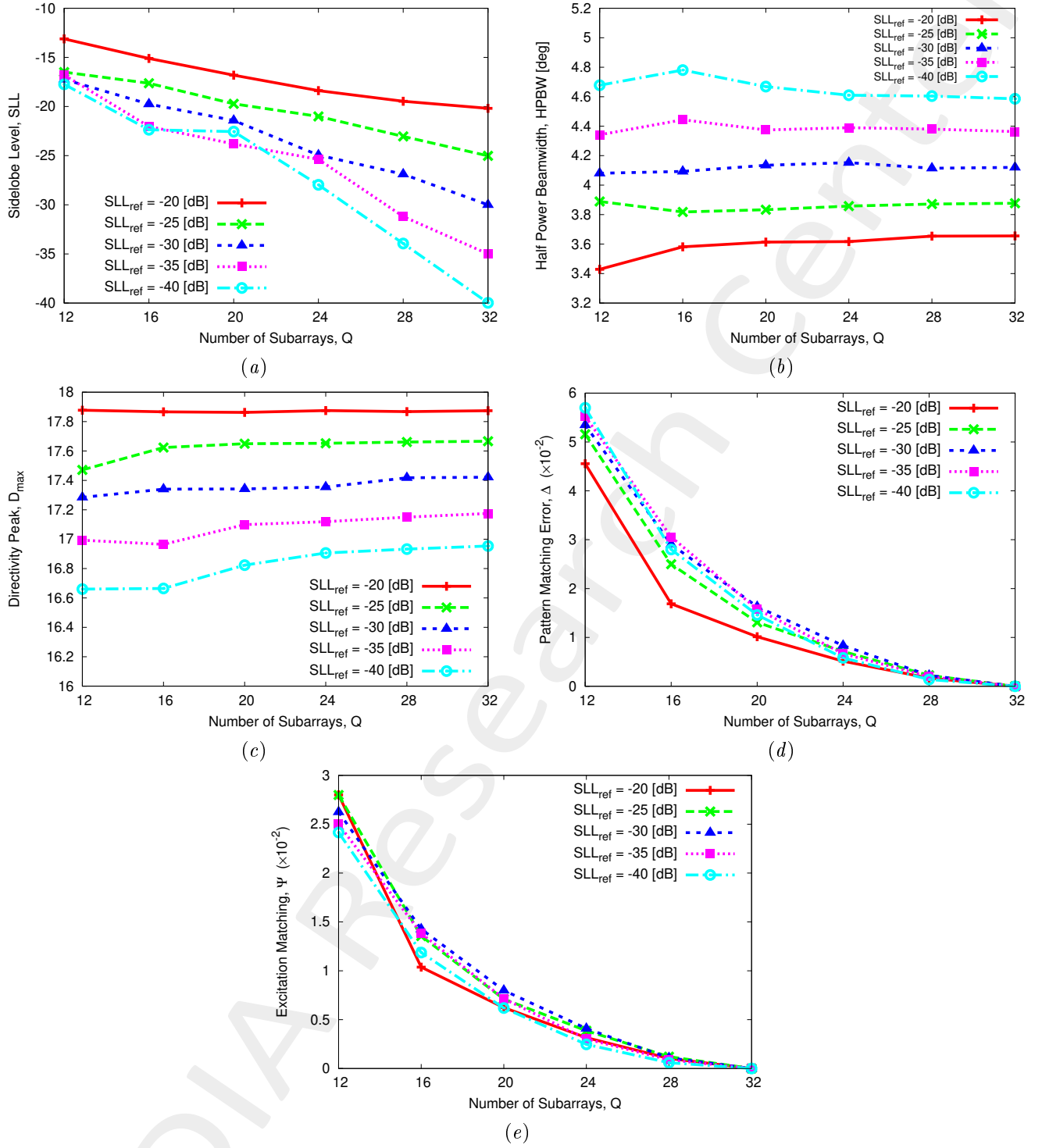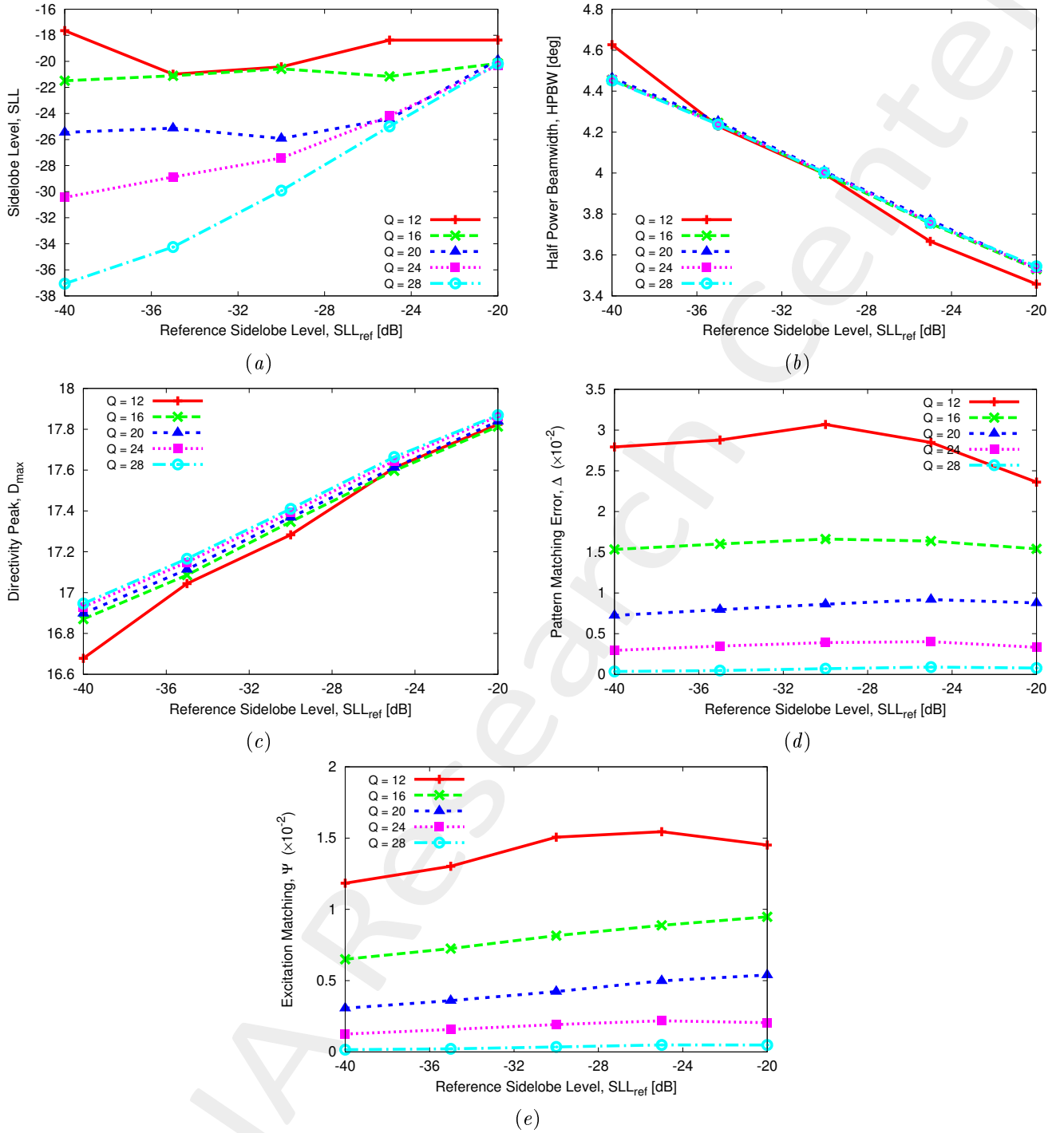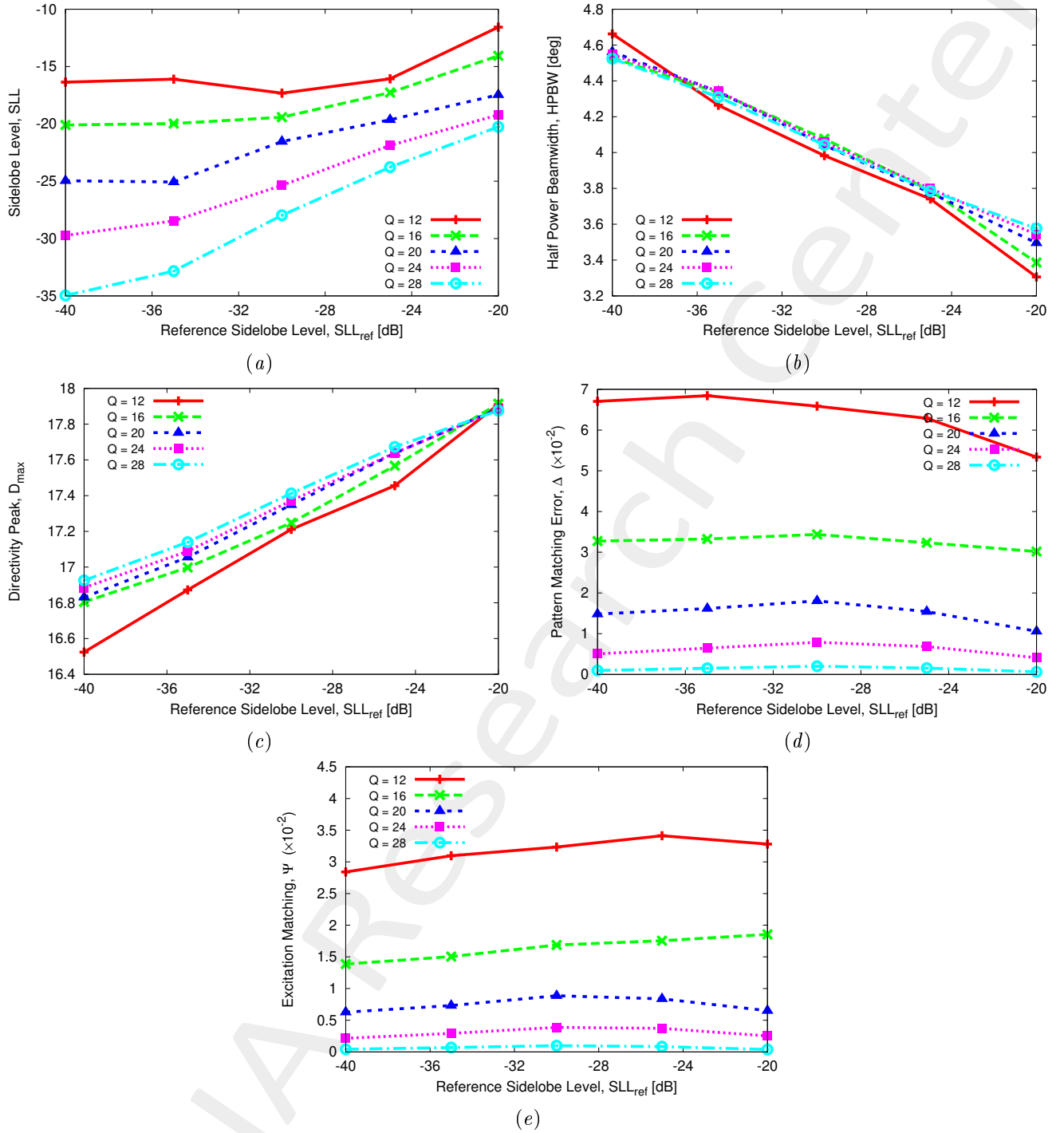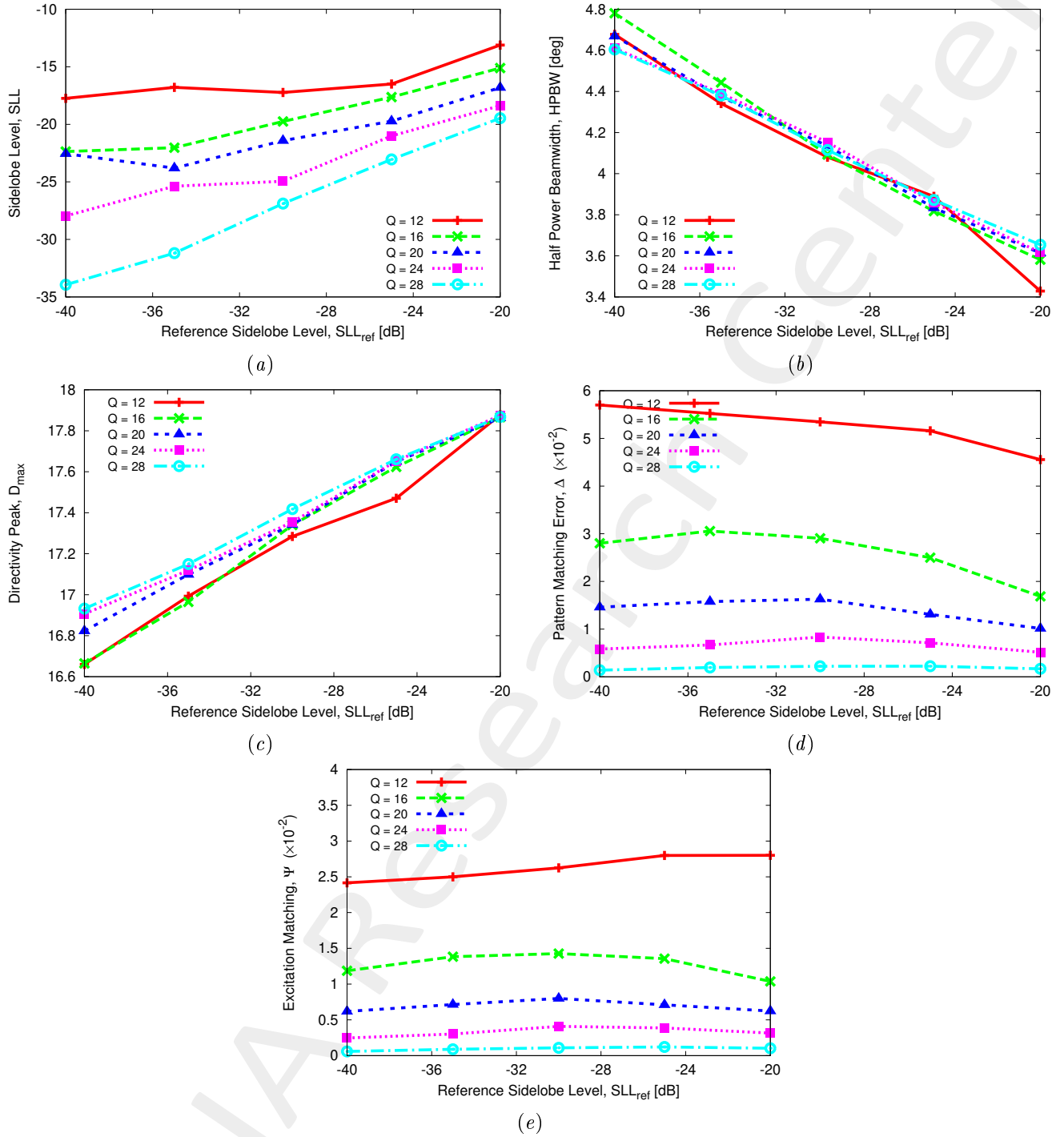
Figure 36: *K-means solutions* - Sidelobe level, SLL, half-power beamwidth, $HPBW$, directivity peak, $D_{\max}$, pattern matching error, Δ, and fitness, Ψ, values as a function of the target sidelobe level, SLL_{ref}.

OUTCOMES:

- As expected, the excitation matching error Ψ and the pattern matching error decreases when the number of subarray Q increases, whatever the sidelobe level of the reference pattern, SLL_{ref};

- Figure $32(a)$ shows that the reduction on the number of subarrays Q has an higher impact on the actual sidelobe level corresponding to the cases with lower SLL_{ref} (e.g., it can be noticed that $\left| \delta SLL \rfloor_{SLL_{ref}=-40dB}^{Q=32 \to 24} \right| = -10.25$ [dB] is higher than $\left| \delta SLL \rfloor_{SLL_{ref}=-20dB}^{Q=32 \to 24} \right| = -0.96$ [dB] when reducing the number of subarrays from $Q = 32$ to $Q = 24$, considering $SLL_{ref} = -40dB$ and $SLL_{ref} = -20dB$, respectively);

- Figure $32(b)$ shows that the half-power beamwidth does not change significantly with Q. For example, considering the case for $SLL_{ref} = -30$ [dB] such pattern feature only changes from $HPBW \rfloor_{Q=32} = 4.04$ [deg] to $HPBW \rfloor_{Q=16} = 4.08$ [deg] when the number of control points is halved (i.e., the number of subarrays decreases from $Q = 32$ to $Q = 16$). Similarly, Fig. $32(c)$ shows that the directivity peak does not change significantly with Q. For example, considering the same case for $SLL_{ref} = -30$ [dB] such pattern feature only changes from $D_{\max} \rfloor_{Q=32} = 17.42$ [dB] to $D_{\max} \rfloor_{Q=16} = 17.25$ [dB] when the number of control points is halved (i.e., the number of subarrays decreases from $Q = 32$ to $Q = 16$);

- Figure $35(c)$ shows that the pattern matching error does not change significantly with SLL_{ref}, especially for $Q > 12$. For example, considering the case for $\theta_0 = -10$ [deg] and with $Q = 16$, the pattern matching error only changes from $\Delta \rfloor_{SLL_{ref}=-20dB} = 3.02 \times 10^{-2}$ to $\Delta \rfloor_{SLL_{ref}=-40dB} = 3.27 \times 10^{-2}$ despite a decrease of 20 [dB] on the reference (i.e., from $SLL_{ref} = -20$ [dB] to $SLL_{ref} = -40$ [dB]). Similarly, the excitation matching error does not change significantly with SLL_{ref}. For example, considering the same case the excitations matching error only changes from $\Psi \rfloor_{SLL_{ref}=-20dB} = 1.86 \times 10^{-2}$ to $\Psi \rfloor_{SLL_{ref}=-40dB} = 1.39 \times 10^{-2}$.

1.3 Taylor Patterns - Analysis varying the Pointing Angle θ_0

OBJECTIVE: In the previous Section the performance of the $K-means$ algorithm have been analyzed keeping a desired beam pointing angle. Under such conditions the changes of sidelobe level of the reference patterns only lead to variations of the excitation amplitude [in the complex plane (see for example Fig. 1), only the distances of the points with respect to the origin are subject to variations while the angles are fixed]. This Section is aimed at studying the performance of the algorithm when changing the beam pointing angle of the patterns and thus the phases of the reference excitations [the angle of the points in the complex plane]. The size of the problem is kept fixed (number of elements: $N = 32$) as well as the tapering on the reference excitations (and accordingly the sidelobe level of the reference pattern).

Array Parameters

- Number of elements: $N = 32$

- Number of subarrays: $Q = 16$

- Inter-element spacing: $d = \lambda/2$

- Taylor excitation amplitudes, $SLL_{ref} = -30$ [dB]

- Pointing angle: $\theta_0 =0, -2, -4, -6, -8, -10, -15, -20$ [deg]

K-means Clustering Method Parameters

- Number of iterations: $I = 100$

- Number of executions: $R = 100$

1.3.1 Taylor Pattern, $N = 32$, $Q = 16$, $SLL_{ref} = -30$ [dB]

$\theta_0 = 0$ [deg] - Target Solution

Figure 37: *Target solution* - (a) target excitations and (b) corresponding radiation pattern.

$\theta_0 = 0$ [deg] - Excitation Matching (EM) K-means Solution

Figure 38: *K-means solution* - (a) Optimized excitations, (b) arising radiation pattern and (c) subarray configuration.

$\theta_0 = -2$ [deg] - Target Solution

(a) (b)

Figure 39: *Target solution* - (a) target excitations and (b) corresponding radiation pattern.

$\theta_0 = -2$ [deg] - Excitation Matching (EM) K-means Solution

(a) (b)

(c)

Figure 40: *K-means solution* - (a) Optimized excitations, (b) arising radiation pattern and (c) subarray configuration.

$\theta_0 = -4$ [deg] - **Target Solution**

(a) $\qquad\qquad\qquad\qquad\qquad\qquad\qquad\qquad$ (b)

Figure 41: *Target solution* - (a) target excitations and (b) corresponding radiation pattern.

$\theta_0 = -4$ [deg] - **Excitation Matching (EM) K-means Solution**

(a) $\qquad\qquad\qquad\qquad\qquad\qquad\qquad\qquad$ (b)

(c)

Figure 42: *K-means solution* - (a) Optimized excitations, (b) arising radiation pattern and (c) subarray configuration.

$\theta_0 = -6$ [deg] - **Target Solution**

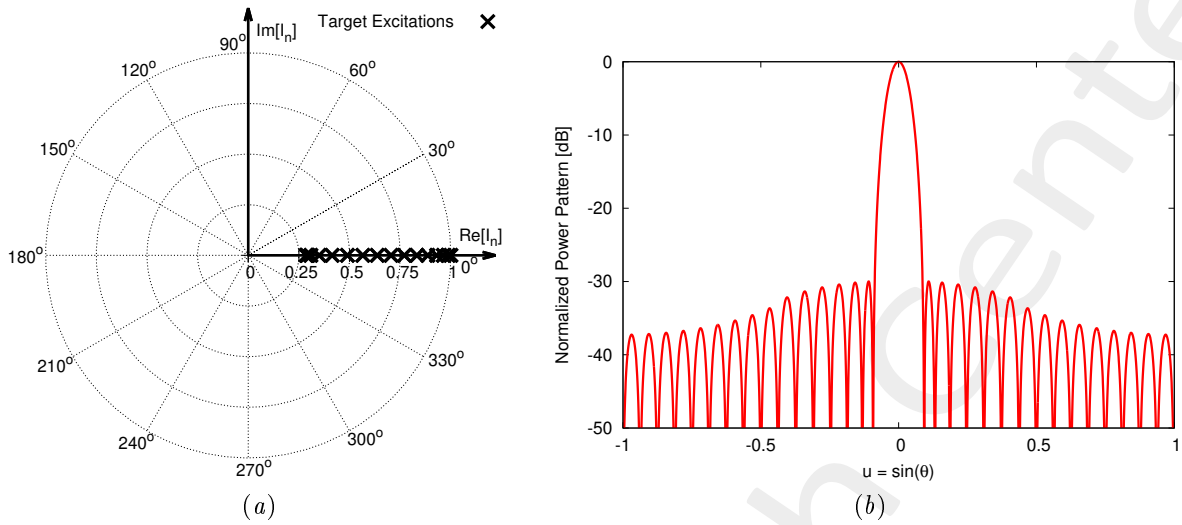
(a) (b)

Figure 43: *Target solution* - (a) target excitations and (b) corresponding radiation pattern.

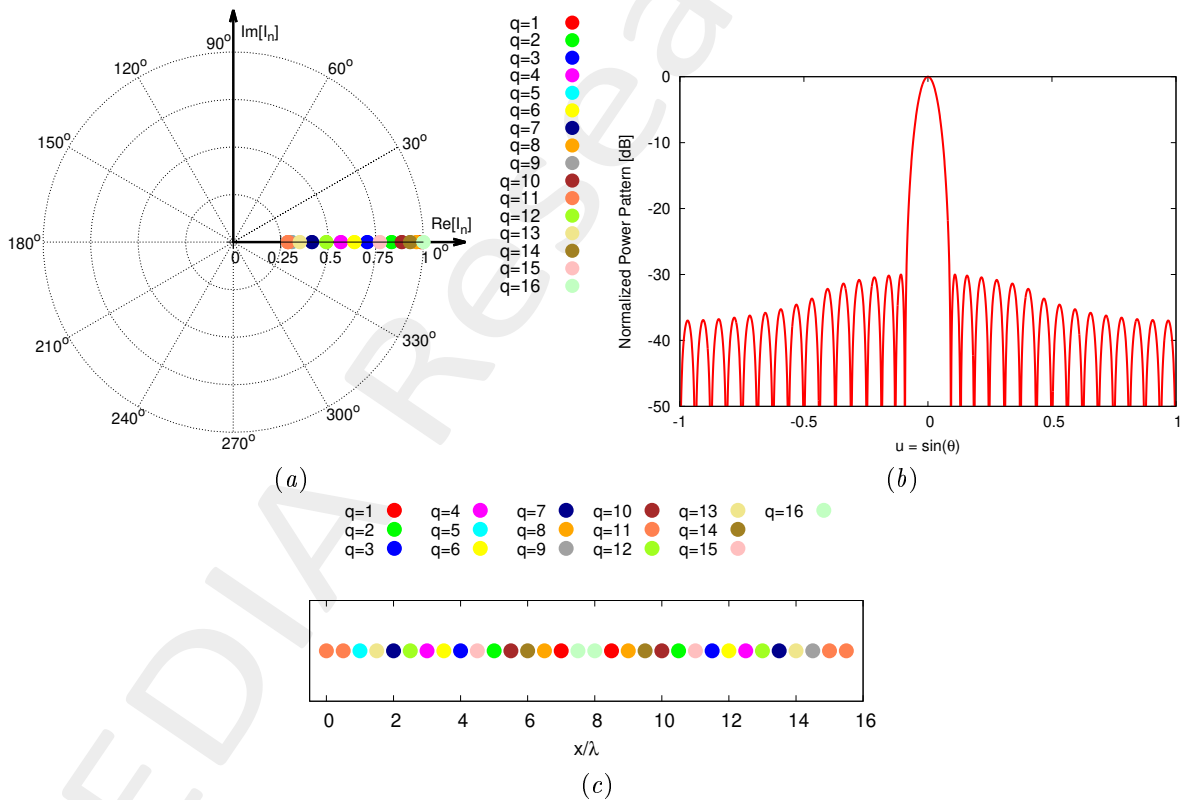$\theta_0 = -6$ [deg] - **Excitation Matching (EM) K-means Solution**

(a) (b)

(c)

Figure 44: *K-means solution* - (a) Optimized excitations, (b) arising radiation pattern and (c) subarray configuration.
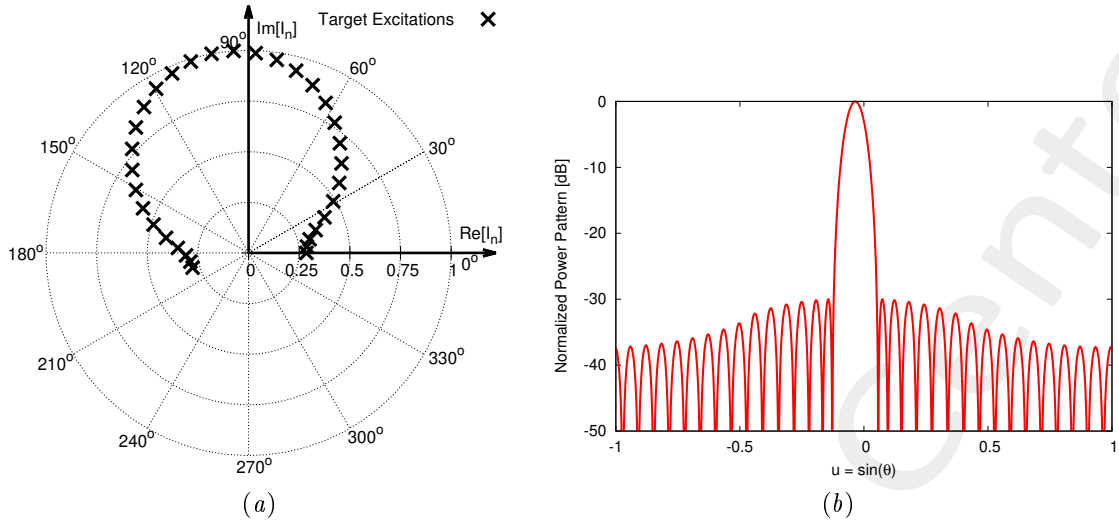
37

$\theta_0 = -8$ [deg] - Target Solution

(a)   (b)

Figure 45: *Target solution* - (a) target excitations and (b) corresponding radiation pattern.

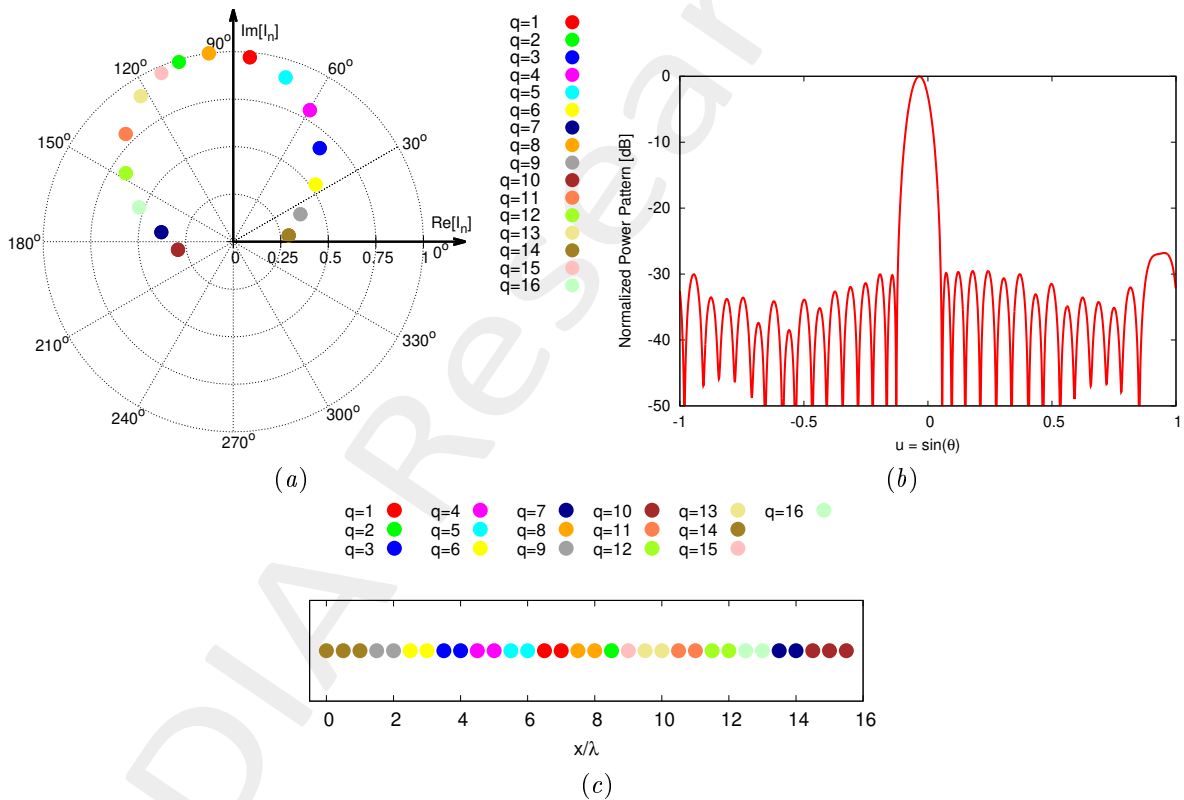$\theta_0 = -8$ [deg] - Excitation Matching (EM) K-means Solution

(a)   (b)

(c)

Figure 46: *K-means solution* - (a) Optimized excitations, (b) arising radiation pattern and (c) subarray configuration.

$\theta_0 = -10$ [deg] - Target Solution

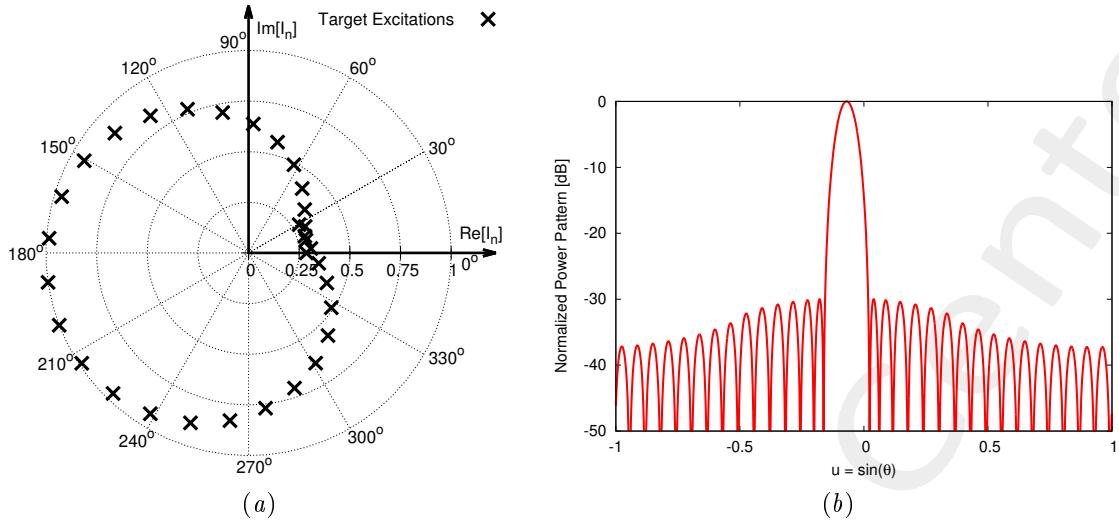(a)   (b)

Figure 47: *Target solution* - (a) target excitations and (b) corresponding radiation pattern.

$\theta_0 = -10$ [deg] - Excitation Matching (EM) K-means Solution

(a)   (b)

(c)

Figure 48: *K-means solution* - (a) Optimized excitations, (b) arising radiation pattern and (c) subarray configuration.

$\theta_0 = -15$ [deg] - Target Solution

(a)   (b)

Figure 49: *Target solution* - (a) target excitations and (b) corresponding radiation pattern.

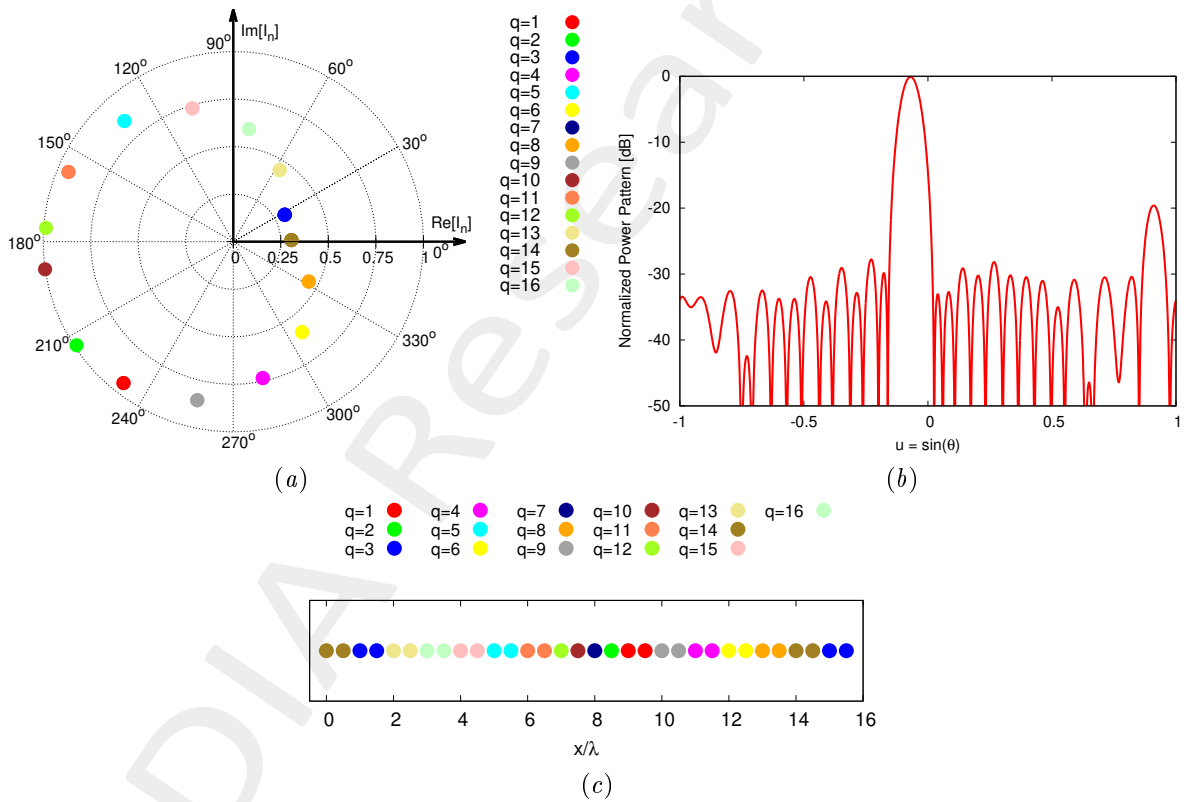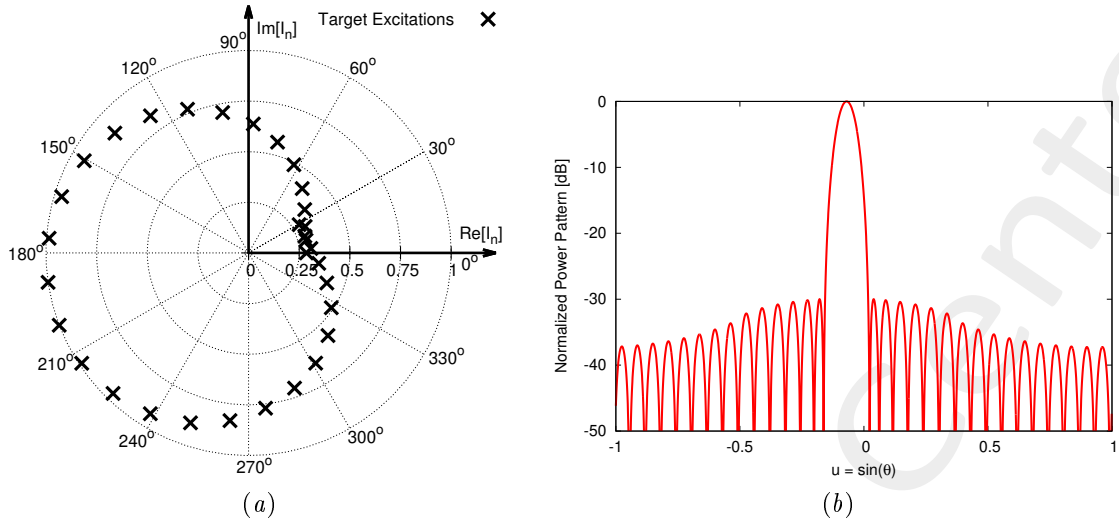**$\theta_0 = -15$ [deg] - Excitation Matching (EM) K-means Solution**

(a)   (b)

(c)
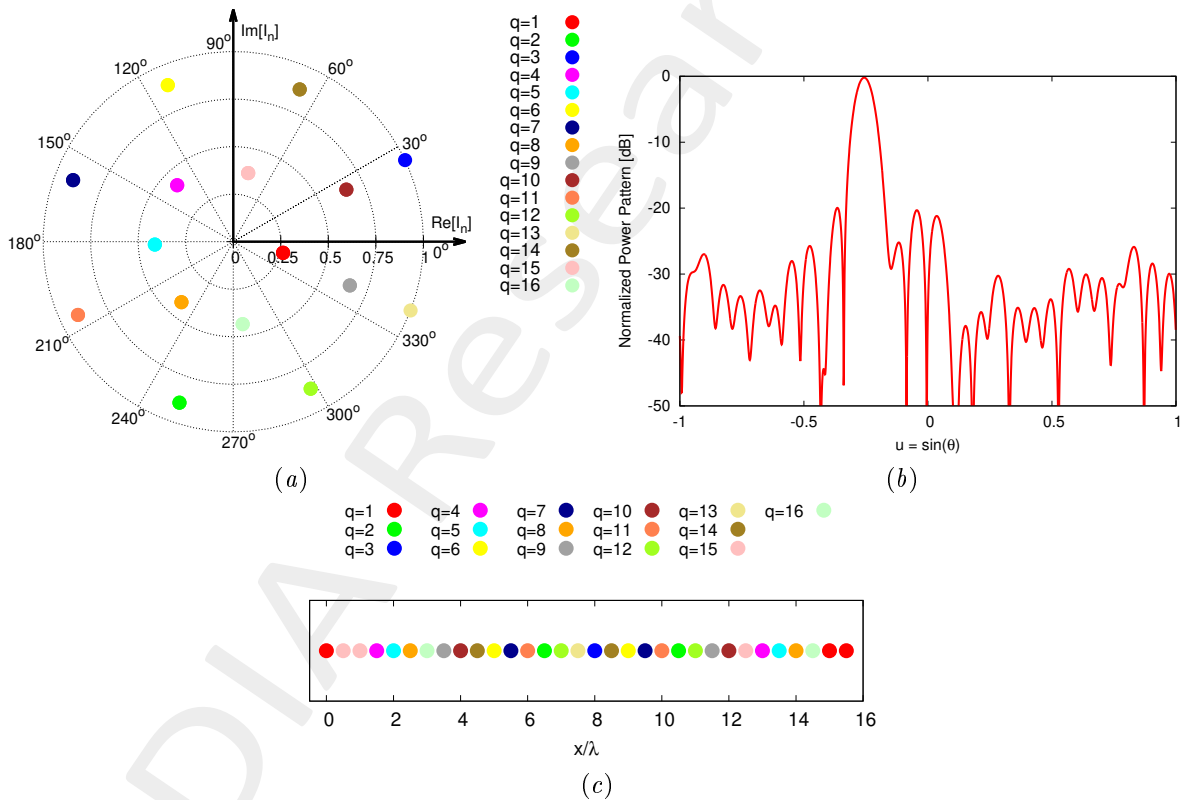
Figure 50: *K-means solution* - (a) Optimized excitations, (b) arising radiation pattern and (c) subarray configuration.

$\theta_0 = -20$ **[deg] - Target Solution**

(a)

(b)
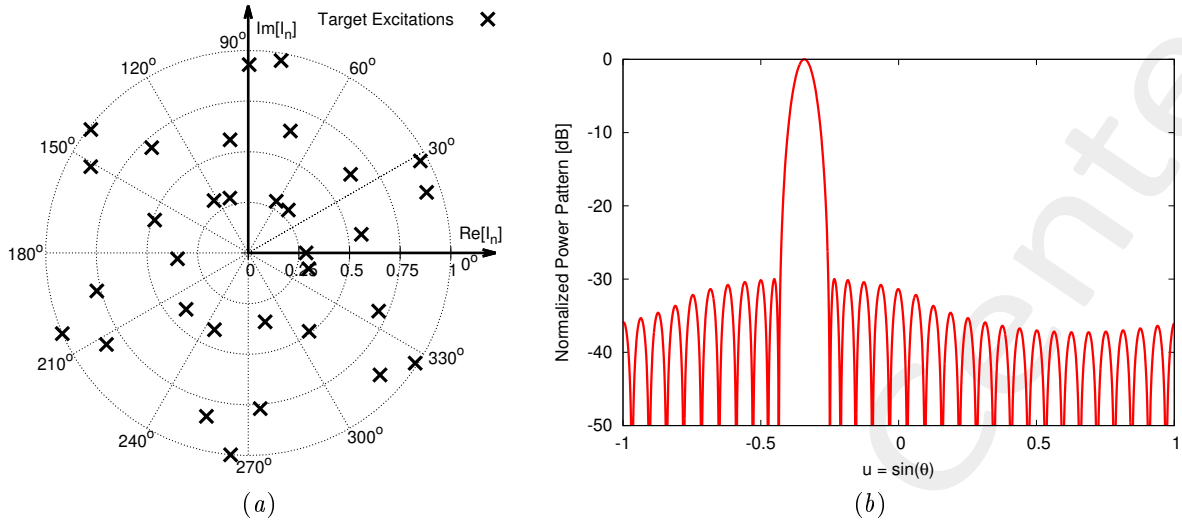
Figure 51: *Target solution* - (a) target excitations and (b) corresponding radiation pattern.

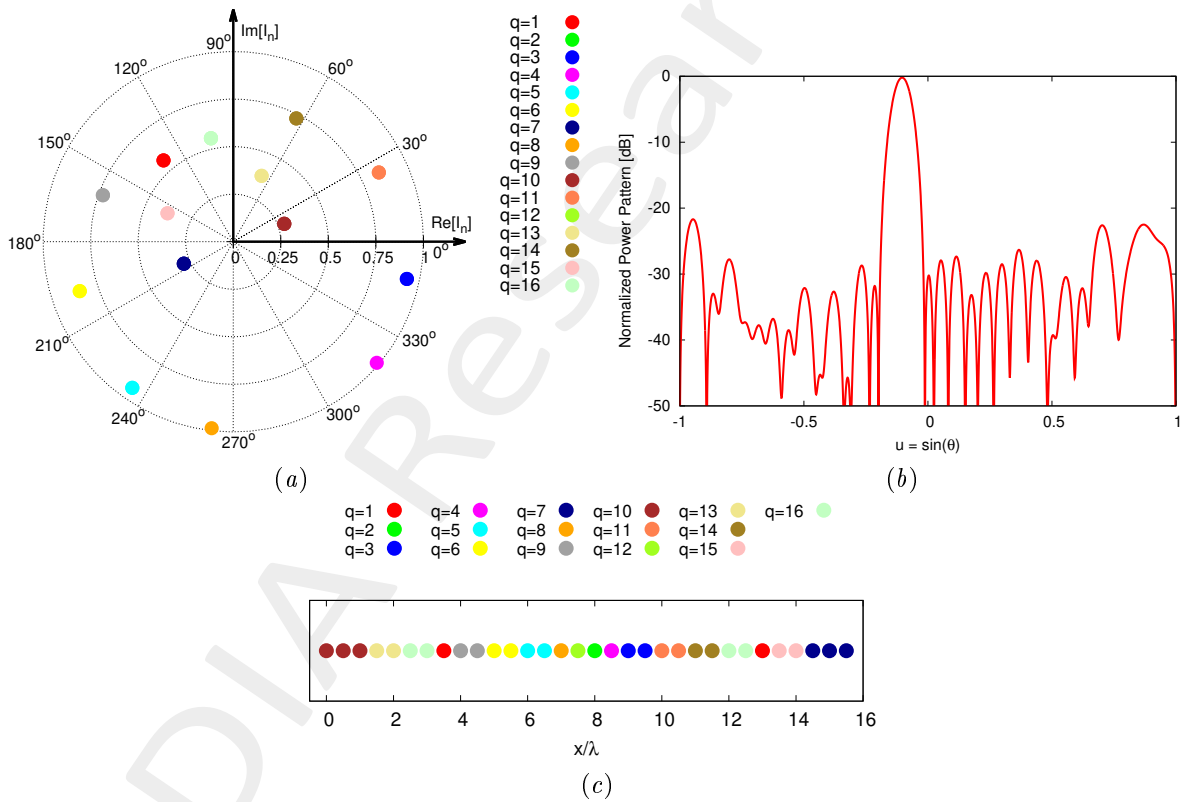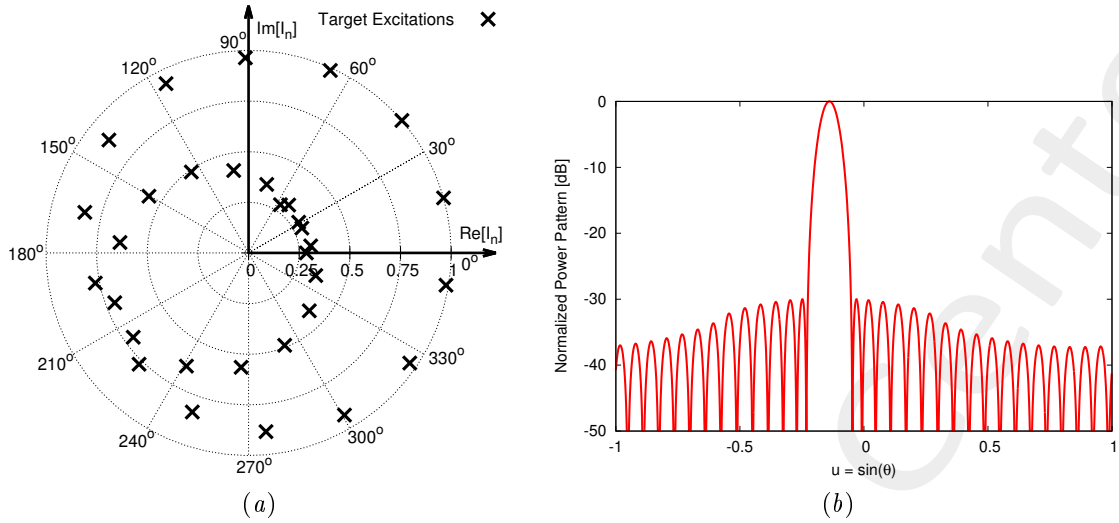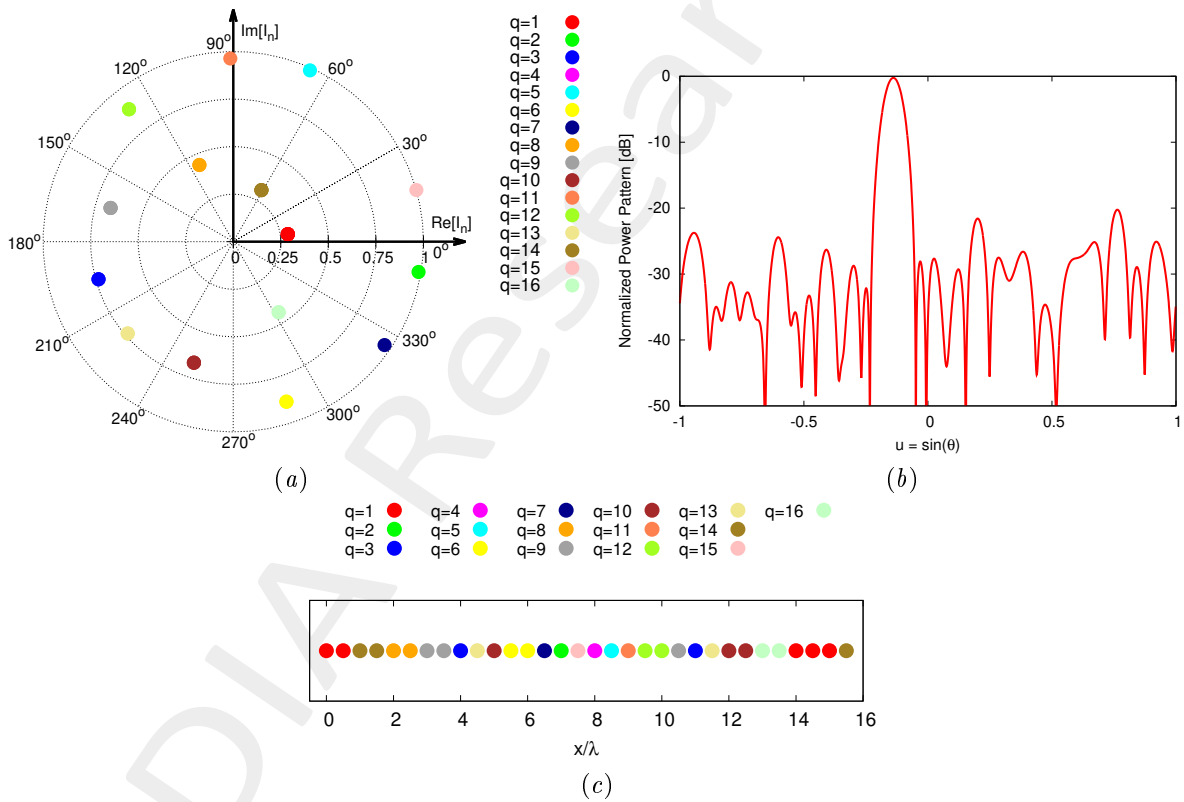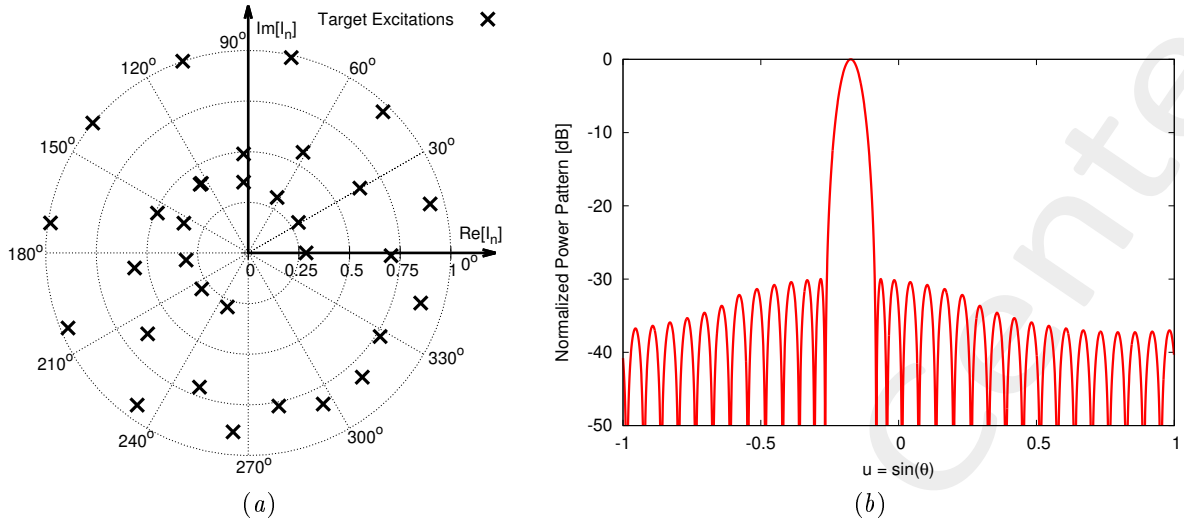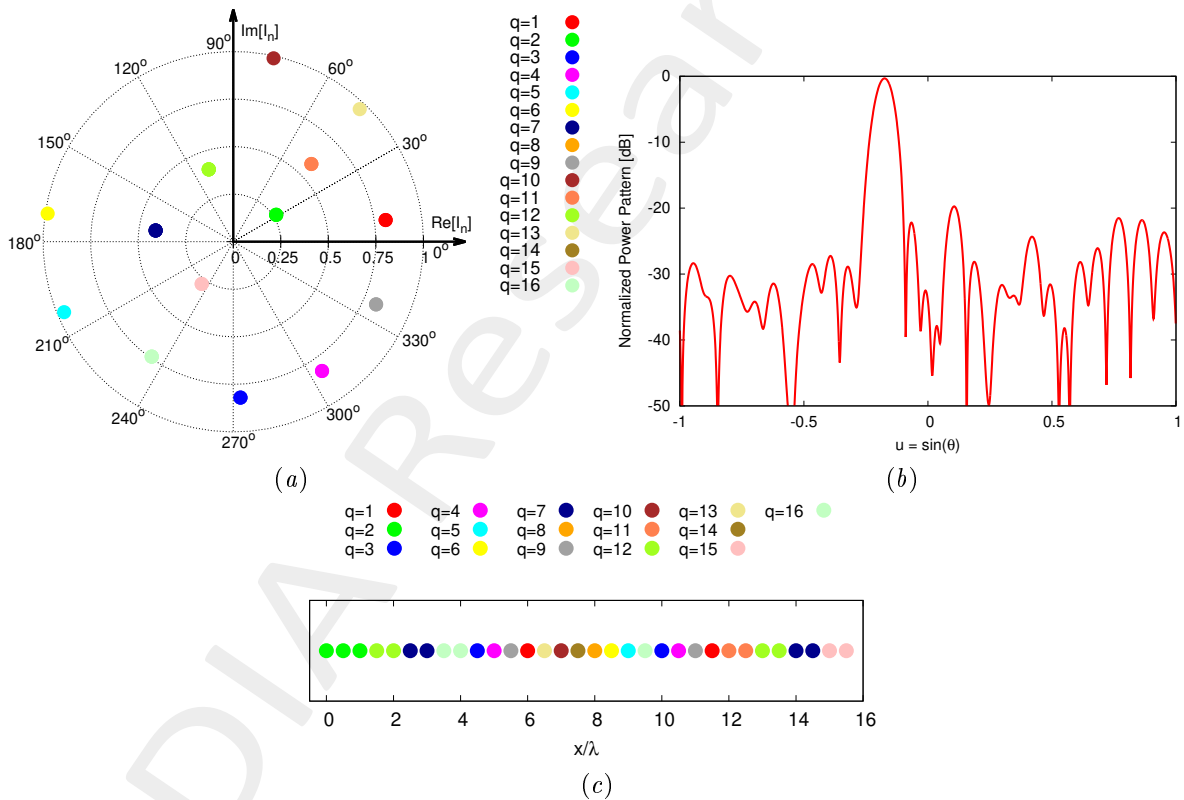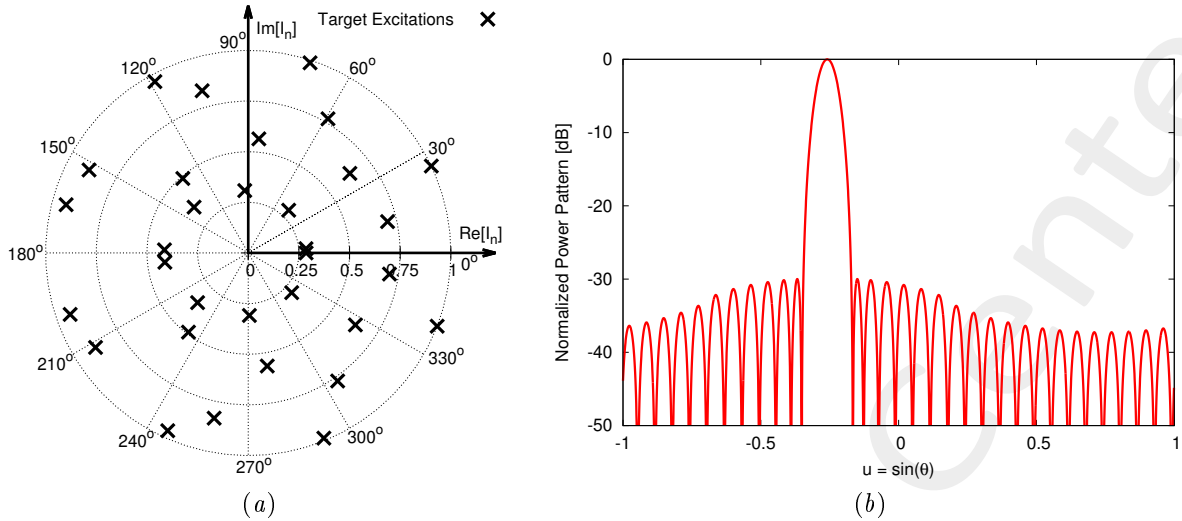$\theta_0 = -20$ **[deg] - Excitation Matching (EM) K-means Solution**

(a)

(b)

(c)
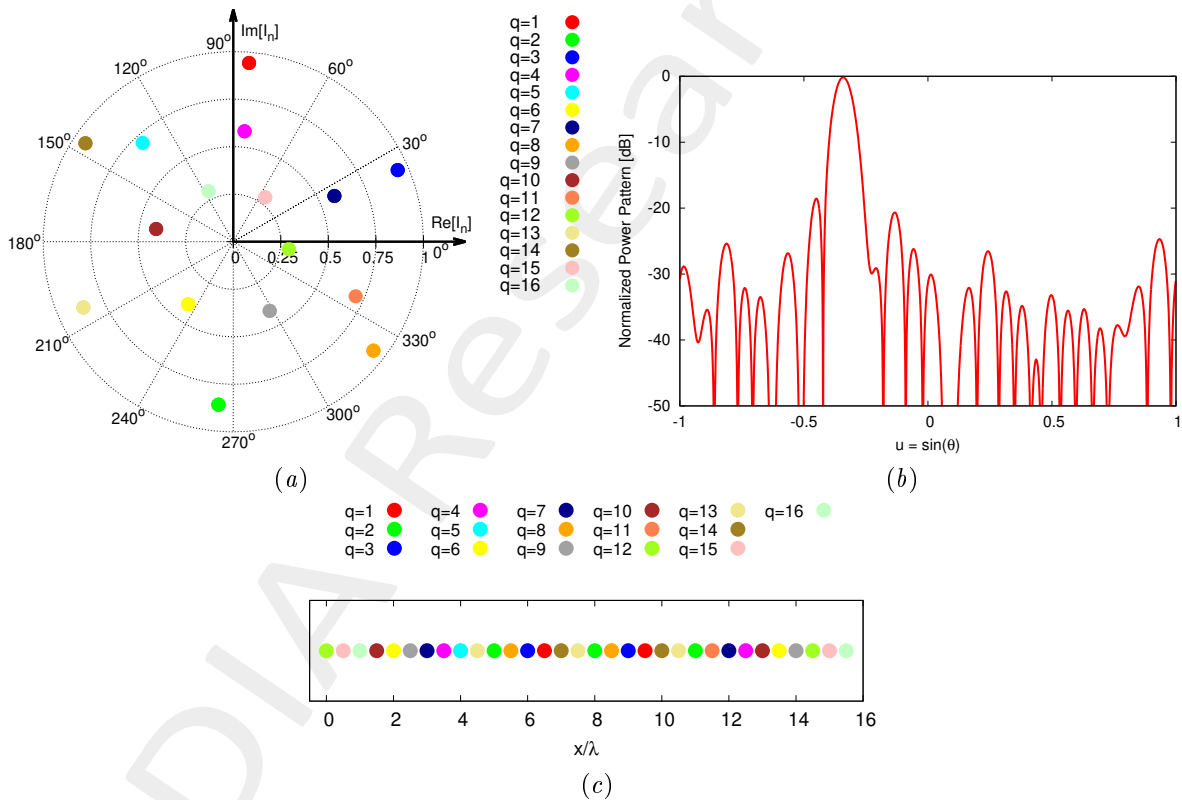
Figure 52: *K-means solution* - (a) Optimized excitations, (b) arising radiation pattern and (c) subarray configuration.

Pattern Features Resume

	SLL [dB]	$HPBW$ [deg]	$D_{\max}$ [dB]	Δ	Ψ
$\theta_0 = 0$ [deg]	-30.20	3.98	17.42	0.0	0.0
$\theta_0 = -2$ [deg]	-28.29	3.96	17.40	4.14×10^{-3}	2.03×10^{-3}
$\theta_0 = -4$ [deg]	-25.01	3.97	17.38	1.08×10^{-2}	5.28×10^{-3}
$\theta_0 = -6$ [deg]	-23.52	3.98	17.32	2.26×10^{-2}	1.11×10^{-2}
$\theta_0 = -8$ [deg]	-22.98	3.96	17.33	2.77×10^{-2}	1.36×10^{-2}
$\theta_0 = -10$ [deg]	-21.42	3.95	17.31	3.44×10^{-2}	1.69×10^{-2}
$\theta_0 = -15$ [deg]	-22.58	4.01	17.38	2.91×10^{-2}	1.43×10^{-2}
$\theta_0 = -20$ [deg]	-20.53	4.07	17.43	2.24×10^{-2}	1.10×10^{-2}

Table VII: *K-means solution* - Sidelobe level, SLL, half-power beamwidth, $HPBW$, directivity peak, $D_{\max}$, pattern matching error, Δ, and fitness, Ψ, values.

1.3.2 Comparative Resume

Analysis vs. Q

(a)

(b)

(c)

(d)

(e)

Figure 53: *K-means solutions* - Sidelobe level, SLL, half-power beamwidth, $HPBW$, directivity peak, $D_{\max}$, pattern matching error, Δ, and fitness, Ψ, values as a function of the number of subarrays, Q.

Analysis vs. θ_0

(*a*)

(*b*)

(*c*)

(*d*)

(*e*)

Figure 54: *K-means solutions* - Sidelobe level, SLL, half-power beamwidth, $HPBW$, directivity peak, $D_{\max}$, pattern matching error, Δ, and fitness, Ψ, values as a function of the number of subarrays, Q.
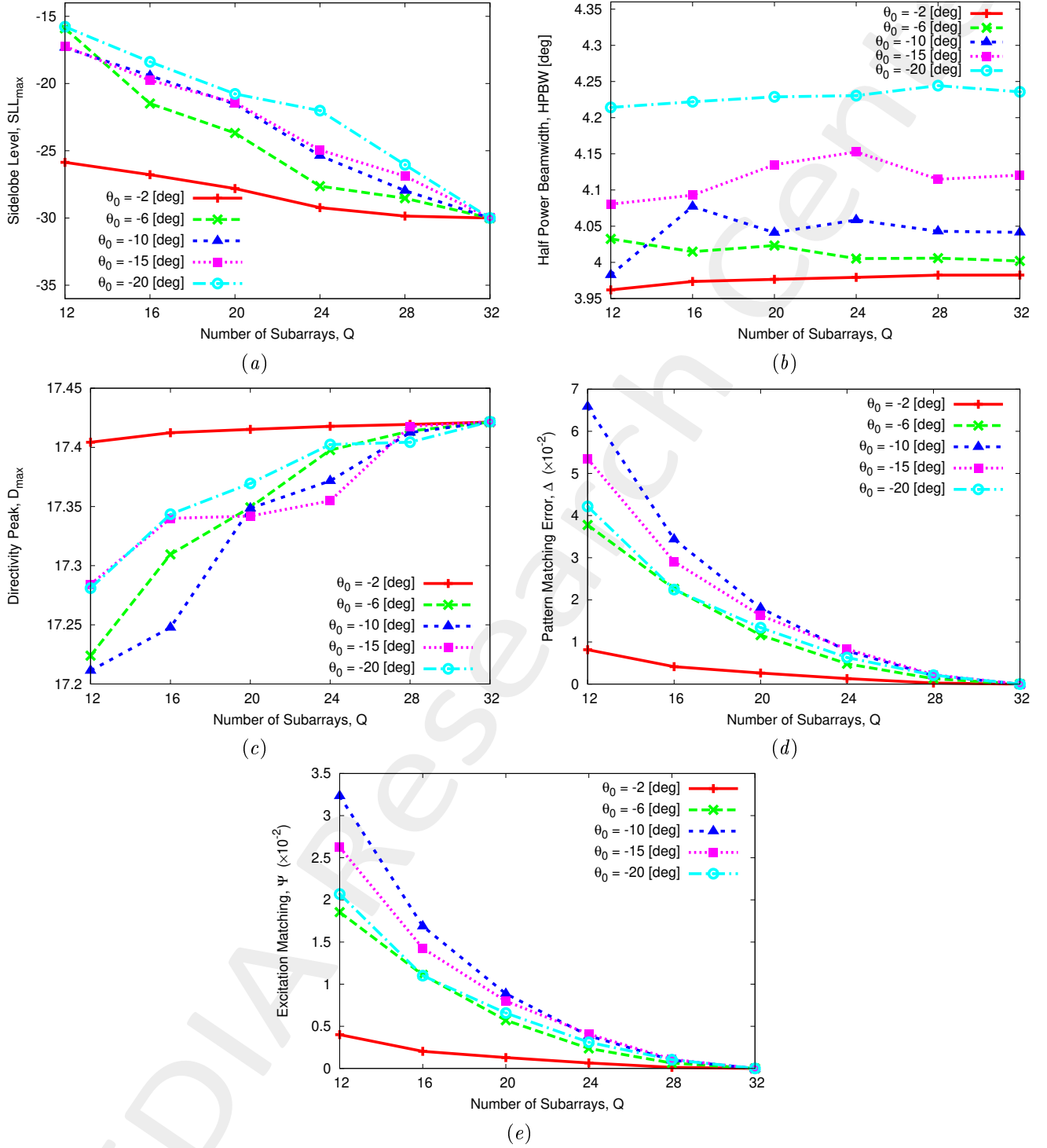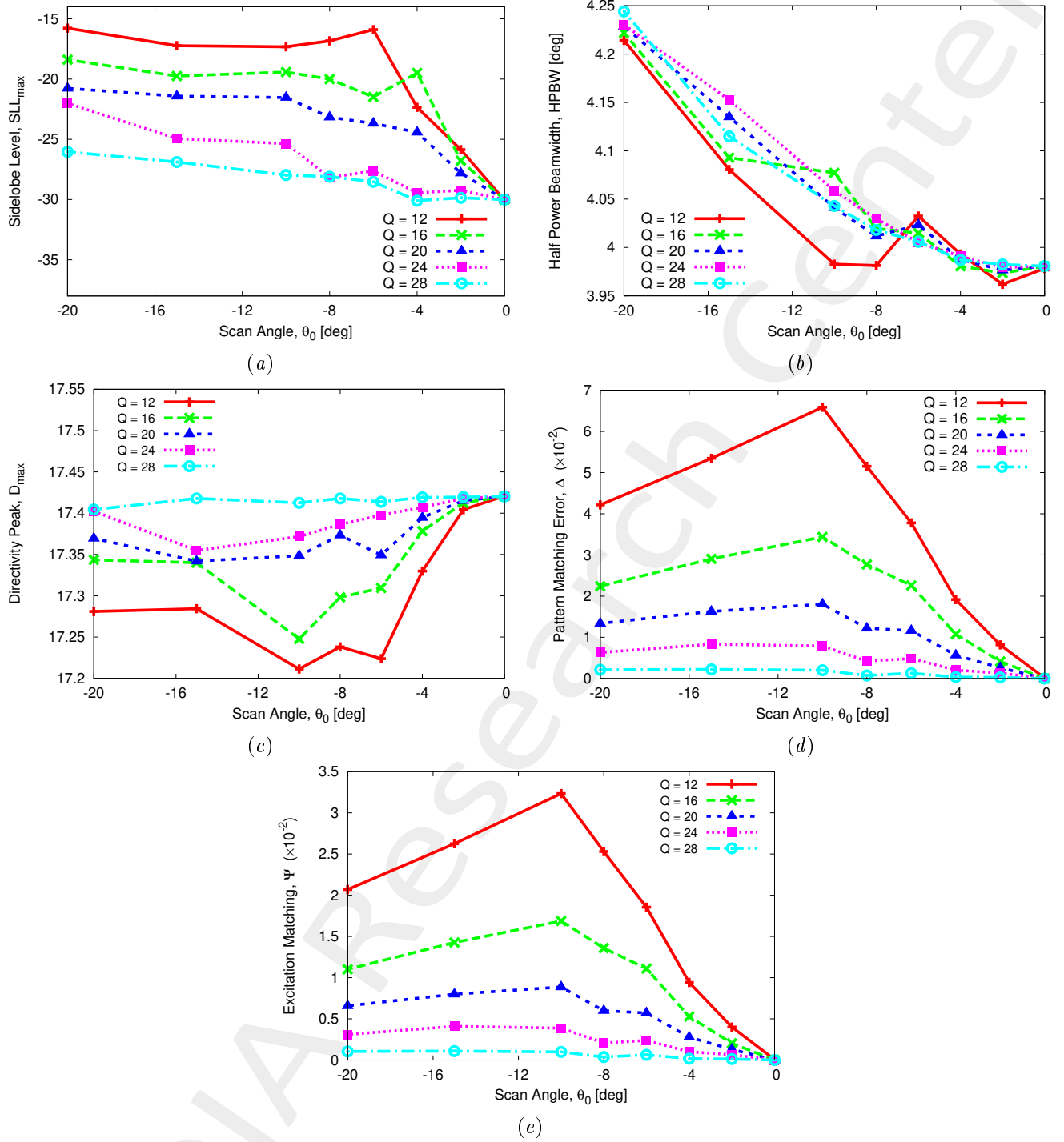
OUTCOMES:

- As expected, the excitation matching error Ψ and the pattern matching error decreases when the number of subarray Q increases, whatever the fixed pointing angle θ_0;

- Figure $53(a)$ shows that the reduction on the number of subarrays Q has an higher impact on the actual sidelobe level corresponding to the cases with higher $|\theta_0|$ (e.g., it can be noticed that $\left| \delta SLL \rfloor_{\theta_0=-20deg}^{Q=32\to24} = \right| = 7.99$ [dB] is higher than $\left| \delta SLL \rfloor_{\theta_0=-2deg}^{Q=32\to24} = \right| = 0.77$ [dB] when reducing the number of subarrays from $Q=32$ to $Q=24$, considering $\theta_0 = -20deg$ and $\theta_0 = -2deg$, respectively);

- Figure $53(b)$ shows that the half-power beamwidth does not change significantly with Q, whatever the pointing angle θ_0. For example, considering the cases with $\theta_0 = -2$ [deg] $\theta_0 = -20$ [deg], such pattern feature only changes from $HPBW\rfloor_{Q=32}^{\theta_0=-2deg} = 3.98$ [deg] to $HPBW\rfloor_{Q=16}^{\theta_0=-2deg} = 3.97$ [deg] and from $HPBW\rfloor_{Q=32}^{\theta_0=-20deg} = 4.23$ [deg] to $HPBW\rfloor_{Q=16}^{\theta_0=-20deg} = 4.22$ [deg], respectively, when the number of control points is halved (i.e., the number of subarrays decreases from $Q=32$ to $Q=16$). Similarly, the directivity peak does not change significantly with Q, whatever the pointing angle θ_0. For example, considering the cases with $\theta_0 = -2$ [deg] $\theta_0 = -20$ [deg], such pattern feature only changes from $D_{\max}\rfloor_{Q=32}^{\theta_0=-2deg} = 17.42$ [dB] to $D_{\max}\rfloor_{Q=16}^{\theta_0=-2deg} = 17.41$ [dB] and from $D_{\max}\rfloor_{Q=32}^{\theta_0=-20deg} = 17.42$ [dB] to $D_{\max}\rfloor_{Q=16}^{\theta_0=-20deg} = 17.34$ [dB], respectively, when the number of control points is halved;

- Figures $53(b)$ shows that the excitation matching error almost linearly increases until $\theta_0 = -10$ [deg] and than it starts to decreases. Such behavior seems strange, but such figure of merit essentially depends on the "sparsification" of the excitations in the complex plane (see for example Figs. $47(a)$ and $51(a)$, corresponding to the cases with the case with $\theta_0 = -10$ [deg] and with $\theta_0 = -20$ [deg], respectively for a qualitative comparison. The **average minimum distance** between two excitations may be a useful index for a quantitative comparison.

1.4 Taylor Patterns - Analysis varying N

OBJECTIVE: In the previous Sections, the size of the problem has been kept fixed. This Section is aimed at studying the performance of the $K-means$ algorithm when changing the array size. A fixed ratio between number of subarrays and total number of elements is considered, in order to deal with the same percentage reduction of the control points. The beam pointing angle as well as the sidelobe level of the reference pattern have been kept fixed.

Array Parameters

- Number of elements: $N = 16, 32, 48, 64$

- Number of subarrays: $Q = N/2$

- Inter-element spacing: $d = \lambda/2$

- Taylor excitation amplitudes, $SLL_{ref} = -30$ [dB]

- Pointing angle: $\theta_0 = -10$ [deg]

K-means Clustering Method Parameters

- Number of iterations: $I = 100$

- Number of executions: $R = 100$

1.4.1 Taylor Pattern, $SLL_{ref} = -30$ [dB], $\theta_0 = -10$ [deg]: $N = 16,\ 48,\ 64$ - $Q = N/2$

$N = 16$ - Target Solution

(a) (b)

Figure 55: *Target solution* - (a) target excitations and (b) corresponding radiation pattern.

$N = 16$ - Excitation Matching (EM) K-means Solution

(a) (b)

(c)

Figure 56: *K-means solution* - (a) Optimized excitations, (b) arising radiation pattern and (c) subarray configuration.

$N = 48$ - **Target Solution**

(a)   (b)

Figure 57: *Target solution* - (a) target excitations and (b) corresponding radiation pattern.

$N = 48$ - **Excitation Matching (EM) K-means Solution**

(a)   (b)

(c)

Figure 58: *K-means solution* - (a) Optimized excitations, (b) arising radiation pattern and (c) subarray configuration.
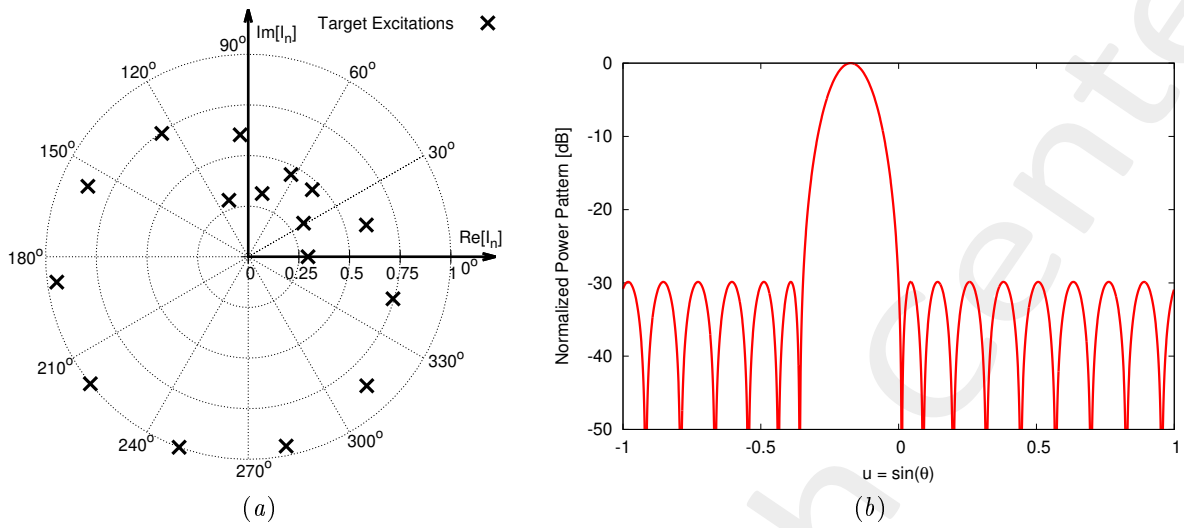
$N = 64$ - **Target Solution**

Figure 59: *Target solution* - (a) target excitations and (b) corresponding radiation pattern.

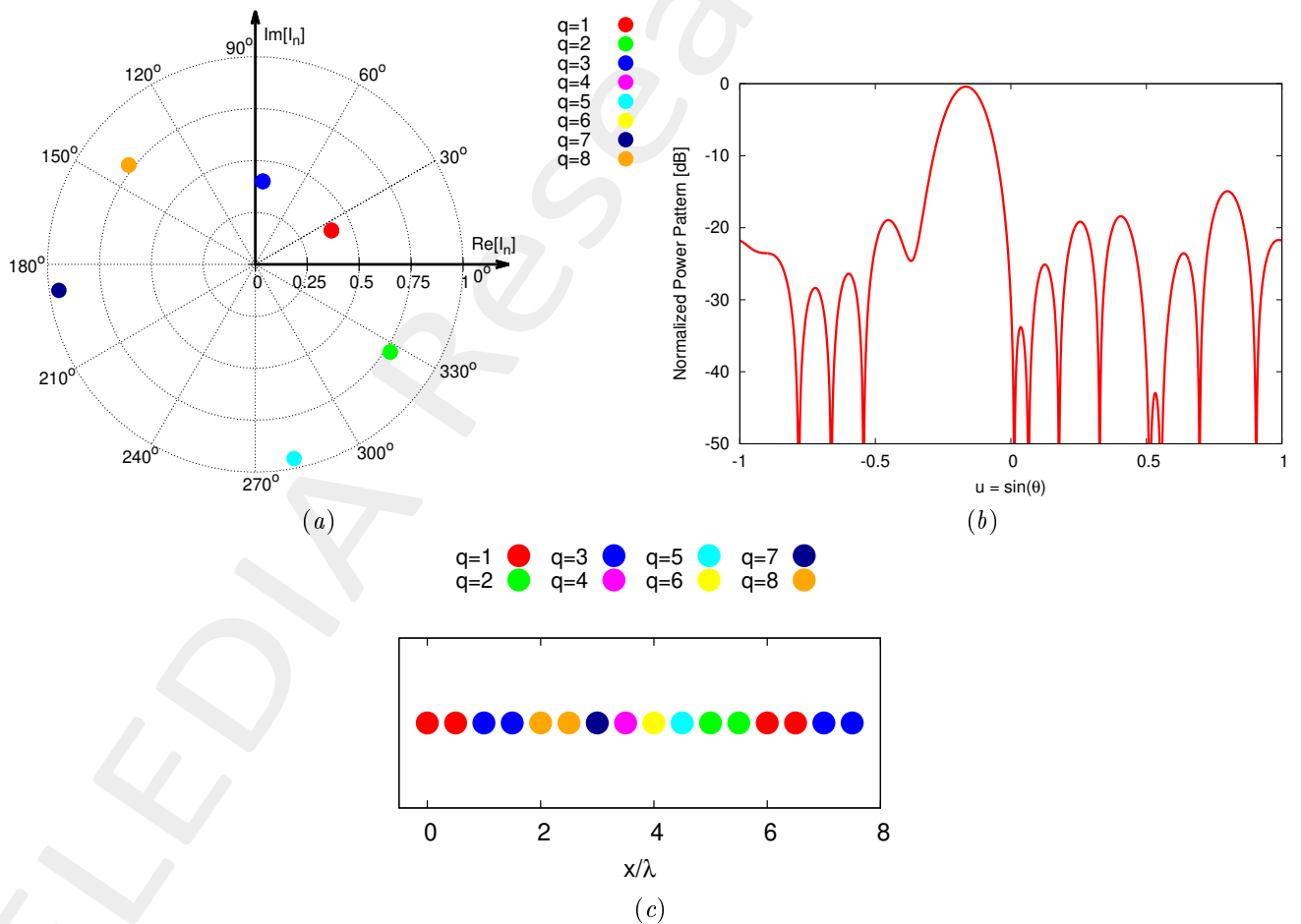## $N = 64$ - **Excitation Matching (EM) K-means Solution**

Figure 60: *K-means solution* - (a) Optimized excitations, (b) arising radiation pattern and (c) subarray configuration.

OUTCOMES:

- The pattern matching error and the excitation matching error generally decrease when the number of elements increases, assuming to keep a fixed ratio $Q/N = 0.5$.

49

1.5 Cosecant-Squared Pattern - Analysis varying Q

OBJECTIVE: In the previous Sections, the performance of the $K-means$ algorithm have been investigated only considering Taylor patterns as reference ones. This Section deals with a different kind pattern (more precisely a cosecant-squared pattern), selected from the published literature. An analysis varying the number of subarrays will be carried out, keeping a fixed beam pointing angle as well as the array size.

Array Parameters

- Number of elements: $N = 17$

- Number of subarrays: $Q = 6, 8, 9, 11, 15$

- Inter-element spacing: $d = \lambda/2$

- Cosecant-squared pattern, $SLL_{ref} \simeq -30$ [dB]

- Pointing angle: $\theta_0 = 0$ [deg]

K-means Clustering Method Parameters

- Number of iterations: $I = 100$

- Number of executions: $R = 100$

1.5.1 Cosecant-Squared Pattern, $N = 17$, $SLL_{ref} \simeq -30$ [dB], $\theta_0 = 0$ [deg]: $Q = 6$, 8, 9, 11, 15
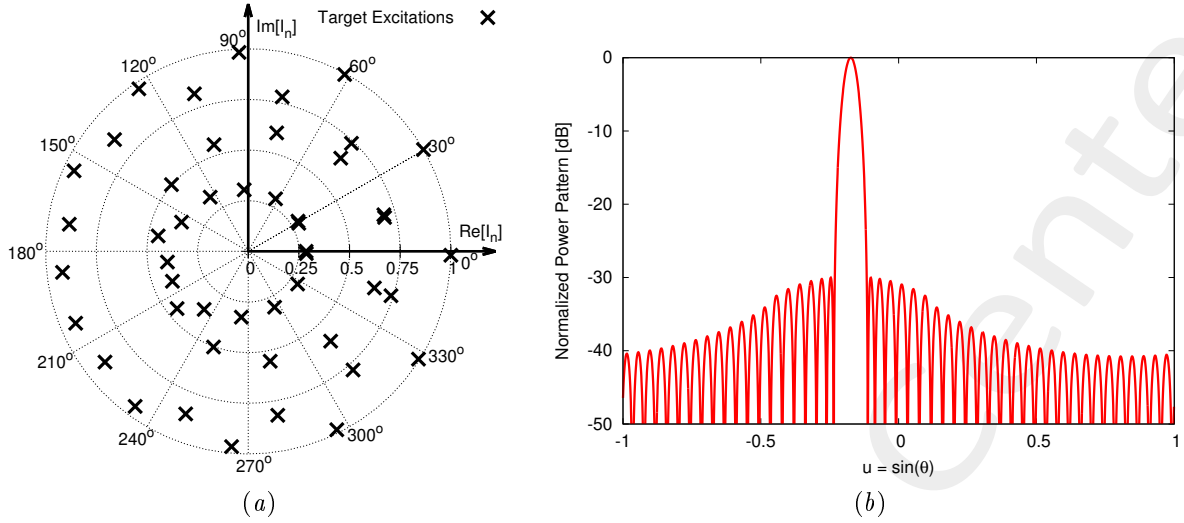
Target Solution

(a)

(b)
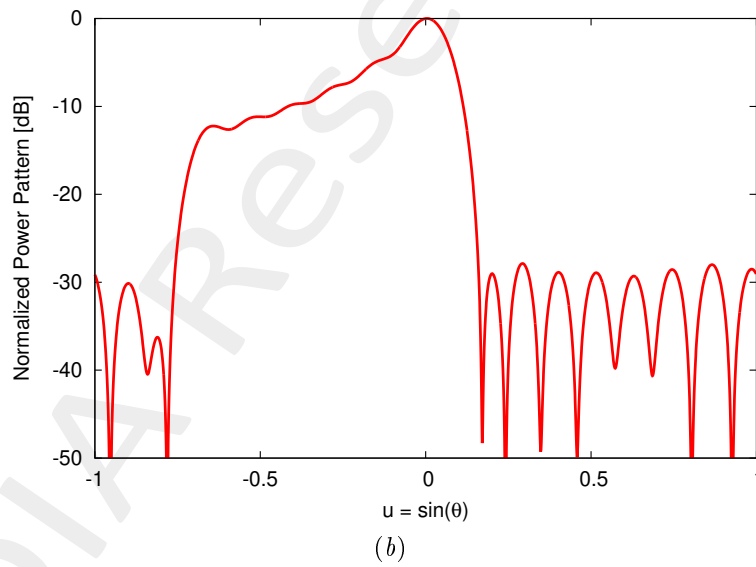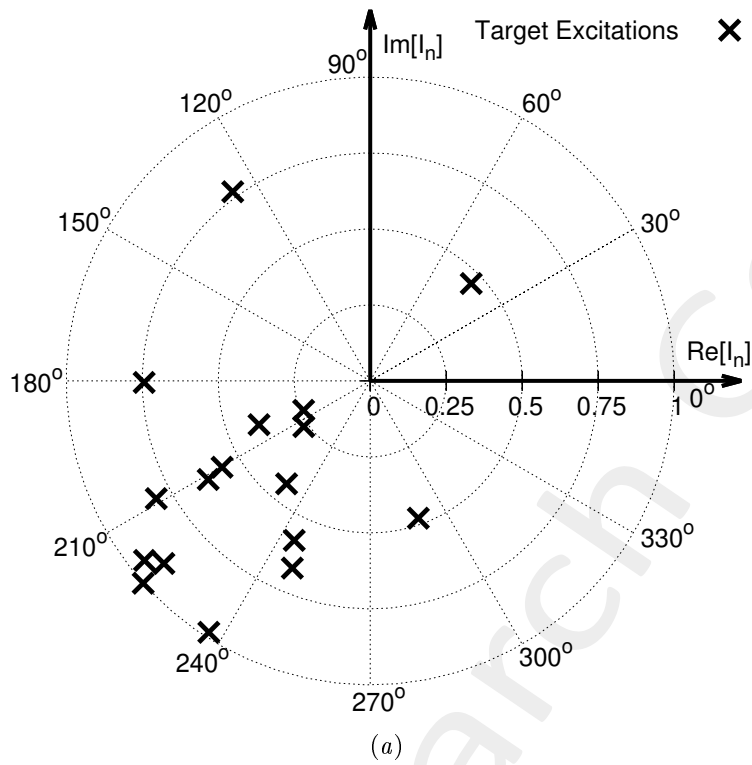
Figure 61: *Target solution* - (*a*) target excitations and (*b*) corresponding radiation pattern.
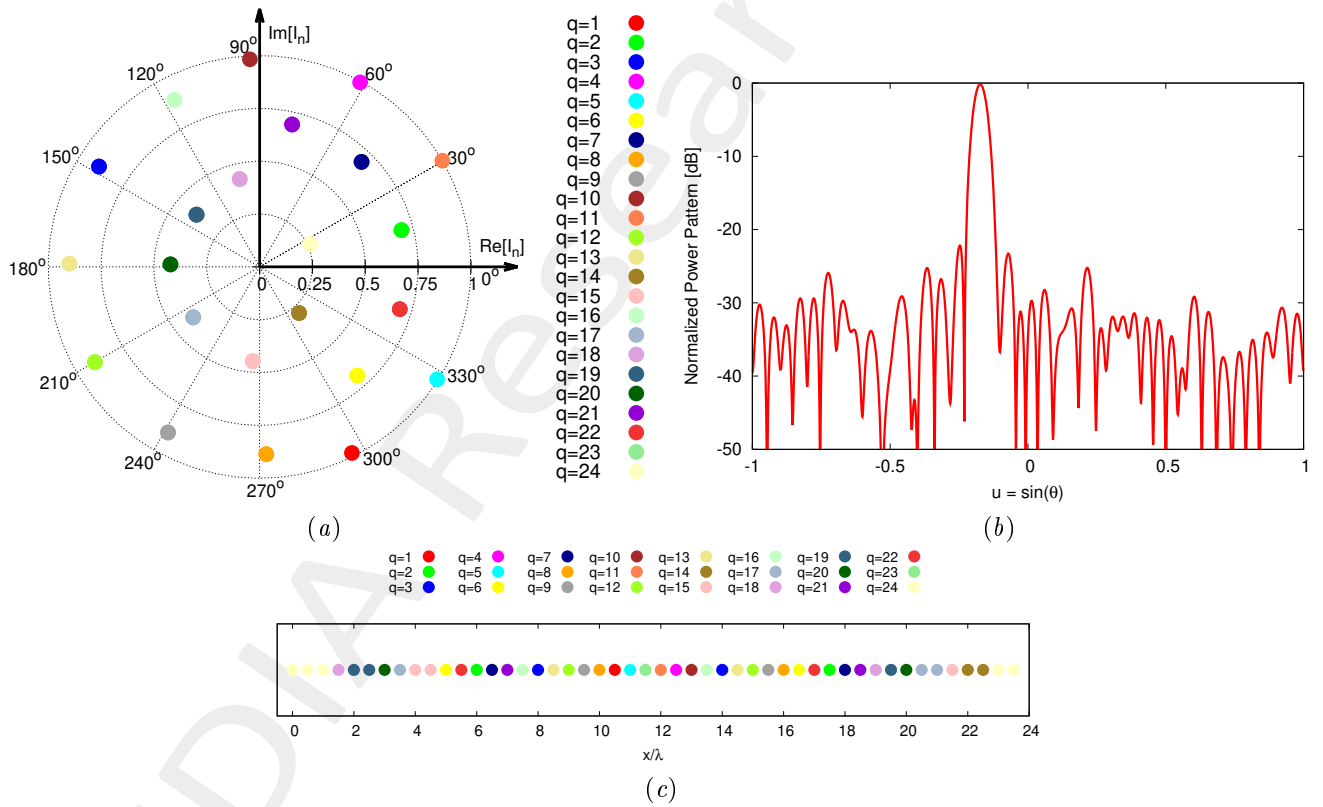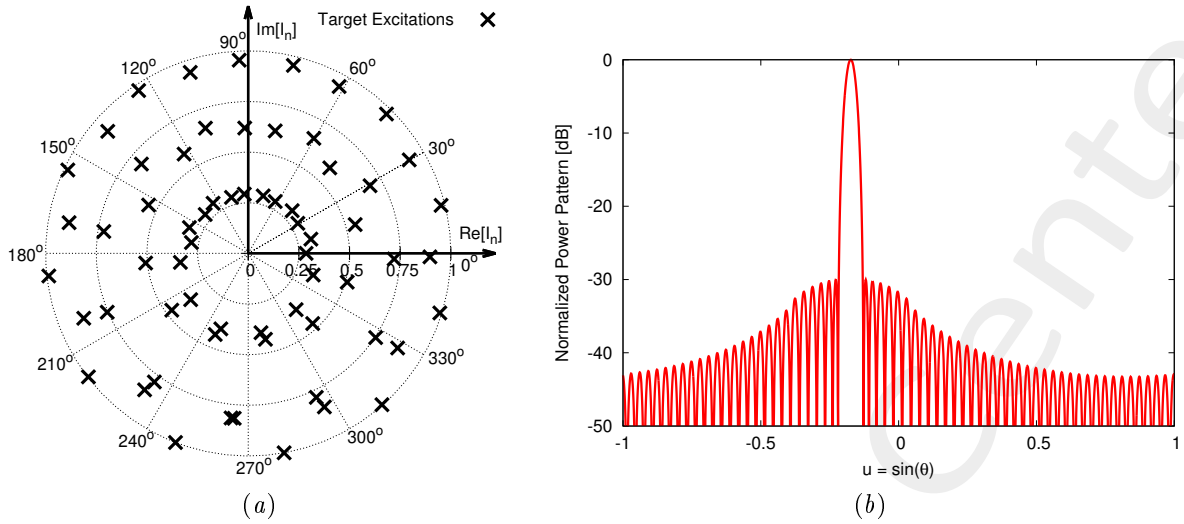
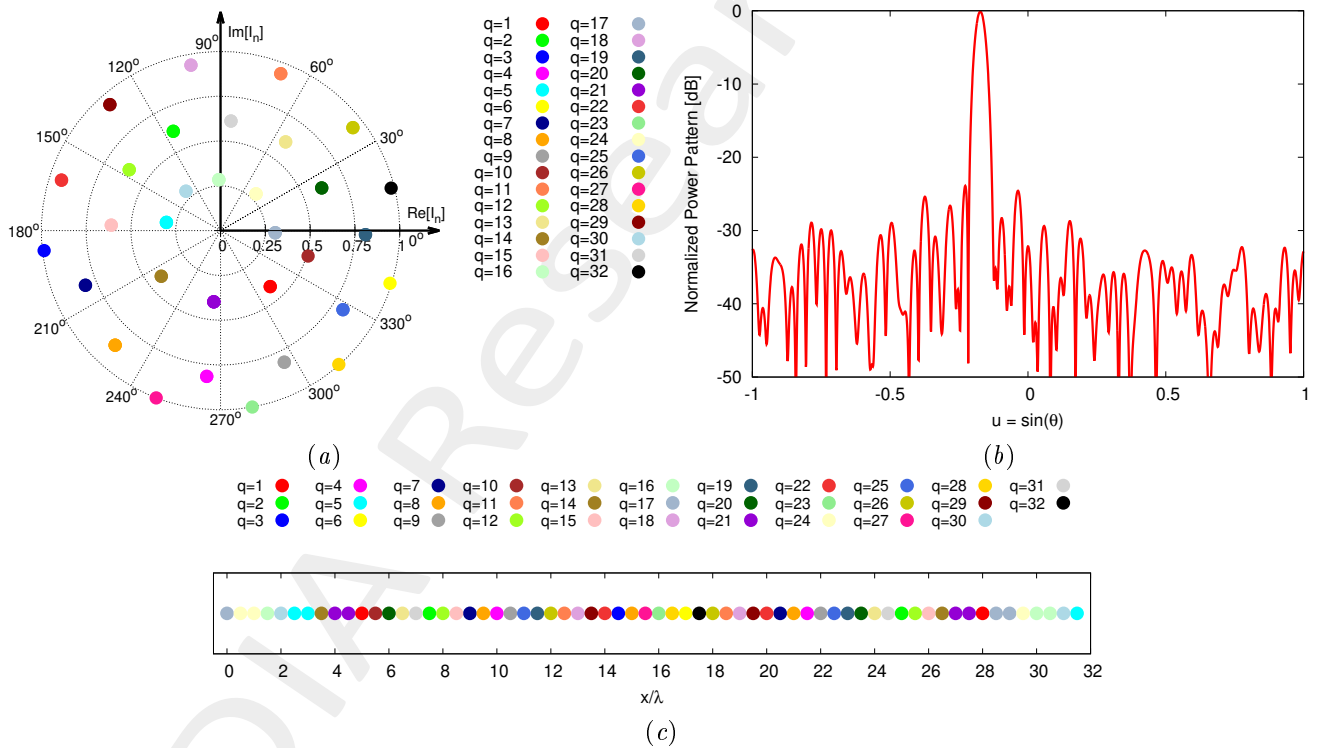**$Q = 6$ - Excitation Matching (EM) K-means Solution**
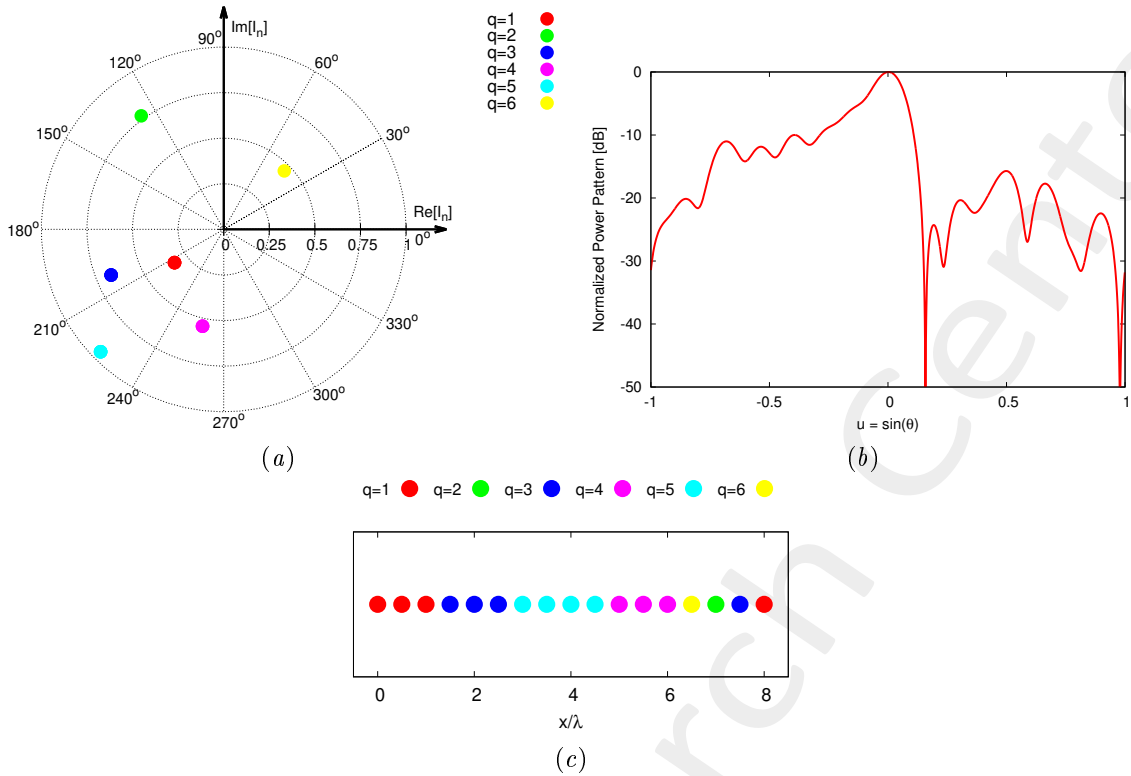
Figure 62: *K-means solution* - (a) Optimized excitations, (b) arising radiation pattern and (c) subarray configuration.

$Q = 8$ - Excitation Matching (EM) K-means Solution
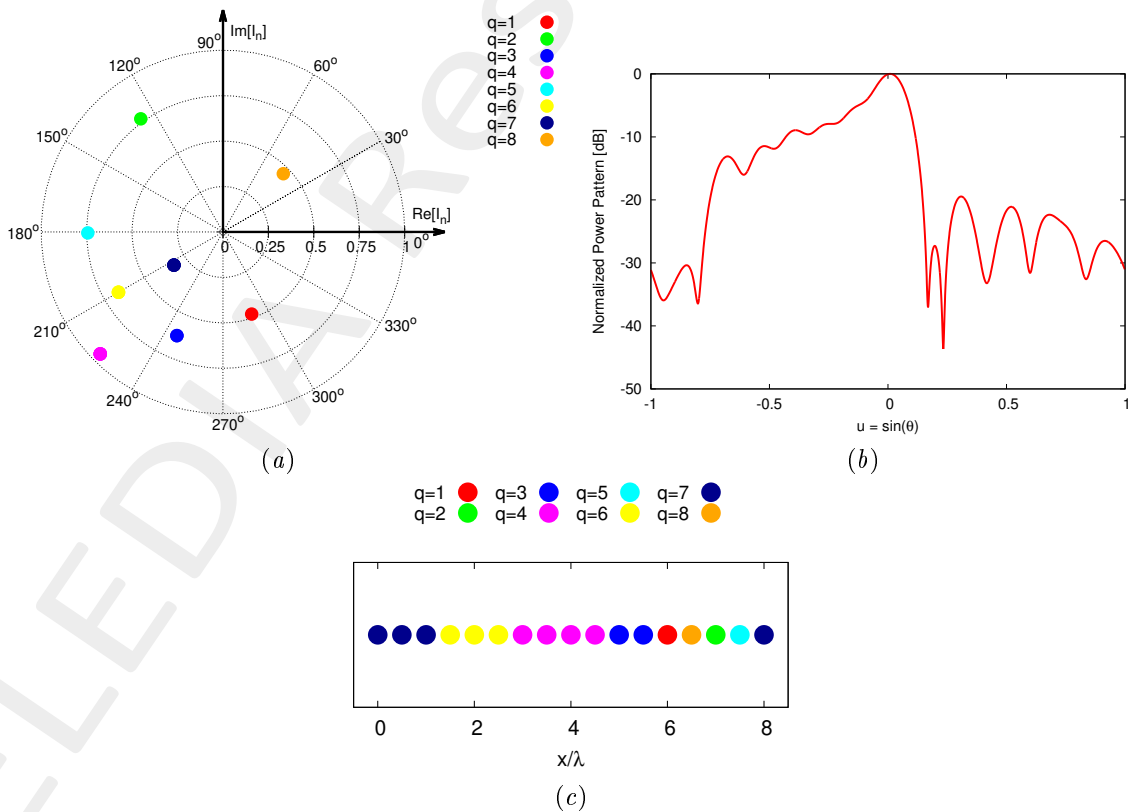
Figure 63: *K-means solution* - (a) Optimized excitations, (b) arising radiation pattern and (c) subarray configuration.

$Q = 9$ - Excitation Matching (EM) K-means Solution

(a)

(b)

(c)
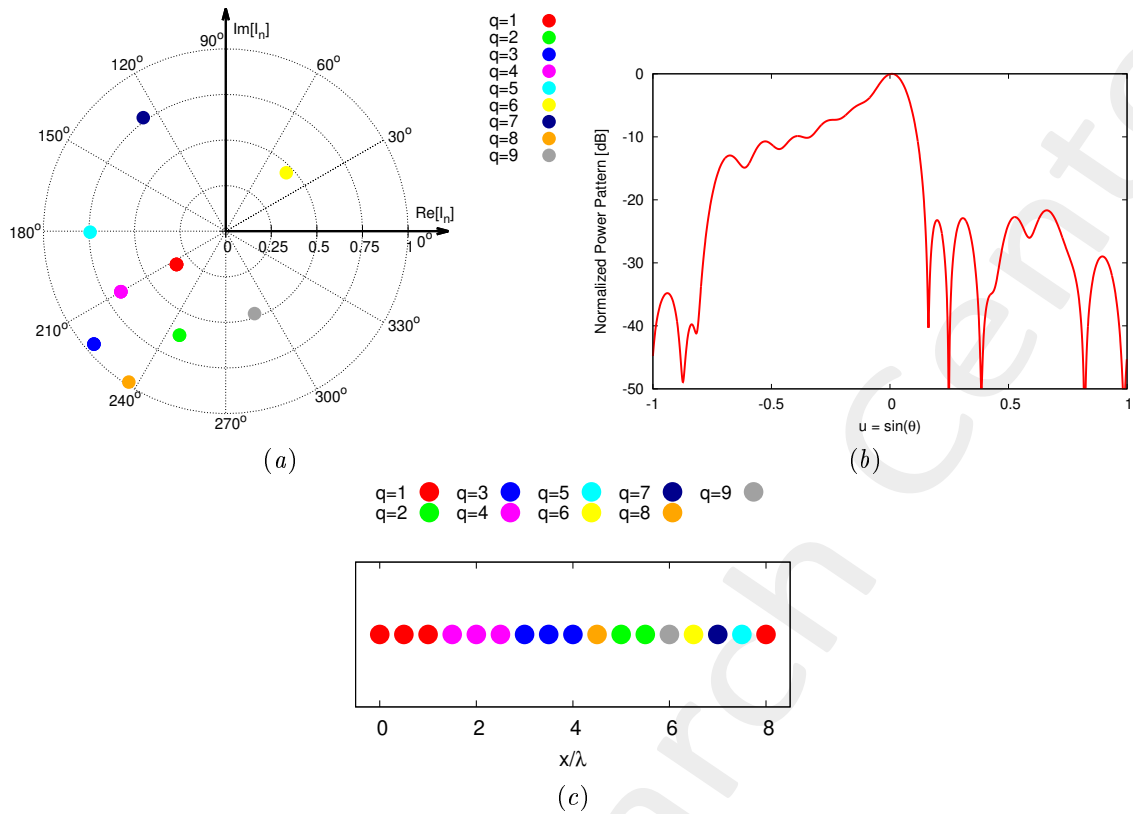
Figure 64: *K-means solution* - (a) Optimized excitations, (b) arising radiation pattern and (c) subarray configuration.

$Q = 11$ - Excitation Matching (EM) K-means Solution

(a)

(b)

(c)

Figure 65: *K-means solution* - (a) Optimized excitations, (b) arising radiation pattern and (c) subarray configuration.

53

$Q = 15$ - Excitation Matching (EM) K-means Solution

Figure 66: *K-means solution* - (a) Optimized excitations, (b) arising radiation pattern and (c) subarray configuration.

Pattern Features Resume

|	Δ	Ψ
$Q = 6$	4.75×10^{-2}	2.20×10^{-2}
$Q = 8$	1.91×10^{-2}	8.85×10^{-3}
$Q = 9$	1.15×10^{-2}	5.32×10^{-3}
$Q = 11$	3.60×10^{-3}	1.67×10^{-3}
$Q = 15$	4.14×10^{-4}	1.92×10^{-4}

Table VIII: *K-means solution* - Pattern matching error, Δ, and fitness, Ψ, values.

OUTCOMES:

- A good trade-off solution is obtained for $Q = 9$. Despite the high reduction in terms of control points (i.e., from $Q = 17$ to $Q = 9$, the reduction percentage is 47.1%), the solution exhibits a good pattern matching error $\Delta = 1.15 \times 10^{-2}$ limiting the degradation of the performance in terms of sidelobe level, that increase from $SLL\rfloor_{Q=17} = -27.9$ [dB] to $SLL\rfloor_{Q=17} = -21.7$ [dB].

1.6 Flat-Top Pattern - Analysis varying Q

OBJECTIVE: Similarly to the test case presented in the previous Section, in this case the performance of the $K - means$ algorithm are investigated considering a kind of pattern alternative to the pencil beam, the flat-top pattern. An analysis varying the number of subarrays will be carried out, keeping a fixed beam pointing angle as well as the array size.

Array Parameters

- Number of elements: $N = 32$

- Number of subarrays: $Q = 12, 16, 20, 28$

- Inter-element spacing: $d = \lambda/2$

- Flat-top pattern, $SLL_{ref} = -20$ [dB]

- Pointing angle: $\theta_0 = 0$ [deg]

K-means Clustering Method Parameters

- Number of iterations: $I = 100$

- Number of executions: $R = 100$

1.6.1 Flat-top Pattern, $N = 32$, $SLL_{ref} = -20$ [dB], $\theta_0 = 0$ [deg]: $Q = 12, 16, 20, 28$

Target Solution

(a)

(b)
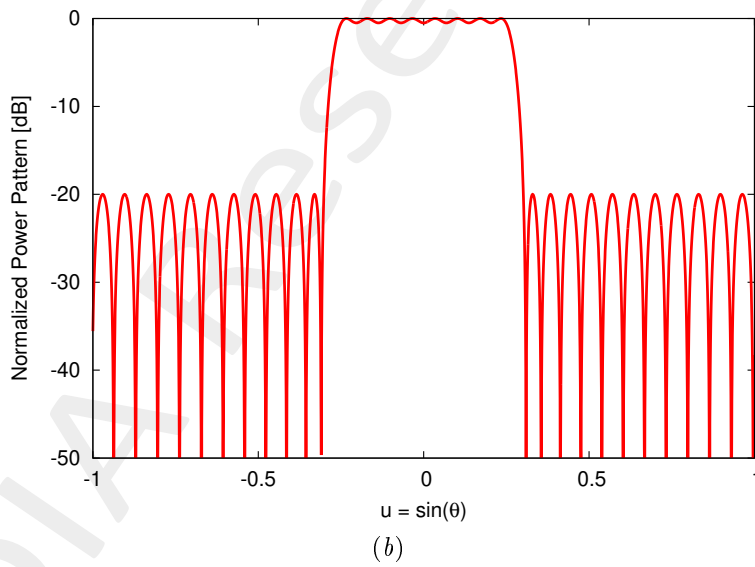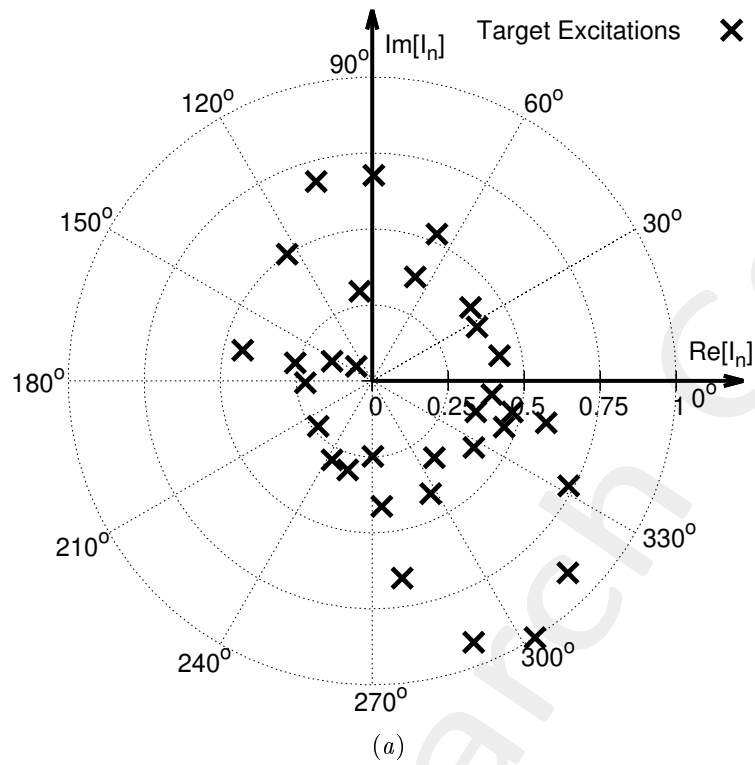
Figure 67: *Target solution* - (a) target excitations and (b) corresponding radiation pattern.

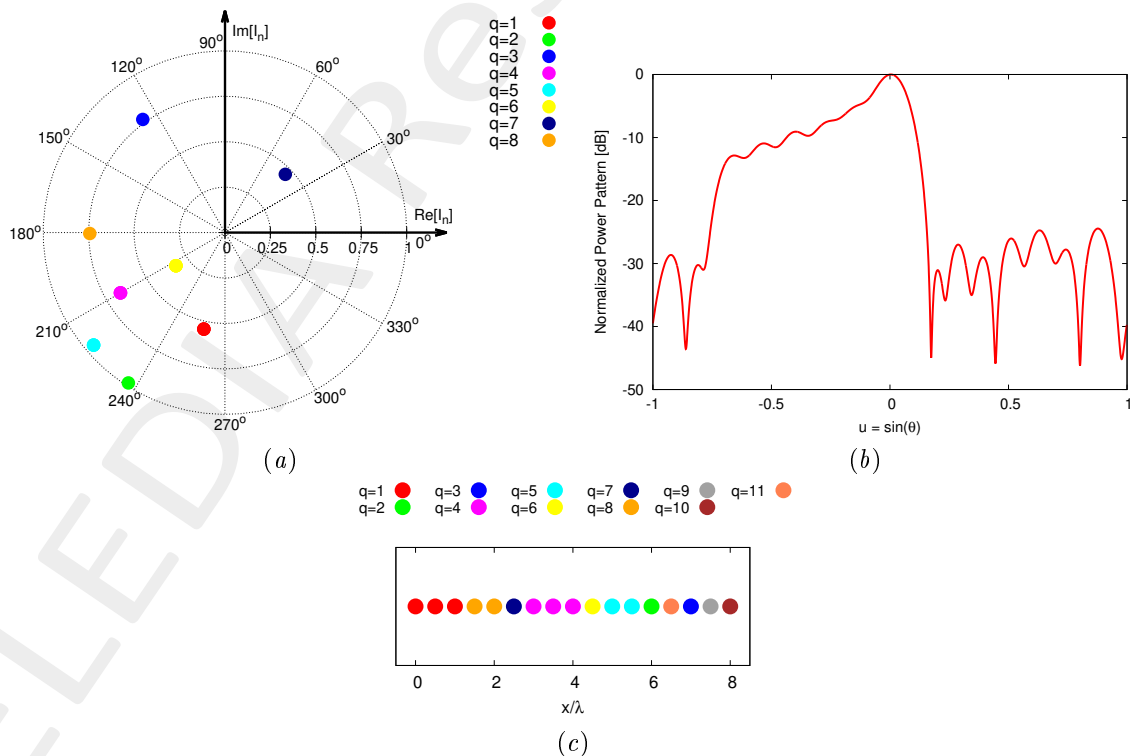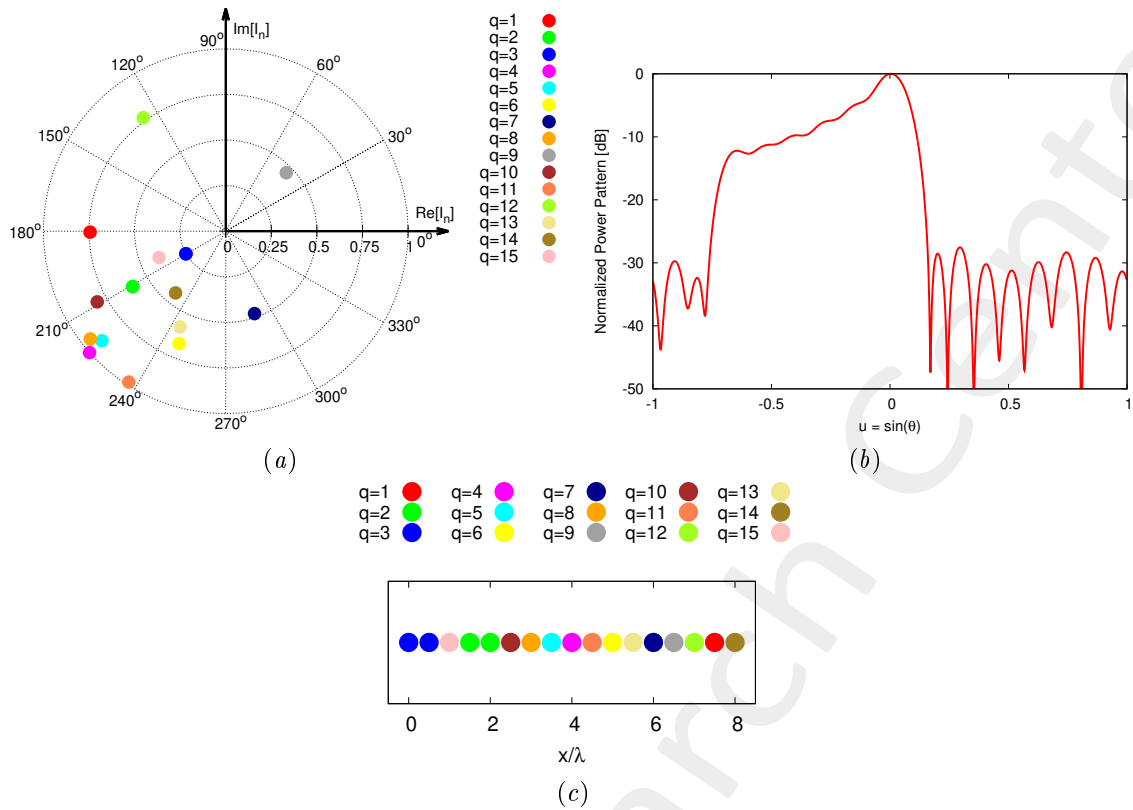**$Q = 12$ - Excitation Matching (EM) K-means Solution**

(a) (b) (c)
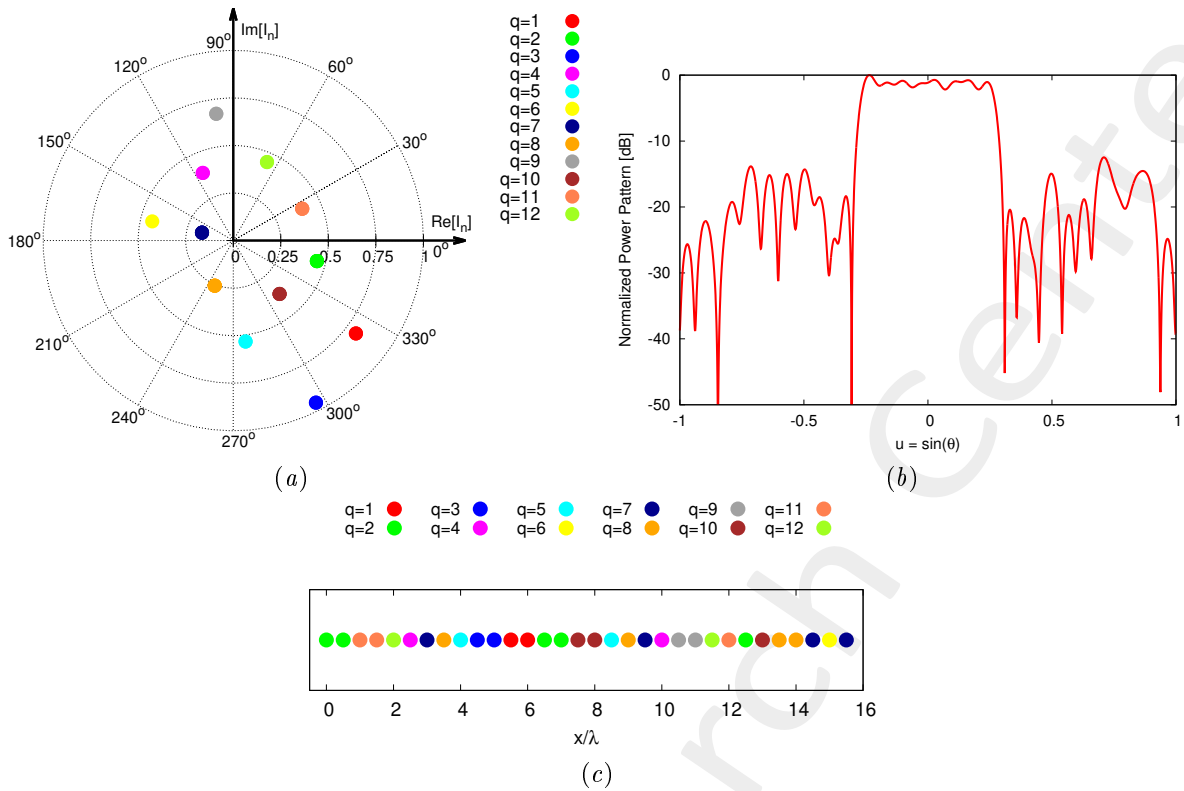
Figure 68: *K-means solution* - (a) Optimized excitations, (b) arising radiation pattern and (c) subarray configuration.

$Q = 16$ - Excitation Matching (EM) K-means Solution

(a) (b) (c)
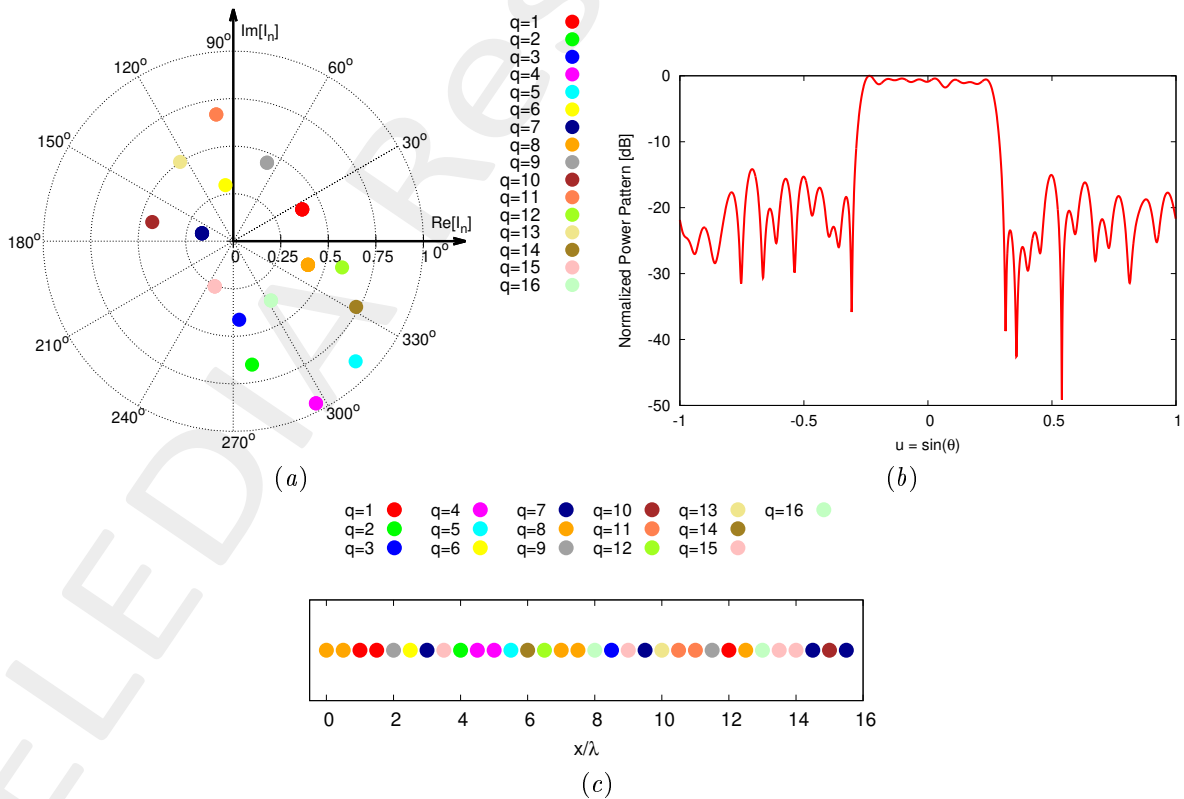
Figure 69: *K-means solution* - (a) Optimized excitations, (b) arising radiation pattern and (c) subarray configuration.

$Q = 20$ - Excitation Matching (EM) K-means Solution

(a)

(b)

(c)
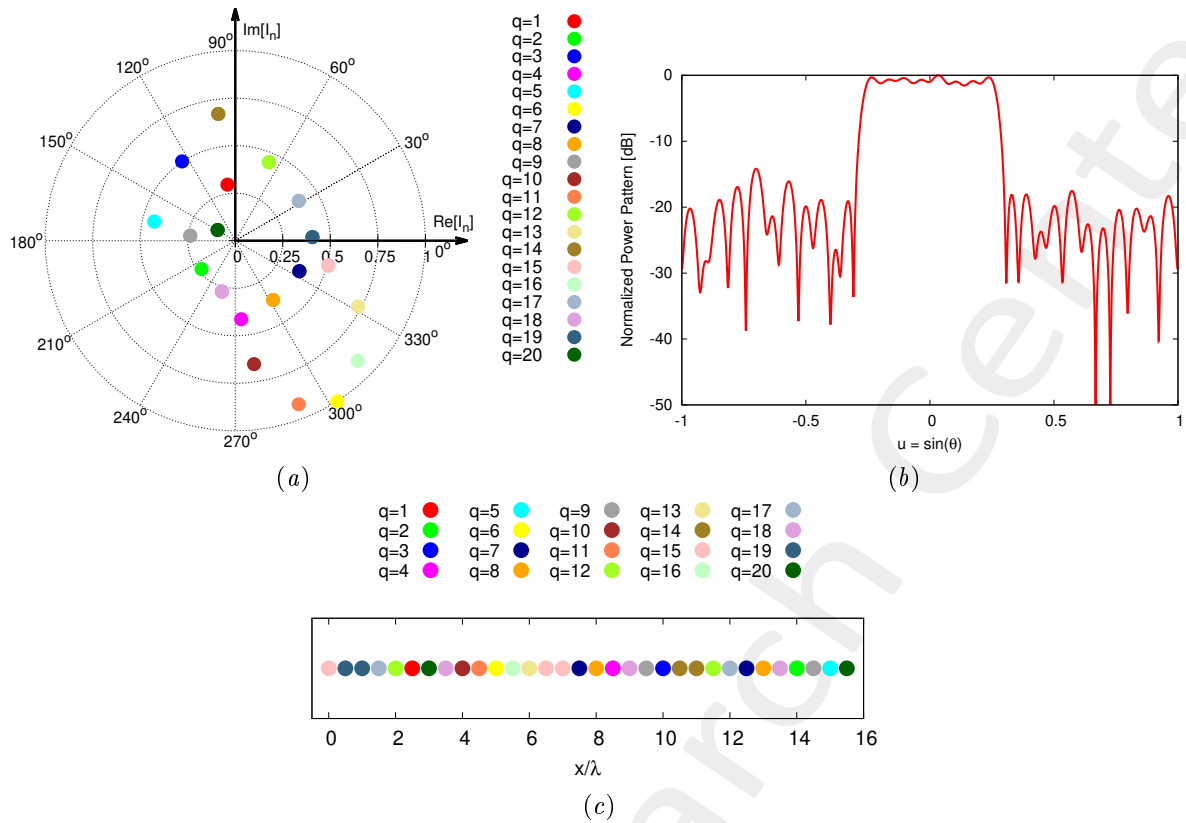
Figure 70: *K-means solution* - (a) Optimized excitations, (b) arising radiation pattern and (c) subarray configuration.

$Q = 28$ - Excitation Matching (EM) K-means Solution
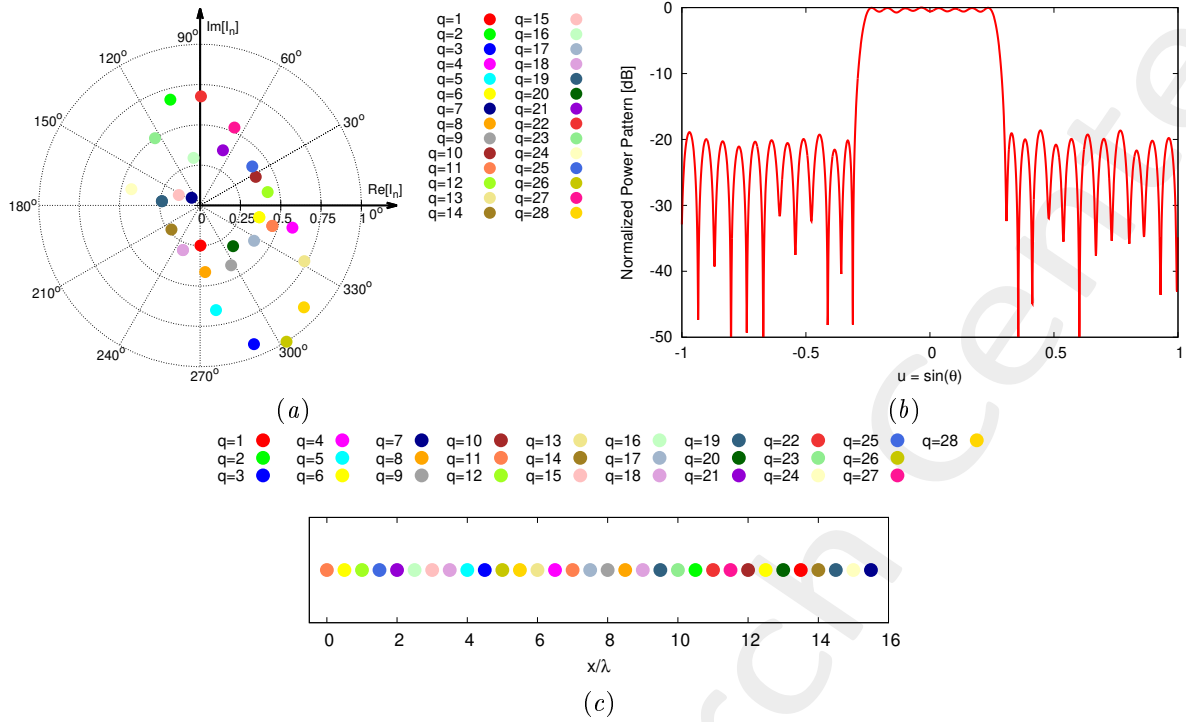
Figure 71: *K-means solution* - (a) Optimized excitations, (b) arising radiation pattern and (c) subarray configuration.

Pattern Features Resume

	Δ	Ψ
$Q = 12$	3.64×10^{-2}	9.23×10^{-3}
$Q = 16$	2.01×10^{-2}	5.09×10^{-3}
$Q = 20$	1.03×10^{-2}	2.62×10^{-3}
$Q = 28$	1.14×10^{-3}	2.88×10^{-4}

Table IX: *K-means solution* - Pattern matching error, Δ, and fitness, Ψ, values.

More information on the topics of this document can be found in the following list of references.

References

[1] P. Rocca, G. Oliveri, R. J. Mailloux, and A. Massa, "Unconventional phased array architectures and design Methodologies - A review," *Proceedings of the IEEE*, vol. 104, no. 3, pp. 544-560, March 2016.

[2] P. Rocca, L. Poli, A. Polo, and A. Massa, "Optimal excitation matching strategy for sub-arrayed phased linear arrays generating arbitrary shaped beams," *IEEE Trans. Antennas Propag.*, vol. 68, no. 6, pp. 4638-4647, Jun. 2020.

[3] G. Oliveri, G. Gottardi and A. Massa, "A new meta-paradigm for the synthesis of antenna arrays for future wireless communications," *IEEE Trans. Antennas Propag.*, vol. 67, no. 6, pp. 3774-3788, Jun. 2019.

[4] P. Rocca, M. H. Hannan, L. Poli, N. Anselmi, and A. Massa, "Optimal phase-matching strategy for beam scanning of sub-arrayed phased arrays," *IEEE Trans. Antennas and Propag.*, vol. 67, no. 2, pp. 951-959, Feb. 2019.

[5] N. Anselmi, P. Rocca, M. Salucci, and A. Massa, "Contiguous phase-clustering in multibeam-on-receive scanning arrays," *IEEE Trans. Antennas Propag.*, vol. 66, no. 11, pp. 5879-5891, Nov. 2018.

[6] L. Poli, G. Oliveri, P. Rocca, M. Salucci, and A. Massa, "Long-Distance WPT Unconventional Arrays Synthesis," *Journal of Electromagnetic Waves and Applications*, vol. 31, no. 14, pp. 1399-1420, Jul. 2017.

[7] G. Gottardi, L. Poli, P. Rocca, A. Montanari, A. Aprile, and A. Massa, "Optimal Monopulse Beamforming for Side-Looking Airborne Radars," *IEEE Antennas Wireless Propag. Lett.*, vol. 16, pp. 1221-1224, 2017.

[8] G. Oliveri, M. Salucci, and A. Massa, "Synthesis of modular contiguously clustered linear arrays through a sparseness-regularized solver," *IEEE Trans. Antennas Propag.*, vol. 64, no. 10, pp. 4277-4287, Oct. 2016.

[9] P. Rocca, G. Oliveri, R. J. Mailloux, and A. Massa, "Unconventional phased array architectures and design Methodologies - A review," *Proceedings of the IEEE = Special Issue on 'Phased Array Technologies', Invited Paper*, vol. 104, no. 3, pp. 544-560, March 2016.

[10] P. Rocca, M. D'Urso, and L. Poli, "Advanced strategy for large antenna array design with subarray-only amplitude and phase contr," *IEEE Antennas and Wireless Propag. Lett.*, vol. 13, pp. 91-94, 2014.

[11] L. Manica, P. Rocca, G. Oliveri, and A. Massa, "Synthesis of multi-beam sub-arrayed antennas through an excitation matching strategy," *IEEE Trans. Antennas Propag.*, vol. 59, no. 2, pp. 482-492, Feb. 2011.

[12] G. Oliveri, "Multi-beam antenna arrays with common sub-array layouts," *IEEE Antennas Wireless Propag. Lett.*, vol. 9, pp. 1190-1193, 2010.

[13] P. Rocca, R. Haupt, and A. Massa, "Sidelobe reduction through element phase control in sub-arrayed array antennas," *IEEE Antennas Wireless Propag. Lett.*, vol. 8, pp. 437-440, 2009.

[14] P. Rocca, L. Manica, R. Azaro, and A. Massa, "A hybrid approach for the synthesis of sub-arrayed monopulse linear arrays," *IEEE Trans. Antennas Propag.* , vol. 57, no. 1, pp. 280-283, Jan. 2009.

[15] L. Manica, P. Rocca, M. Benedetti, and A. Massa, "A fast graph-searching algorithm enabling the efficient synthesis of sub-arrayed planar monopulse antennas," *IEEE Trans. Antennas Propag.*, vol. 57, no. 3, pp. 652-664, Mar. 2009.

[16] P. Rocca, L. Manica, A. Martini, and A. Massa, "Compromise sum-difference optimization through the iterative contiguous partition method," *IET Microwaves, Antennas & Propagation*, vol. 3, no. 2, pp. 348-361, 2009.

[17] L. Manica, P. Rocca, and A. Massa, "An excitation matching procedure for sub-arrayed monopulse arrays with maximum directivity," *IET Radar, Sonar & Navigation*, vol. 3, no. 1, pp. 42-48, Feb. 2009.

[18] L. Manica, P. Rocca, and A. Massa, "Design of subarrayed linear and planar array antennas with SLL control based on an excitation matching approach," *IEEE Trans. Antennas Propag.*, vol. 57, no. 6, pp. 1684-1691, Jun. 2009.

[19] L. Manica, P. Rocca, A. Martini, and A. Massa, "An innovative approach based on a tree-searching algorithm for the optimal matching of independently optimum sum and difference excitations," *IEEE Trans. Antennas Propag.*, vol. 56, no. 1, pp. 58-66, Jan. 2008.

[20] P. Rocca, L. Manica, and A. Massa, "An effective excitation matching method for the synthesis of optimal compromises between sum and difference patterns in planar arrays," *Progress in Electromagnetic Research B*, vol. 3, pp. 115-130, 2008.

[21] P. Rocca, L. Manica, and A. Massa, "Directivity optimization in planar sub-arrayed monopulse antenna," *Progress in Electromagnetic Research L*, vol. 4, pp. 1-7, 2008.

[22] P. Rocca, L. Manica, M. Pastorino, and A. Massa, "Boresight slope optimization of sub-arrayed linear arrays through the contiguous partition method," *IEEE Antennas Wireless Propag. Lett.*, vol. 8, pp. 253-257, 2008.

[23] P. Rocca, L. Manica, and A. Massa, "Synthesis of monopulse antennas through the iterative contiguous partition method," *Electronics Letters*, vol. 43, no. 16, pp. 854-856, Aug. 2007.

[24] P. Rocca, L. Manica, A. Martini, and A. Massa, "Synthesis of large monopulse linear arrays through a tree-based optimal excitations matching," *IEEE Antennas Wireless Propag. Lett.*, vol. 7, pp. 436-439, 2007.

[25] P. Rocca, N. Anselmi, A. Polo, and A. Massa, "An irregular two-sizes square tiling method for the design of isophoric phased arrays," *IEEE Trans. Antennas Propag.*, vol. 68, no. 6, pp. 4437-4449, Jun. 2020.

[26] P. Rocca, N. Anselmi, A. Polo, and A. Massa, "Modular design of hexagonal phased arrays through diamond tiles," *IEEE Trans. Antennas Propag.*, vol.68, no. 5, pp. 3598-3612, May 2020.

[27] N. Anselmi, L. Poli, P. Rocca, and A. Massa, "Design of simplified array layouts for preliminary experimental testing and validation of large AESAs," *IEEE Trans. Antennas Propag.*, vol. 66, no. 12, pp. 6906-6920, Dec. 2018.

[28] G. Oliveri, G. Gottardi, F. Robol, A. Polo, L. Poli, M. Salucci, M. Chuan, C. Massagrande, P. Vinetti, M. Mattivi, R. Lombardi, and A. Massa, "Co-design of unconventional array architectures and antenna elements for 5G base station," *IEEE Trans. Antennas Propag.*, vol. 65, no. 12, pp. 6752-6767, Dec. 2017.

[29] N. Anselmi, P. Rocca, M. Salucci, and A. Massa, "Irregular phased array tiling by means of analytic schemata-driven optimization," *IEEE Trans. Antennas Propag.*, vol. 65, no. 9, pp. 4495-4510, September 2017.

[30] N. Anselmi, P. Rocca, M. Salucci, and A. Massa, "Optimization of excitation tolerances for robust beamforming in linear arrays," *IET Microwaves, Antennas & Propagation*, vol. 10, no. 2, pp. 208-214, 2016.

[31] P. Rocca, R. J. Mailloux, and G. Toso, "GA-Based optimization of irregular sub-array layouts for wideband phased arrays desig," *IEEE Antennas and Wireless Propag. Lett.*, vol. 14, pp. 131-134, 2015.

[32] P. Rocca, M. Donelli, G. Oliveri, F. Viani, and A. Massa, "Reconfigurable sum-difference pattern by means of parasitic elements for forward-looking monopulse radar," *IET Radar, Sonar & Navigation*, vol 7, no. 7, pp. 747-754, 2013.

[33] P. Rocca, L. Manica, and A. Massa, "Ant colony based hybrid approach for optimal compromise sum-difference patterns synthesis," *Microwave Opt. Technol. Lett.*, vol. 52, no. 1, pp. 128-132, Jan. 2010.

[34] P. Rocca, L. Manica, and A. Massa, "An improved excitation matching method based on an ant colony optimization for suboptimal-free clustering in sum-difference compromise synthesis," *IEEE Trans. Antennas Propag.*, vol. 57, no. 8, pp. 2297-2306, Aug. 2009.

[35] P. Rocca, L. Manica, and A. Massa, "Hybrid approach for sub-arrayed monopulse antenna synthesis," *Electronics Letters*, vol. 44, no. 2, pp. 75-76, Jan. 2008.

[36] P. Rocca, L. Manica, F. Stringari, and A. Massa, "Ant colony optimization for tree-searching based synthesis of monopulse array antenna," *Electronics Letters*, vol. 44, no. 13, pp. 783-785, Jun. 19, 2008.